Supporting Information for:

Consecutive C-H and O_2 activation at a Pt(II) Center to Produce Pt(IV) Aryls

David Watts, Peter Y. Zavalij, Andrei N. Vedernikov*

Department of Chemistry and Biochemistry, University of Maryland, College Park, MD 20742

E-mail: avederni@umd.edu

I. Materials and Methods

All manipulations were carried out under argon atmosphere unless otherwise noted. SEPIX 560 40 – 63 µm silica gel was purchased from ZEOCHEM and used for all column chromatography purifications. Potassium tetrachloroplatinate(II) was purchased from Pressure Chemical and used without purification. 2,2,2-Trifluoroethanol was purchased from Sigma-Aldrich or Oakwood Chemical, dried over calcium hydride, purified by vacuum transfer and was stored in an argon-filled glovebox. The storage of 2,2,2-trifluoroethanol over molecular sieves leads to slow alkalinization of the solvent and so was not employed. THF solvent was dried over and distilled from sodium / benzophenone adduct under argon and stored over molecular sieves. Deuterium-labeled solvents C_6D_6, $CDCl_3$, DMSO-d_6 were purchased from Cambridge Isotope Laboratories and TFE-d_1 was purchased from Sigma Aldrich. 1H (400 Mhz, 500 MHz, and 600 Mhz) and 13C NMR (125 MHz) spectra were recorded on a Bruker DRX-500 or Bruker AVIII-600MHz spectrometer. Chemical shifts are reported in parts per million (ppm) (δ) and referenced to residual solvent resonance peaks. Multiplicities are reported as follows: br (broad signal), s (singlet), d (doublet), t (triplet), q (quartet), quin (quintet), sex (sextet), m (multiplet), dd (doublet of doublets), ddd (doublet of doublet of doublets), qd (quartet of doublets). Coupling constants (J) are reported in Hz. High Resolution Mass Spectrometry (HRMS) experiments were performed using a JEOL AccuTOF-CS instrument.

II. Ligand Synthesis

Synthesis of H(Ph-dpms):

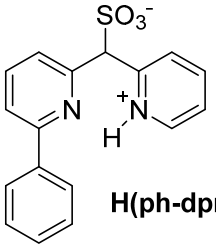

H(ph-dpms)

The synthesis of H(Ph-dpms) was carried out according to the published procedure.[1]

^{1}H NMR (400 MHz, 22 ^{o}C, DMSO-d_6), δ: 5.94 (s, 1H), 7.45 (overlapping multiplets, 3H), 7.81 (d, $^{3}J_{HH}$ = 7.4 Hz, 1H), 7.92 (d, $^{3}J_{HH}$ = 7.8 Hz, 1H), 7.94 - 8.01 (overlapping multiplets, 4H), 8.35 (d, $^{3}J_{HH}$ = 7.8 Hz, 1H), 8.59 (ddd, $^{3}J_{HH}$ = 8.6, 8.2 Hz, $^{4}J_{HH}$ = 1.6 Hz, 1H), 8.97 (dd, $^{3}J_{HH}$ = 5.8 Hz, $^{4}J_{HH}$ = 0.9 Hz, 1H). The expected signal of the NH – proton in H(Ph-dpms) could not be observed in either $CDCl_3$ or $CDCl_2$ solution. A very broad signal at about 3 ppm is seen in DMSO solutions which might result from a fast proton exchange between the NH^+ group and the solvent residual water.

^{13}C NMR (125 MHz, 22 ^{o}C, DMSO-d_6), δ: 68.8, 119.3, 124.0, 125.4, 126.7, 128.8, 128.9, 129.2, 138.0, 138.1, 141.5, 145.4, 151.8, 153.6, 154.7.

ESI-MS(-) of solution of H(Ph-dpms) in methanol doped with KOH, H(Ph-dpms) = 325.08. Calculated for H(Ph-dpms) = $C_{17}H_{13}N_2O_3S$, 325.07.

Synthesis of Li(Ph-dpms):

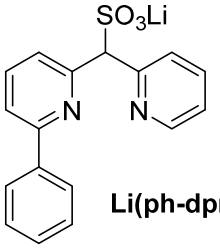

Li(ph-dpms)

The synthesis of Li(Ph-dpms) was carried out according to the published procedure.[2] Alternatively, Li(Ph-dpms) could be produced from H(Ph-dpms) by the following method: Under air, H(Ph-dpms) (0.25 g, 0.75 mmol) was dispersed in 10 mL deionized H_2O along with $LiOH{\cdot}H_2O$ (0.035 g, 0.83 mmol, 1.1 eq.) in a 50 mL round bottom flask. The slurry was stirred at 60 °C until all H(Ph-dpms) had dissolved (approx. 15 min) resulting in an orangish solution with a pH of ~10. The solvent was removed *in vacuo*. To remove excess LiOH, the resulting residue was flushed through a short silica column (2:2:1 EtOAc:DCM:MeOH) to give a white powder which was dried overnight at 60 °C in a vacuum oven, yielding dry Li(Ph-dpms) (0.23 g, 68mmol, 91 % yield). Aqueous solutions of the resulting Li(Ph-dpms) had a pH of ~7.

^{1}H NMR (400 MHz, 22 ^{o}C, MeOD), δ: 5.80 (s, 1H), 7.34 (ddd, $^{3}J_{HH}$ = 7.2, 4.8 Hz, $^{4}J_{HH}$ = 0.8 Hz, 1H), 7.38-7.45 (m, 3H), 7.75 (dd, $^{3}J_{HH}$ = 7.6 Hz, $^{4}J_{HH}$ = 0.8 Hz, 1H), 7.82-7.92 (m, 3H), 8.00-8.02 (m, 2H), 8.26 (d, $^{3}J_{HH}$ = 8.0 Hz, 1H), 8.47 (dd, $^{3}J_{HH}$ = 4.0 Hz, $^{4}J_{HH}$ = 0.4 Hz, 1H).

^{13}C NMR (125 MHz, 22 ^{o}C, MeOD), δ: 73.6, 117.3, 121.1, 121.6, 124.0, 125.1, 126.7, 127.0, 135.0, 135.5, 137.8, 146.3, 154.0, 154.7, 154.9.

ESI-MS(-) of a solution of Li(Ph-dpms) in water, $[Ph\text{-}dpms]^-$ = 325.09. Calculated for $[Ph\text{-}dpms]^-$: $C_{17}H_{13}N_2O_3S$, 325.07.

III. Synthesis of Pt Complexes

Synthesis of (C_6H_4-dpms)Pt(H_2O), 4:[1]

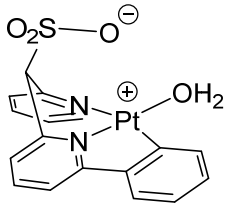

4

The synthesis of (C_6H_4-dpms)Pt(H_2O), **4**, was carried out according to the published procedure.[1]

Synthesis of (C_6H_4-dpms)Pt(OCH_2CF_3)(OH), 8:[2]

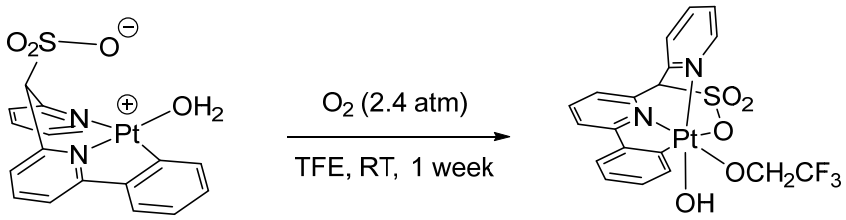

4 **8**

To a 25 mL Schlenk tube was added **4** (40.0 mg, 74.4 µmol) along with 5 mL TFE. A stir bar was added, the head space was purged with O_2, and then the tube was pressurized to 20 psi O_2 (total pO_2 of ~35 psi) before being sealed. The solution was stirred vigorously at room temperature over the course of one week. The color initially changed to deep purple and then slowly to yellow. A 0.05 mL aliquot was removed, dried, dissolved in DMSO-d_6, and submitted to a ^{1}H-NMR analysis which showed one new species, identified as complex **8** in a 0.7:1 ratio with (C_6H_4-dpms)Pt(DMSO-d_6) (41% NMR yield of **8**). The TFE solution was dried *in vacuo* leaving a light yellow residue which was purified by column chromatography on silica (1:10 MeOH:DCM) to give pure **8** as a white powder (13.2 mg, 21 µmol, 28 %). XRD quality crystals could be grown from a TFE solution of **8** layered with Et_2O and the crystal structure has been published.[2] Samples of complex **8** are stable when stored in the freezer but slowly decompose at room temperature. In TFE solution the decomposition takes weeks at RT whereas in DMSO-d_6 it is on the order of a few days.

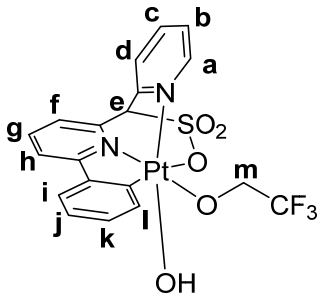

^{1}H NMR (600 MHz, 22 °C, TFE-d_1), δ: 6.18 (s, 1H$_e$), 7.40 (m, 2H$_{j,k}$), 7.61 (ddd, $^3J_{HH}$ = 8.2, 6.6 Hz, $^4J_{HH}$ = 1.3 Hz, 1H$_b$), 7.67 (dd, $^3J_{HH}$ = 7.1 Hz, $^4J_{HH}$ = 2.2 Hz, 1H$_i$), 7.73 (d, $^3J_{HH}$ = 7.8 Hz, 1H$_f$), 7.78 (dd, $^3J_{HH}$ = 7.3 Hz, $^4J_{HH}$ = 1.8 Hz, 1H$_l$), 7.90 (overlapping d, $^3J_{HH}$ = 8.2 Hz, 2H$_{d,h}$), 8.13 (m, 2H$_{g,c}$), 8.81 (dd, $^3J_{HH}$ = 5.8 Hz, $^4J_{HH}$ = 1.0 Hz). The

Pt-OCH_2CF_3 protons (H_m) could not be found in TFE-d_1, presumably due to overlap with the large solvent -CH_2- resonance.

^{1}H NMR (400 MHz, 22 °C, DMSO-d_6), δ: 1.53 (brs, 1H), 3.77 (dq, $^2J_{HH}$ = 12.7 Hz, $^3J_{HF}$ = 10.1 Hz, 1H), 4.01 (dq, $^2J_{HH}$ = 12.7 Hz, $^3J_{HF}$ = 10.1 Hz, 1H), 6.88 (s, 1H), 7.35 (m, 2H), 7.62 (m, 1H), 7.78 (ddd, $^3J_{HH}$ = 8.1, 5.8 Hz, $^4J_{HH}$ = 1.3 Hz, 1H), 7.86 (dd, $^3J_{HH}$ = 7.2 Hz, $^4J_{HH}$ = 1.4 Hz, 1H), 7.90 (m, 1H), 8.01 (dd, $^3J_{HH}$ = 8.0 Hz, $^4J_{HH}$ = 0.7 Hz, 1H), 8.23 – 8.32 (m, 3H), 8.67 (dd, $^3J_{HH}$ = 5.9 Hz, $^4J_{HH}$ = 1.5 Hz, 1H).

^{19}F NMR (376 MHz, 21 °C, DMSO-d_6), δ: -73.49 (brt, $^3J_{HF}$ = 10.1 Hz)

ESI-MS(+) of solution of **8** in TFE with a drop of HBF_4, [**8**+H]$^-$ = 636.05. Calculated for [**15**+H]$^+$ $C_{19}H_{16}F_3N_2O_5PtS^-$, 636.04.

Synthesis of Li[(C_6H_4-dpms)PtPh], Li(12a):

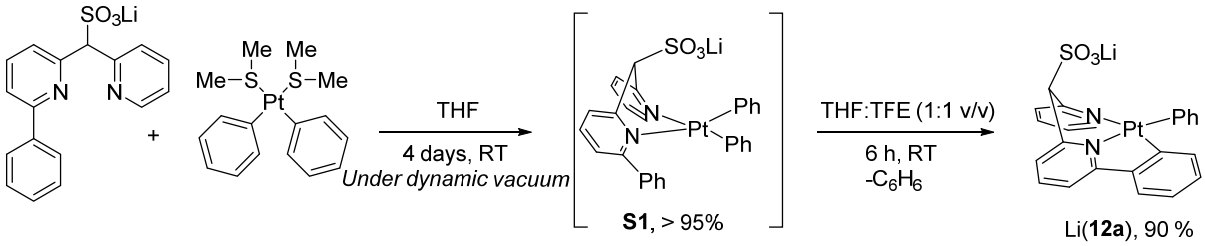

The precursor $Ph_2Pt(SMe2)_2$ was prepared according to the literature method.[3] In an argon filled glovebox, Li(Ph-dpms) (166 mg, 0.500 mmol) was dissolved in 4 mL anhydrous de-gassed THF and a stir bar was added. In a separate vial, $Ph_2Pt(SMe_2)_2$ (238 mg, 0.500 mmol) was dissolved in 4 mL anhydrous de-gassed THF. The two solutions were then combined and left to stir for 24 h after which a yellow precipitate had formed. The solvent was then removed under vacuum. The residue was then dispersed in 8 mL anhydrous THF and stirred for another 24 h. This process was repeated 4 times (96 h total) or until the precipitate disappeared and the solution became clear. The solvent was removed, resulting in a yellow powder weighing 320 mg. A sample was dissolved in a 1:1 mixture of THF-d_8:MeOD. Subsequent ^{1}H-NMR analysis showed primarily one species with 22 H in the aromatic region (one of which is likely the bridging methine C-H) which was tentatively assigned as **S1**. No SMe_2 was observed in the spectrum.

The yellow powder (**S1**) was then dispersed in 5 mL of a de-gassed 1:1 THF:TFE solvent mixture. The slurry was stirred for 6 h before the solvent was removed resulting in a yellowish orange residue. Recrystallization from MeOH with Et_2O yielded Li(**12a**) as a pale yellow semi-crystalline powder (262 mg, 90%).

^{1}H-NMR (400 MHz, 22 °C, DMSO-d6), δ: 5.85 (s, 1H), 6.80-6.95 (m, 4H), 6.98, (vt, $^3J_{HH}$ = 7.3 Hz, 2H), 7.17 (m, 2H), 7.25 (m, 1H), 7.55 (dd, $^3J_{HH}$ = 7.5 Hz, $^4J_{HH}$ = 1.3 Hz, 2H), 7.64 (vd, $^3J_{HH}$ = 7.9 Hz, 1H), 7.77 (vd, $^3J_{HH}$ = 7.9 Hz, 1H), 7.90-8.01 (m, 3H), 8.22 (dd, $^3J_{HH}$ = 5.9 Hz, $^4J_{HH}$ = 1.5 Hz, 1H)

^{13}C-NMR (125 MHz, 22 °C, MeOD), δ: 109.1, 113.2, 113.9, 115.1 ($^3J_{PtC}$ = 45.7 Hz, Pt-C_6H_4 C-*o*), 115.9, 117.0, 118.6 (2C, $^3J_{PtC}$ = 69.8 Hz, Pt-Ph C-*o*), 120.5, 121.3, 129.0, 129.6, 129.7, 130.4, 137.7, 137.8, 142.6, 144.4, 144.7, 145.9, 157.3.

El. Analysis, calculated for $C_{23}H_{17}LiN_2O_3PtS\cdot(CH_3OH)$: C, 45.36; H, 3.33; N, 4.41. Found C, 45.07; H, 3.46; N, 4.39.

ESI-MS(-) of a solution of Li[**12a**] in MeOH, [**12a**]$^-$: 596.37. Calculated for [**12a**]$^-$: $C_{23}H_{17}N_2O_3PtS$, 596.06.

A combination of ^{1}H-NMR NOE and COSY provided assignments for all protons belonging to Li(**12a**) in TFE solvent. 1D NOE experiments also provide evidence for the κ^3-CNN (as opposed to κ^3-CNO) structure assignment via the observed 0.9 % spin-spin coupling between the ortho pyridyl H_a and ortho phenyl H_b in Li(**12a**) (Figure S1).

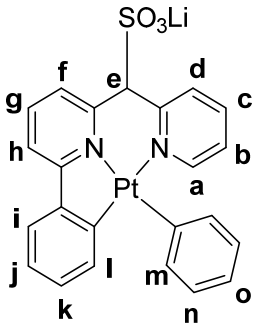

^{1}H-NMR (500 MHz, 22 °C, TFE), δ: 5.78 (s, 1H$_e$), 7.06 – 7.13 (m, 2H$_{k,o}$), 7.13 – 7.22 (m, 4H$_{b,j,n}$), 7.35 (d, $^{3}J_{HH}$ = 7.4 Hz, 1H$_l$), 7.60 (d, $^{3}J_{HH}$ = 8.1 Hz, 1H$_f$), 7.67 (d, $^{3}J_{HH}$ = 7.4 Hz, 2H$_m$), 7.71 (d, $^{3}J_{HH}$ = 8.1 Hz, 1H$_i$), 7.76 (vd, $^{3}J_{HH}$ = 8.1 Hz, 1H$_d$), 7.93 (m, 2H$_{c,h}$), 7.98 (vt, $^{3}J_{HH}$ = 7.8 Hz, 1H$_g$), 8.36 (d, $^{3}J_{HH}$ = 5.9 Hz).

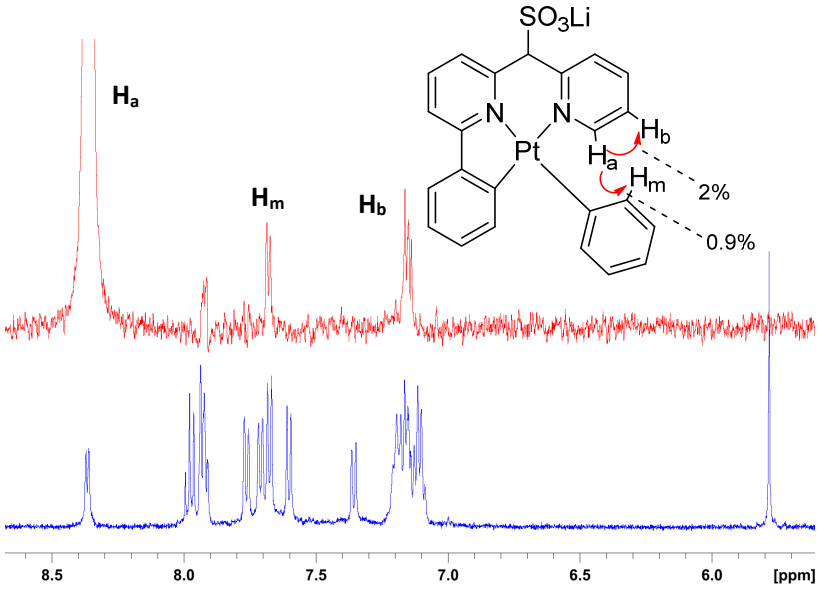

Figure S1. Red Trace - Selective irradiation of H_a in Li(12a) shows NOE coupling to neighboring protons H_m and H_b. Blue Trace – Normal ^{1}H-NMR spectrum of Li(12a) in TFE.

Synthesis of Li(13a) from Li(12a) via oxidation with O_2:

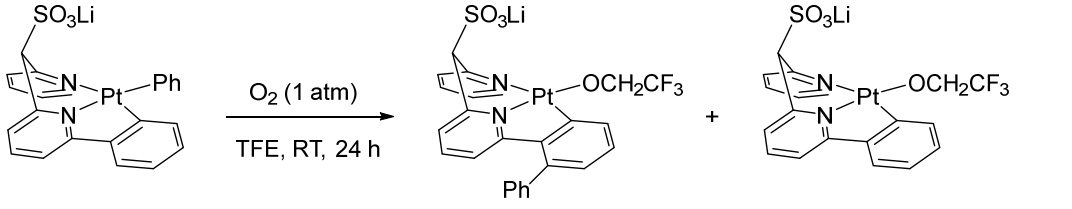

Li(**12a**) Li(**13a**), 80 % Li[(C$_6$H$_4$-dpms)Pt(OCH$_2$CF$_3$], 20%

In an argon filled glovebox, Li(**12a**) (4.0 mg, 6.6 µmol) was placed in vial along with 0.6 mL de-gassed TFE. Due to the low solubility of Li(**12a**) in TFE, not all solids dissolved and the mixture was passed through a Teflon syringe filter to give a yellow saturated TFE solution of Li(**12a**) (2.8 mM as measured by ^{1}H-NMR). The solution was transferred to a 25 mL Schlenk tube and the headspace flushed with O_2. After vigorously stirring for 1 day, an aliquot was taken, the solvent removed under vacuum, and the residue dissolved in DMSO-d_6. The ^{1}H-NMR spectrum showed two products, Li(**13a**) and [(C_6H_4-dpms)Pt(OCH_2CF_3)]$^-$, in an 8:2 ratio, respectively (Figure S2). The ^{1}H-NMR spectrum in TFE showed the same two products. An additional NOE experiment in TFE supports the assigned κ^3-CNN ligand arrangement (Figure S2).

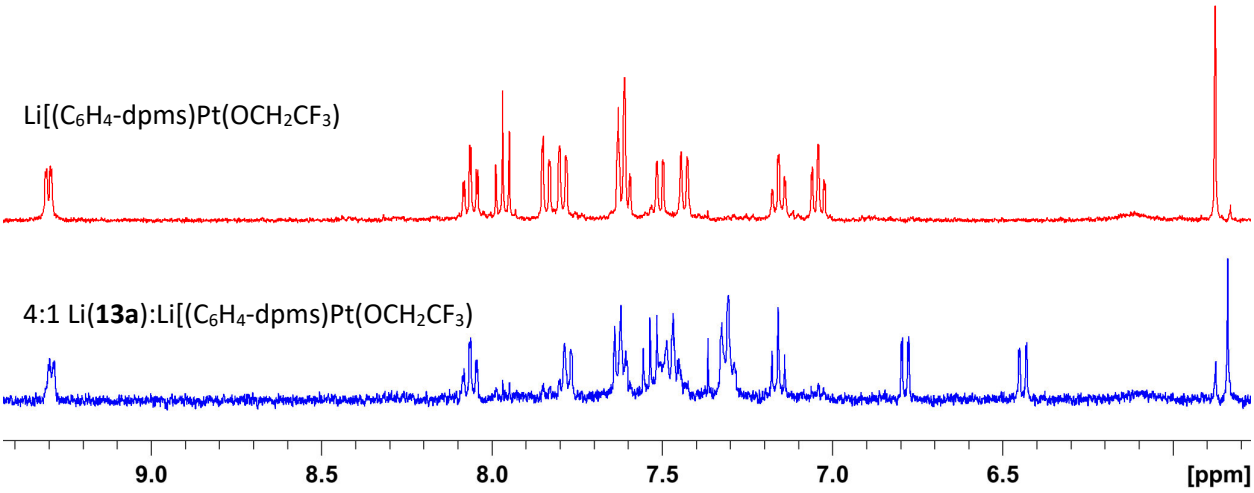

Figure S2. Red Trace – Independently synthesized Li[(C_6H_4-dpms)Pt(OCH_2CF_3)] in DMSO-d_6. Blue trace – 8:2 mixture of Li(**13a**) and Li[(C_6H_4-dpms)Pt(OCH_2CF_3] resulting from the oxidation of Li(**12a**) by O_2 in TFE.

Characterization data for Li(**13a**):

^{1}H NMR (400 MHz, 22 °C, DMSO-d_6), δ: 4.21 (two overlapping dq, 2H), 5.84 (s, 1H), 6.44 (dd, $^3J_{HH}$ = 8.4 Hz, $^4J_{HH}$ = 1.0 Hz, 1H), 6.79 (dd, $^3J_{HH}$ = 7.5 Hz, $^4J_{HH}$ = 1.3 Hz, 1H), 7.16 (t, $^3J_{HH}$ = 7.5 Hz, 1H), 7.31 (m, 3H), 7.44 – 7.56 (m, 4H), 7.62 (vt, $^3J_{HH}$ = 7.5 Hz, 1H), 7.78 (d, $^3J_{HH}$ = 7.8 Hz, 1H), 8.06 (ddd, $^3J_{HH}$ = 8.2, 7.5 Hz, $^4J_{HH}$ = 1.3 Hz, 1H), 9.29 (d, $^3J_{HH}$ = 5.9 Hz, 1H).

^{1}H NMR (400 MHz, 22 °C, MeOD), δ: 4.32 (dq, $^2J_{HH}$ = 10.8 Hz, $^3J_{HF}$ = 9.6 Hz, 1H), 4.41 (dq, $^2J_{HH}$ = 10.8 Hz, $^3J_{HH}$ = 9.6 Hz, 1H), 5.89 (s, 1H), 6.61 (d, $^3J_{HH}$ = 8.4 Hz, 1H), 6.84 (d, $^3J_{HH}$ = 7.5 Hz, 1H), 7.17 (vt, $^3J_{HH}$ = 8.0 Hz, 1H), 7.30 (vt, $^3J_{HH}$ = 7.5 Hz, 2H), 7.36 (d, $^3J_{HH}$ = 7.5, 1H), 7.39 – 7.50 (m, 5 H), 7.62 (vt, $^3J_{HH}$ =7.5 Hz, 1H), 7.67 (d, $^3J_{HH}$ = 7.5, 1H), 7.87 (d, $^3J_{HH}$ = 8.0 Hz, 1H), 8.07 (vt, $^3J_{HH}$ = 7.5 Hz, 1H), 9.41 (d, $^3J_{HH}$ = 5.6 Hz, 1H).

ESI-MS(-) of the crude reaction mixture containing both Li[**13a**] and Li[(C_6H_4-dpms)Pt(OCH_2CF_3)] in TFE, [**13a**]$^-$: 693.97. Calculated for [**12a**]$^-$: $C_{19}H_{14}F_3N_2O_4PtS$, 694.06.

4:1 mixture of Li(**13a**):Li[(C_6H_4-dpms)Pt(OCH_2CF_3)]

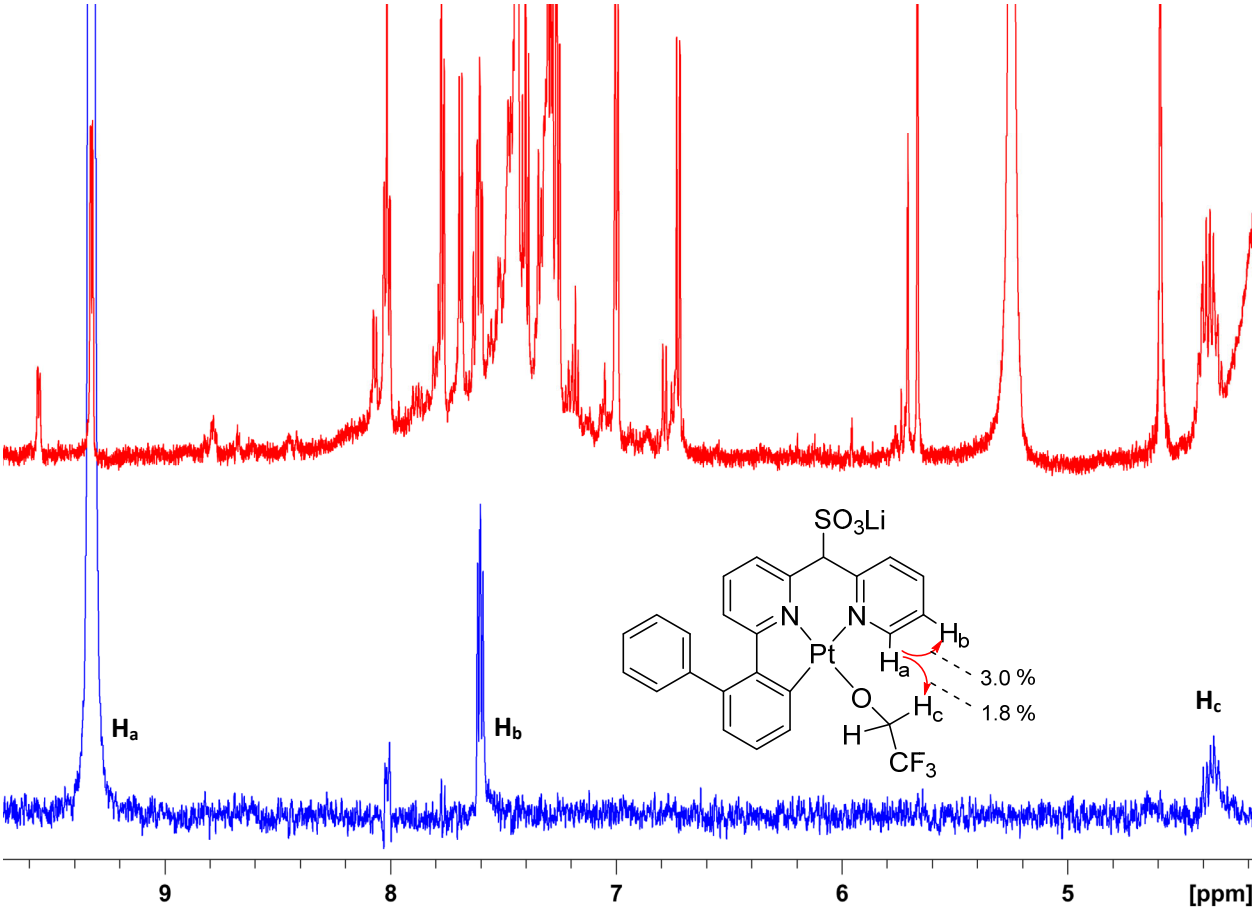

Figure S3. Red trace – Spectrum of aerobic oxidation product of Li(**12a**) in TFE showing 8:2 ratio of Li(**13a**) and Li[(C_6H_4-dpms)Pt(OCH_2CF_3)]. Blue trace – Selective irradiation of H_a in Li(**12a**) show NOE coupling to neighboring protons H_b and H_c.

Synthesis of Li(13a) from Li(12a) via oxidation with H_2O_2:

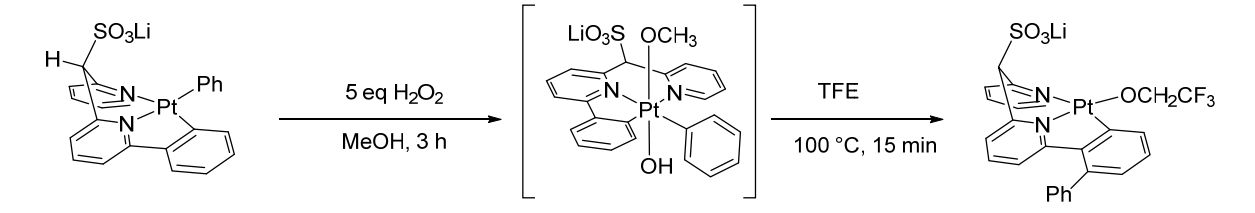

Li[(C_6H_4-dpms)PtPh], Li(**12a**) Li[(C_6H_4-dpms)Pt(Ph)(OH)(OCH_3)], **S2** Li[(Ph-C_6H_3-dpms)PtOCH_2CF_3], Li(**13a**)

Li(**12a**) (183mg, 0.303 mmol) was dissolved in 5 mL MeOH. While stirring, 0.155 mL of a 30% H_2O_2 (1.51 mmol, 5 eq.) solution was added. The color changed from yellow to murky white. After stirring for 3 h the methanol was removed in vacuo. The residue was stirred in 5 mL anhydrous DCM for 30 min and passed through a 20 µm Teflon syringe filter to produce a clear solution. The DCM was reduced in volume to ~ 1 mL and diluted with 3 mL hexanes to produce a white precipitate. The supernatant was decanted off and the residue washed with hexanes and then dried under high vacuum

to produce **S2** as an off-white powder (190 mg, 96%) which decomposes slowly at room temperature but is stable if stored in the freezer. The NMR and ESI-MS data are consistent with the proposed structure for **S2**, however the exact ligand arrangement might be different.

Characterization data for **S2**:

^{1}H NMR (400 MHz, 22 °C, MeOD), δ: 2.16 (s, $^{3}J_{PtH}$ = 40.5 Hz, 3H), 6.44 (s, 1H), 6.83 (dd, $^{3}J_{HH}$ = 8.0, $^{4}J_{HH}$ = 1.1 Hz, JPt-H = 41.9 Hz, 1H), 6.97 (ddd, $^{3}J_{HH}$ = 8.3, 7.1 Hz, $^{4}J_{HH}$ = 1.4 Hz, 1H), 7.17 (ddd, $^{3}J_{HH}$ = 8.3, 7.1 Hz, $^{4}J_{HH}$ = 1.1 Hz, 1H), 7.24 – 7.36 (m, 4H), 7.67 – 7.79 (m, $^{3}J_{PtH}$ = 30.7 Hz, 1H), 7.85 (dd, J = 7.9, 1.3 Hz, 1H), 7.95 (dd, J = 7.7, 0.7 Hz, 1H), 7.99 – 8.10 (m, 3H), 8.16 (t, $^{3}J_{HH}$ = 7.8 Hz, 1H), 8.32 (dd, $^{3}J_{HH}$ = 8.5 Hz, $^{4}J_{HH}$ = 0.8 Hz, 1H), 8.55 (dd, $^{3}J_{HH}$ = 5.8 Hz, $^{4}J_{HH}$ = 1.3 Hz, $^{3}J_{PtH}$ = 20.2 Hz, 1H).

^{13}C NMR (125 MHz, 22 °C, MeOD), δ: 56.6, 78.8, 120.7, 125.8, 126.1, 126.2, 126.5, 128.4, 128.6, 128.8, 128.9, 131.0, 131.6, 132.2, 132.7, 135.7, 137.6, 138.0, 140.1, 141.2, 143.6, 152.7, 154.0, 164.1.

ESI-MS(-) of a solution of in TFE, $[(C_6H_4\text{-dpms})Pt(Ph)(OH)(OCH_3)]^-$: 644.11. Calculated for $[(C_6H_4\text{-dpms})Pt(Ph)(OH)(OCH_3)]^-$: $C_{24}H_{21}N_2O_5PtS^-$, 644.08

Li[$(C_6H_4$-dpms)Pt(Ph)(OH)(OCH_3)], **S2**, (14.4 mg, 22.1 µmol) was dissolved in 0.6 mL TFE and heated at 100 °C for 15 min. Analysis of the ^{1}H-NMR in TFE showed Li[$(C_6H_4$-dpms)Pt(Ph)(OH)(OCH_3)] had been entirely consumed and a new complex, formed in 85 % NMR yield (as judged by the bridging methine C-H singlet), had appeared along with 1 eq. methanol (measured by integration of its 3.42 ppm singlet). The solution was passed through a 0.20 µm Teflon syringe filter and the solvent was removed to yield 15.4 mg Li(**13a**) as a yellow residue. Recrystallization from TFE with Et_2O yielded 10.1 mg Li(**13a**) as a yellow powder (65 % yield). The ^{1}H-NMR spectrum in MeOD and DMSO-d_6 matches that of the Li(**13a**) produced from the oxidation of Li(**12a**) by O_2 in TFE.

Synthesis of (Ph-C_6H_3-dpms)Pt(H_2O), 9a, and (Ph-C_6H_3-dpms)Pt(PPh_3), 10a:

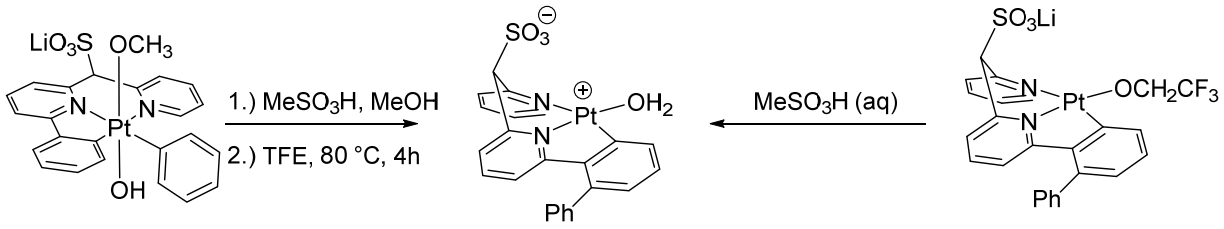

Li[$(C_6H_4$-dpms)Pt(Ph)(OH)(OCH_3)], **S2** **9a** Li(**13a**)

Li[$(C_6H_4$-dpms)Pt(Ph)(OH)(OCH_3)), **S2**, (224 mg, 0.344 mmol) was dissolved in 3 mL MeOH. To this solution was added 2.3 mL of a 0.150 M methanol solution of $MeSO_3H$ (1 eq.). A large amount of white precipitate formed almost immediately and, after swirling for ~20 seconds, was collected by filtration and washed with 2 mL cold MeOH. The collected solids were then dispersed in 3 mL TFE and transferred to a 25 mL Schlenk tube before being heated at 80 °C for 4 h. The resulting orange-yellow solution was passed through a 0.20 µm Teflon syringe filter and then dried to yield a yellow powder. In an argon filled glovebox, the powder was dissolved in a minimal amount of de-gassed TFE and recrystallized with H_2O to give **9a** as a yellow powder (181 mg, 86%). The ^{1}H-NMR analysis presented is of the **9a**-DMSO complex, formed upon dissolution of **9a** in DMSO-d_6.

^{1}H-NMR (400 MHz, 22 °C, DMSO-d6), δ: 6.25 (s, 1H), 6.63 (dd, $^3J_{HH}$ = 8.45 Hz, $^4J_{HH}$ = 1.0 Hz, 1H), 7.06 (dd, $^3J_{HH}$ = 7.4, $^4J_{HH}$ = 1.0 Hz, 1H), 7.19-7.31 (broad s, 1H), 7.28 (vt, $^3J_{HH}$ = 7.6 Hz, 1H), 7.32-7.41 (broad s, 1H), 7.48 (vt, $^3J_{HH}$ = 7.3 Hz, 1H), 7.49-7.57 (broad s, 1H), 7.58-7.66 (broad s, 1H), 7.65 (dd, $^3J_{HH}$ = 8.1, $^4J_{HH}$ = 1.0 Hz, 1H), 7.69 (ddd, $^3J_{HH}$ = 8.0, 5.5, $^3J_{HH}$ = 1.4 Hz, 1H), 7.77 (dd, $^3J_{HH}$ = 7.6, $^3J_{HH}$ = 1.1 Hz, 1H), 7.86 (vt, $^3J_{HH}$ = 7.9 Hz, 1H), 7.99 (d, $^3J_{HH}$ = 8.0 Hz, 1H), 8.25 (td, $^3J_{HH}$ = 7.5, $^4J_{HH}$ = 1.5 Hz, 1H), 9.07 (dd, $^3J_{HH}$ = 6.2, $^4J_{HH}$ = 1.0 Hz, 1H).

ESI-MS(-) of a solution of **9a** in TFE doped with KOH, [**9a**-H]$^-$: 612.03. Calculated for [**9a**-H]$^-$: $C_{23}H_{17}N_2O_4PtS$, 612.06.

Alternatively, **9a** could be produced from Li(**13a**):
In a vial, Li(**13a**) (8.3 mg, 12 µmol) was dissolved in 5 mL deionized H_2O. The pH was adjusted to ~2 with $MeSO_3H$, after which a large amount of precipitate was observed. The mixture was left in the fridge for ~18 h. The supernatant was then pipetted off and the solids washed with additional deionized H_2O to remove excess acid. The solids were then dried under high vacuum for 24 h. The solids were then dissolved in DMSO-d_6 and subsequent ^{1}H-NMR analysis showed **9a**-DMSO as the only species present.

Attempts to grow XRD quality crystals of **9a** were unsuccessful.
The PPh_3 derivative, **10a**, was synthesized by combining **9a** (22 mg, 36 µmol) in TFE with PPh_3 (10 mg, 38 µmol). Removal of solvent yielded an off-white powder that was washed with Et_2O to remove excess PPh_3. The residue was then dissolved in DCM, layered with ether, and placed in the freezer for 18 h to yield XRD quality crystals of PPh_3 derivative **10a**.

Synthesis of Na[(C_6H_4-dpms)Pt(OCH_2CF_3)]:

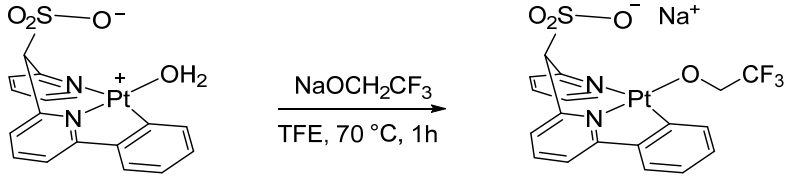

2 Na[(C_6H_4-dpms)Pt(OCH_2CF_3)]
Quantitative

In an argon filled glovebox, **4** (7.0 mg, 13 µmol) was dissolved in 1.0 mL dry, de-gassed TFE. To the orange-red solution was then added 59 µL of a 0.22 M stock solution of $NaOCH_2CF_3$ in TFE (1 eq. $NaOCH_2CF_3$). The solution became yellow in color. ^{1}H-NMR analysis showed two species in roughly equal concentration, presumed to be Na[(C_6H_4-dpms)Pt(OCH_2CF_3)] and the hydroxy analog, Na[(C_6H_4-dpms)Pt(OH)]. The solution was heated at 70 °C for 1 h, after which the only complex in solution was Na[(C_6H_4-dpms)Pt(OCH_2CF_3)] in quantitative yield as assessed using the solvent signal as an internal standard. The solvent was removed under vacuum and the residue dissolved in DMSO-d_6 for farther ^{1}H-NMR analysis.

^{1}H-NMR (400 MHz, 22 °C, TFE): 4.37 (m, overlapping w/ solvent peak), 5.72 (s, 1H), 7.20 (vt, $^3J_{HH}$ = 7.8 Hz, 1H), 7.31 (vt, $^3J_{HH}$ = 7.8 Hz, 1H), 7.42 (d, $^3J_{HH}$ = 7.8 Hz, 1H), 7.58 (d, $^3J_{HH}$ = 7.8 Hz, 1H), 7.62 (vt, $^3J_{HH}$ = 7.8 Hz, 1H), 7.73 (d, $^3J_{HH}$ = 8.5 Hz, 1H), 7.78 (d, $^3J_{HH}$ = 7.8 Hz, 1H), 7.90 (vt, $^3J_{HH}$ = 7.8 Hz, 1H), 8.02 (vt, $^3J_{HH}$ = 7.7 Hz, 1H), 9.32 (d, $^3J_{HH}$ = 5.9 Hz, 1H).

^{1}H-NMR (400 MHz, 22 °C, DMSO-d_6): 4.20 (two overlapping dq, $^{2}J_{HH}$ = 10.2 Hz, $^{3}J_{HF}$ = 9.9 Hz, 2H), 5.88 (s, 1H), 7.04 (ddd, $^{3}J_{HH}$ = 7.8, 7.5 Hz, $^{4}J_{HH}$ = 1.1 Hz, 1H), 7.16 (ddd, $^{3}J_{HH}$ = 7.8, 7.5 Hz, $^{4}J_{HH}$ = 1.1 Hz, 1H), 7.43 (dd, $^{3}J_{HH}$ = 7.5 Hz, $^{3}J_{HH}$ = 1.1 Hz, 1H), 7.51 (dd, $^{3}J_{HH}$ = 7.5 Hz, $^{4}J_{HH}$ = 0.9 Hz, 1H), 7.61 (m, 2H), 7.79 (d, $^{3}J_{HH}$ = 7.8 Hz, 1H), 7.84 (dd, $^{3}J_{HH}$ = 8.3 Hz, $^{4}J_{HH}$ = 1.1 Hz, 1H), 7.97 (vt, $^{3}J_{HH}$ = 8.3, 7.8 Hz, $^{4}J_{HH}$ = 1.6 Hz, 1H), 9.30 (dd, $^{3}J_{HH}$ = 5.8 Hz, $^{4}J_{HH}$ = 1.5 Hz, 1H).

^{13}C NMR (125 MHz, 22 °C, DMSO-d_6), δ: 76.1, 117.1, 122.7, 123.1, 123.2, 126.2, 128.4, 129.0, 131.7, 137.0, 137.2, 145.6, 146.0, 152.7, 153.1, 166.8. Two quaternary carbons could not be located due to the low S/N ratio.

ESI-MS(-) of a solution of Na[(C_6H_4-dpms)Pt(OCH_2CF_3)] in TFE, [(C_6H_4-dpms)Pt(OCH_2CF_3)]$^{-}$ = 618.07. Calculated for [(C_6H_4-dpms)Pt(OCH_2CF_3)]$^{-}$ $C_{19}H_{14}F_3N_2NaO_4PtS^{-}$, 618.02.

Synthesis of (C_6H_4-dpms)Pt^{IV}(Aryl)(OH) Complexes, 7a – 7h:

General Method A, 7a – 7e – Using electron rich arenes**:**

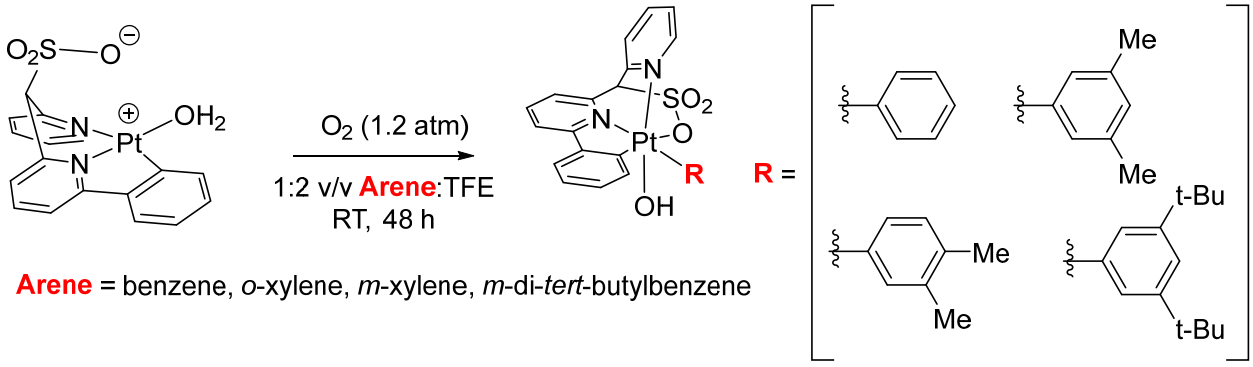

Arene = benzene, *o*-xylene, *m*-xylene, *m*-di-*tert*-butylbenzene

(C_6H_4-dpms)Pt(H_2O) (13.1 mg, 24.4 µmol) was weighed out into a 20 mL vial. Under air, TFE (2 mL) was added and the mixture swirled until all solids had dissolved. The appropriate arene (1 mL) was then added and the orange solution transferred to a 25 mL Schlenk tube along with a small Teflon coated stir bar. The Schlenk tube was pressurized with 1 atm O_2, bringing the total pO_2 to ~1.2 atm. The reaction was stirred vigorously for 2 days (*except in the case of *m*-di-*tert*-butylbenzene), showing a color change to deep red/purple over the first hour followed by a slow change to yellow throughout the remainder of the reaction. Some white cloudy precipitate could be observed after the first day.

*In the case that the arene was *m*-di-*tert*-butylbenzene, the reaction had to be continued for 7 days to see appreciable conversion due to immiscibility with TFE.

A 50 µL aliquot was removed, dried, and redissolved in DMSO-d_6 for subsequent ^{1}H-NMR analysis to determine the conversion and NMR yield of each product. To isolate the LPt^{IV}(Aryl) product, the solution was first doped with 100 µL of a stock solution of $KOCH_2CF_3$ in TFE (0.31 M, 1.3 eq.) and stirred for an additional few minutes. Avoiding this step results in the simultaneous elution of both Pt^{IV} products off the subsequent silica column. The solvent was then removed *in vacuo* leaving a red residue which was purified by column chromatography on silica (10:1 DCM:MeOH), producing the (C_6H_4-dpms)Pt^{IV}(Aryl)(OH) product as a white powder. Further purification was achieved by partially dissolving

the white powder in acetone and layering with pentanes. After being left in the freezer for 12 – 18 h, the supernatant was pipetted off and the white solid dried for 24 h under high vacuum at RT.

General Method B, 7f- 7g – Using electron poor arenes:

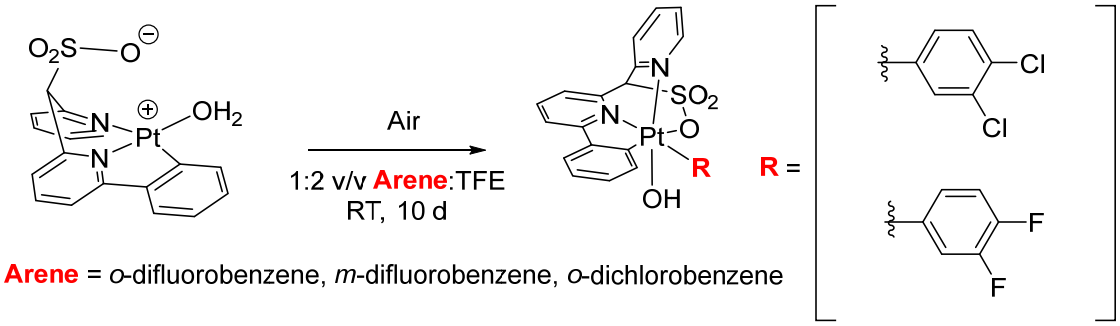

(C_6H_4-dpms)Pt(H_2O) (13.1 mg, 24.4 µmol) was weighed out into a 20 mL vial. Under air, TFE (2 mL) was added and the mixture swirled until all solids had dissolved. The appropriate arene (1 mL) was then added and the orange solution transferred to a 25 mL Schlenk tube along with a small Teflon coated stir bar. The reaction was then stirred vigorously for 10 days under air, showing a color change to deep red/purple over the first hour followed by a slow change to yellow throughout the remainder of the reaction. Some white cloudy precipitate could be observed after one week.

The workup and purification were the same as outlined in General Method A for (C_6H_4-dpms)Pt^{IV}(Aryl)(OH) complexes derived from electron rich arenes. The results are summarized in Table S1.

Table S1. Oxidation with O_2 of complex **4** in TFE : arene 2 : 1 (vol.) mixtures at 20 °C and 1 atm O_2.

Arene	Yield of **7**+**8**+**9** after 1 day[23]	**8** / **7** / **9** ratio
C_6H_6 **5a**, C_6D_6 **5b**	68%	1 / 1 / 0.1
1,2-$Me_2C_6H_4$ **5c**	73%	1 / 1 / 0.1
1,3-$Me_2C_6H_4$ **5d**	69%	1 / 1 / 0.1
1,3-*t*-$Bu_2C_6H_4$ **5e**	34%	1 / 1 / 0.1
1,2-$Cl_2C_6H_4$ **5f**	19%	1 /0.6 / -
1,2-$F_2C_6H_4$ **5g**	23%	1 /0.5 / -

(C_6H_4-dpms)Pt(C_6H_5)(OH), 7a:

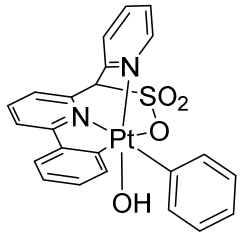

7a

The product was prepared according to General Method A, using C_6H_6 as the arene, Rf: 0.33. Isolated yield of **7a**: 3.0 mg, 20 %. Analysis by ^{13}C-NMR was carried out by combining **7a** and **7b** (in approximately 0.25:0.75 ratio) in order to achieve a high enough concentration. ^{1}H NOE and COSY experiments provided a full proton assignment for **7a** in DMSO-d_6 and are consistent with the solid state structure (Figure S4).

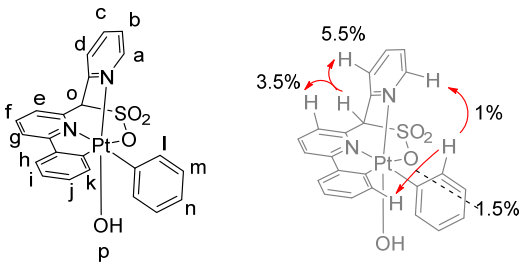

Figure S4. Left – proton assignment for ^{1}H-NMR analysis of **7a**. Right – Spin-spin coupling percentages derived from NOE experiments.

^{1}H NMR (600 MHz, 22 °C, DMSO-d_6), δ: 0.52 (s, 1H$_p$), 6.83 (s, 1H$_o$), 7.08 (dd, $^3J_{HH}$ = 7.8 Hz, $^4J_{HH}$ = 1.4 Hz, 2H$_l$), 7.12 – 7.17 (m, 3H = 2H$_m$ + 1H$_n$), 7.20 (ddd, $^3J_{HH}$ = 7.7, 7.5 Hz, $^4J_{HH}$ = 1.7 Hz, 1H$_j$), 7.27 (ddd, $^3J_{HH}$ = 8.4, 7.5 Hz, $^4J_{HH}$ = 1.1 Hz, 1H$_i$), 7.33 (dd, $^3J_{HH}$ = 7.7 Hz, $^4J_{HH}$ = 1.1 Hz, 1H$_k$), 7.55 (ddd, $^3J_{HH}$ = 7.5, 6.6 Hz, $^4J_{HH}$ = 1.5 Hz, 1H$_b$), 7.87 (dd, $^3J_{HH}$ = 7.0 Hz, $^4J_{HH}$ = 1.6 Hz, 1H$_e$), 7.92 (dd, $^3J_{HH}$ = 7.5 Hz, $^4J_{HH}$ = 1.6 Hz, 1H$_h$), 8.05 (dd, $^3J_{HH}$ = 7.9 Hz, $^4J_{HH}$ = 1.1 Hz, H$_d$), 8.26 (ddd, $^3J_{HH}$ = 8.3, 7.6 Hz, $^4J_{HH}$ = 1.4 Hz, 1H$_c$), 8.28 – 8.32 (m, 2H = H$_f$ + H$_g$), 8.46 (dd, $^3J_{HH}$ = 5.8 Hz, $^4J_{HH}$ = 1.6 Hz, $^3J_{HPt}$ = 26.5 Hz, 1H$_a$).

^{1}H NMR (600 MHz, 22 °C, TFE-d_1), δ: 6.18 (s, 1H), 7.12 (d, $^3J_{HH}$ = 6.9 Hz, 2H), 7.25 (m, 3H), 7.31 (dd, $^3J_{HH}$ = 7.0, 6.8 Hz, 1H), 7.33 (dd, $^3J_{HH}$ = 7.5, 6.8 Hz, 1H), 7.38 (dd, $^3J_{HH}$ = 7.7, 6.7 Hz, 1H), 7.51 (d, $^3J_{HH}$ = 7.9 Hz, 1H), 7.73 (dd, $^3J_{HH}$ = 7.8 Hz, $^4J_{HH}$ = 1.2 Hz, 1H), 7.76 (d, $^3J_{HH}$ = 7.6 Hz, 1H), 7.89 (d, $^3J_{HH}$ = 8.0 Hz, 1H), 7.99 (d, $^3J_{HH}$ = 8.2 Hz, 1H), 8.10 (ddd, $^3J_{HH}$ = 8.2, 7.8 Hz, $^4J_{HH}$ = 1.2 Hz, 1H), 8.13 (dd, $^3J_{HH}$ = 8.7, 8.0 Hz, 1H), 8.46 (d, $^3J_{HH}$ = 5.6 Hz, 1H).

^{13}C-NMR (151 MHz, 22 °C, DMSO-d_6), δ: 72.2, 120.0, 123.6, 124.9, 125.1, 126.1, 126.2, 127.0, 127.2, 129.4, 130.1, 131.5, 132.2, 133.8, 134.3, 137.1, 142.6, 142.9, 143.8, 151.0, 152.9, 153.2, 160.0.

ESI(+)-MS of **7a** in TFE/H_2O doped with dilute HBF_4 [**7a**+H]$^+$: 614.14. Calculated for [**7a**+H]$^+$: $C_{23}H_{19}N_2O_4PtS$, 614.07.

(C_6H_4-dpms)Pt(C_6D_5)(OH), 7b:

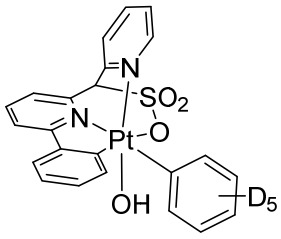

7b

The product was prepared according to General Method A, using C_6D_6 as the arene, Rf:0.33. Isolated yield of **7b**: 3.3 mg, 24 %. Isolated samples of **7b** consistently had a ~15% proton incorporation into the phenyl ring, likely originating from H/D exchange between C_6D_6 and TFE prior to oxidation.

^{1}H NMR (600 MHz, 22 °C, TFE-d_1), δ: 6.18 (s, 1H), 7.25 (dd, $^3J_{HH}$ = 8.7, 7.4 Hz, 1H), 7.33 (dd, $^3J_{HH}$ = 7.5, 6.8 Hz, 1H), 7.38 (dd, $^3J_{HH}$ = 7.7, 6.7 Hz, 1H), 7.51 (d, $^3J_{HH}$ = 7.9 Hz, 1H), 7.73 (dd, $^3J_{HH}$ = 7.8 Hz, $^4J_{HH}$ = 1.2 Hz, 1H), 7.76 (d, $^3J_{HH}$ = 7.6 Hz, 1H), 7.89 (d, $^3J_{HH}$ = 8.0 Hz, 1H), 7.99 (d, $^3J_{HH}$ = 8.2 Hz, 1H), 8.10 (ddd, $^3J_{HH}$ = 8.2, 7.8 Hz, $^4J_{HH}$ = 1.2 Hz, 1H), 8.13 (dd, $^3J_{HH}$ = 8.7, 8.0 Hz, 1H), 8.46 (d, $^3J_{HH}$ = 5.6 Hz, 1H).

^{13}C-NMR (151 MHz, 22 °C, DMSO-d_6), δ: 72.2, 120.0, 123.6, 124.9, 125.1, 126.1, 126.2, 127.0, 127.2, 129.4, 130.1, 131.5, 132.2, 133.8, 134.3, 137.1, 142.6, 142.9, 143.8, 151.0, 152.9, 153.2, 160.0.

ESI(+)-MS of **7b** in TFE/H_2O doped with dilute HBF_4 [**7b**+H]$^+$: 619.08. Calculated for [**7b**+H]$^+$: $C_{23}H_{14}D_5N_2O_4PtS$, 619.10.

(C_6H_4-dpms)Pt(3,4-dimethylphenyl)(OH), 7c:

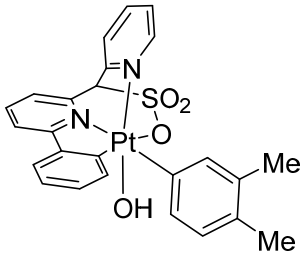

7c

Product was prepared according to General Method A, using *o*-xylene as the arene, Rf: 0.32. Samples of the crude reaction mixture in DMSO-d_6 showed that **7c** is the major LPt^{IV}(Aryl) isomer by no less than 85 %. Isolated Yield: 5.0 mg, 32 %.

^{1}H NMR (600 MHz, 22 °C, DMSO-d_6) δ: 0.32 (s, 1H), 2.17 (s, 3H), 2.22 (s, 3H), 6.73 (dd, $^3J_{HH}$ = 8.0 Hz, $^4J_{HH}$ = 1.6 Hz, 1H), 6.85 (s, 1H), 6.85 (d, $^3J_{HH}$ = 8.6 Hz, 1H), 6.90 (d, $^3J_{HH}$ = 8.0 Hz, 1H), 7.18 (ddd, $^3J_{HH}$ = 8.1, 7.6 Hz, $^4J_{HH}$ = 1.5 Hz, 1H), 7.25 (ddd, $^3J_{HH}$ = 8.1, 7.4 Hz, $^4J_{HH}$ = 1.1 Hz, 1H), 7.33 (dd, $^3J_{HH}$ = 8.0 Hz, $^4J_{HH}$ = 1.1 Hz, 1H), 7.54 (ddd, $^3J_{HH}$ = 7.8, 6.8 Hz, $^4J_{HH}$ = 1.4 Hz), 7.86 (dd, $^3J_{HH}$ = 7.2 Hz, $^4J_{HH}$ = 1.2 Hz, 1H), 7.91 (dd, $^3J_{HH}$ = 7.5 Hz, $^4J_{HH}$ = 1.6 Hz, 1H), 8.04 (dd, $^3J_{HH}$ = 7.9 Hz, $^4J_{HH}$ = 1.2 Hz, 1H), 8.25 (ddd, $^3J_{HH}$ = 8.3, 7.7 Hz, $^4J_{HH}$ = 1.7 Hz, 1H), 8.26 – 8.31 (m, 2H), 8.47 (dd, $^3J_{HH}$ = 5.8 Hz, $^4J_{HH}$ = 1.4 Hz, 1H).

^{1}H NMR (600 MHz, 22 °C, CF_3CH_2OD), δ: 2.26 (s, 3H), 2.30 (s, 3H), 6.17 (s, 1H), 6.77 (d, $^3J_{HH}$ = 7.4 Hz, 1H), 6.91 (s, 1H), 7.25 (dd, $^3J_{HH}$ = 9.0, 8.0 Hz, 1H), 7.32 (dd, $^3J_{HH}$ = 8.0, 7.5 Hz, 1H), 7.37 (dd, $^3J_{HH}$ = 7.9, 6.9 Hz,

1H), 7.53 (d, $^3J_{HH}$ = 8.0 Hz, 1H), 7.73 (d, $^3J_{HH}$ = 7.5 Hz, 1H), 7.75 (d, $^3J_{HH}$ = 7.7 Hz, 1H), 7.88 (d, $^3J_{HH}$ = 7.7 Hz, 1H), 7.99 (d $^3J_{HH}$ = 8.2 Hz, 1H), 8.09 (dd, $^3J_{HH}$ = 8.1, 7.5 Hz, 1H), 8.13 (dd, $^3J_{HH}$ = 8.6, 8.0 Hz, 1H), 8.49 (d, $^3J_{HH}$ = 5.6 Hz, 1H).

ESI(+)-MS of **7c** in TFE/H_2O doped with dilute HBF_4 [**7c**+H]$^+$: 642.11. Calculated for [**7c**+H]$^+$: $C_{25}H_{23}N_2O_4PtS$, 642.10.

(C_6H_4-dpms)Pt(3,5-dimethylphenyl)(OH), 7d:

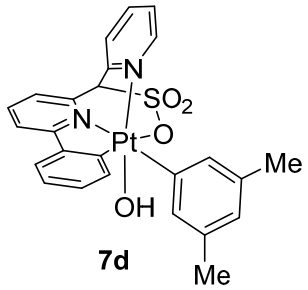

7d

Product was prepared according to General Method A, Rf: 0.36. Samples of the crude reaction mixture in DMSO-d_6 showed that **7d** is the major LPt^{IV}(Aryl) isomer by no less than 90 %. Isolated yield: 27 %.

^{1}H NMR (600 MHz, 22 °C, DMSO-d_6) δ: 0.34 (s, 1H), 2.21 (s, 6H), 6.67 (brs, 2H), 6.81 (s, 1H), 6.86 (s, 1H), 7.18 (ddd, $^3J_{HH}$ = 8.3, 7.6 Hz, $^4J_{HH}$ = 1.5 Hz, 1H), 7.25 (ddd, $^3J_{HH}$ = 7.4, 7.2 Hz, $^4J_{HH}$ = 1.1 Hz, 1H), 7.32 (dd, $^3J_{HH}$ = 8.0 Hz, $^4J_{HH}$ = 1.1 Hz, 1H), 7.55 (ddd, $^3J_{HH}$ = 7.0, 6.8 Hz, $^4J_{HH}$ = 1.4 Hz, 1H), 7.86 (dd, $^3J_{HH}$ = 7.1 Hz, $^4J_{HH}$ = 1.4 Hz, 1H), 7.91 (dd, $^3J_{HH}$ = 7.6 Hz, $^4J_{HH}$ = 1.6 Hz, 1H), 8.04 (dd, $^3J_{HH}$ = 7.9 Hz, $^4J_{HH}$ = 1.1 Hz, 1H), 8.26 (ddd, $^3J_{HH}$ = 8.1, 7.8 Hz, $^4J_{HH}$ = 1.6 Hz, 1H), 8.26 – 8.30 (m, 2H), 8.47 (dd, $^3J_{HH}$ = 5.9, $^4J_{HH}$ = 1.9 Hz, 1H).

^{1}H NMR (600 MHz, 22 °C, CF_3CH_2OD), δ: 2.28 (s, 6H), 6.16 (s, 1H), 6.72 (s, 2H), 6.99 (s, 1H), 7.25 (dd, $^3J_{HH}$ = 8.5, 7.6 Hz, 1H), 7.32 (dd, $^3J_{HH}$ = 7.7, 7.5 Hz, 1H), 7.38 (dd, $^3J_{HH}$ = 7.8, 7.2 Hz, 1H), 7.52 (d, $^3J_{HH}$ = 8.0 Hz, 1H), 7.72 (d, $^3J_{HH}$ = 8.0 Hz, 1H), 7.75 (d, $^3J_{HH}$ = 7.8 Hz, 1H), 7.88 (d $^3J_{HH}$ = 7.8 Hz, 1H), 7.99 (d, $^3J_{HH}$ = 8.0 Hz, 1H), 8.09 (ddd, $^3J_{HH}$ = 8.4, 8.0 Hz, $^4J_{HH}$ = 1.1 Hz, 1H), 8.13 (dd, $^3J_{HH}$ = 9.0, 8.0 Hz), 8.48 (d, $^3J_{HH}$ = 5.8 Hz, 1H).

ESI(+)-MS of **7d** in TFE/H_2O doped with dilute HBF_4 [**7d**+H]$^+$: 642.00. Calculated for [**7d**+H]$^+$: $C_{25}H_{23}N_2O_4PtS$, 642.10.

(C_6H_4-dpms)Pt(3,5-di-*tert*-butylphenyl)(OH), 7e:

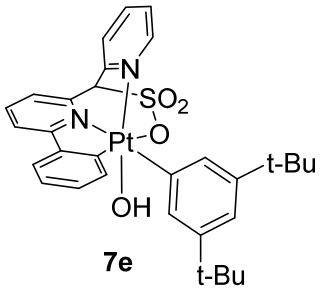

7e

The product was prepared according to General Method A (except with a longer reaction time of one week) using *m*-di-*tert*-butylbenzene (which is immiscible in TFE) as the arene, Rf: 0.38. Samples of the crude reaction mixture in DMSO-d_6 showed that **7e** is the only visible LPt^{IV}(Aryl) isomer.

Yield: 5.1 mg, 29 %.

^{1}H NMR (600 MHz, 22 °C, DMSO-d_6) δ: 0.43 (s, 1H), 1.23 (s, 18H), 6.86 (s, 1H), 6.90 (brs, 2H), 7.15 – 7.20 (m, 2H), 7.26 (ddd, $^3J_{HH}$ = 8.0, 7.5 Hz, $^4J_{HH}$ = 1.0 Hz, 1H), 7.37 (dd, $^3J_{HH}$ = 8.0 Hz, $^4J_{HH}$ = 1.0 Hz, 1H), 7.53 (ddd, $^3J_{HH}$ = 7.7, 6.7 Hz, $^4J_{HH}$ = 1.4 Hz, 1H), 7.88 (dd, $^3J_{HH}$ = 7.4 Hz, $^4J_{HH}$ = 1.1 Hz, 1H), 7.93 (dd, $^3J_{HH}$ = 7.8 Hz, $^4J_{HH}$ = 1.6 Hz, 1H), 8.04 (dd, $^3J_{HH}$ = 8.0 Hz, $^4J_{HH}$ = 1.1 Hz, 1H), 8.26 (ddd, $^3J_{HH}$ = 8.3, 7.9 Hz, $^4J_{HH}$ = 1.6 Hz, 1H), 8.28 (dd, $^3J_{HH}$ = 8.3, 7.7 Hz, 1H), 8.30 (ddd, $^3J_{HH}$ = 8.3, 8.3 Hz, $^4J_{HH}$ = 1.1 Hz, 1H), 8.39 (dd, $^3J_{HH}$ = 5.8 Hz, $^4J_{HH}$ = 1.5 Hz, 1H).

^{1}H NMR (600 MHz, 22 °C, CF_3CH_2OD), δ: 1.30 (s, 18H), 6.16 (s, 1H), 6.98 (bs, 2H), 7.25 (dd, $^3J_{HH}$ = 8.4, 7.4 Hz, 1H), 7.33 (dd, $^3J_{HH}$ = 7.8, 7.4 Hz, 1H), 7.35 (dd, $^3J_{HH}$ = 7.4, 7.3 Hz, 1H), 7.48 (s, 1H), 7.58 (d, $^3J_{HH}$ = 8.0 Hz, 1H), 7.74 (dd, $^3J_{HH}$ = 7. Hz, $^4J_{HH}$ = 0.9 Hz, 1H), 7.76 (d, $^3J_{HH}$ = 7.6 Hz, 1H), 7.88 (d, $^3J_{HH}$ = 8.0 Hz, 1H), 8.00 (d, $^3J_{HH}$ = 8.0 Hz, 1H), 8.09 (ddd, $^3J_{HH}$ = 8.4, 8.5 Hz, $^4J_{HH}$ = 1.0 Hz, 1H), 8.13 (dd, $^3J_{HH}$ = 8.4, 8.0 Hz, 1H), 8.45 (d, $^3J_{HH}$ = 5.5 Hz, 1H).

ESI(+)-MS of **7e** in TFE/H_2O doped with dilute HBF_4 [**7e**+H]$^+$: 726.21. Calculated for [**7e**+H]$^+$: $C_{31}H_{35}N_2O_4PtS$, 726.20.

(C_6H_4-dpms)Pt(3,4-dichlorophenyl)(OH), 7f:

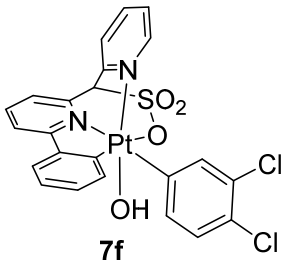

7f

The product was prepared according to General Method B using *o*-dichlorobenzene as the arene, Rf: 0.36. Samples of the crude reaction mixture in DMSO-d_6 showed that **7f** is the major LPt^{IV}(Aryl) isomer by no less than 90 %. Isolated yield: 3.2 mg, 19 %.

^{1}H NMR (600 MHz, 22 °C, DMSO-d_6) δ: 1.14 (brs, 1H), 6.90 (s, 1H), 7.00 (dd, $^3J_{HH}$ = 8.3 Hz, $^4J_{HH}$ = 2.0 Hz, 1H), 7.21 (m, 1H), 7.24 – 7.30 (m, 3H), 7.42 (d, $^3J_{HH}$ = 8.4 Hz, 1H), 7.57 (ddd, $^3J_{HH}$ = 7.6, 6.7 Hz, $^4J_{HH}$ = 1.4

Hz, 1H), 7.87 (dd, $^3J_{HH}$ = 6.5 Hz, $^4J_{HH}$ = 2.0 Hz, 1H), 7.93 (dd, $^3J_{HH}$ = 7.8Hz, $^4J_{HH}$ = 1.6 Hz, 1H), 8.07 (dd, $^3J_{HH}$ = 7.9 Hz, $^4J_{HH}$ = 1.2 Hz, 1H), 8.28 (ddd, $^3J_{HH}$ = 7.9, 7.9 Hz, $^4J_{HH}$ = 1.6 Hz, 1H), 8.27 – 8.32 (m, 2H), 8.55 (dd, $^3J_{HH}$ = 5.8 Hz, $^4J_{HH}$ = 1.1 Hz, 1H).

^{1}H NMR (600 MHz, 22 °C, CF_3CH_2OD), δ: 6.20 (s, 1H), 6.98 (dd, $^3J_{HH}$ = 8.4 Hz, $^4J_{HH}$ = 1.8 Hz, 1H), 7.27 (m, 2H), 7.34 (m, 2H), 7.39 (d, $^3J_{HH}$ = 8.0 Hz, 1H), 7.42 (dd, $^3J_{HH}$ = 7.4, 7.0 Hz, 1H), 7.74 (d, $^3J_{HH}$ = 7.6 Hz, 1H), 7.77 (d, $^3J_{HH}$ = 7.77 Hz, 1H), 7.94 (d, $^3J_{HH}$ = 7.9 Hz, 1H), 7.99 (d, $^3J_{HH}$ = 8.4 Hz, 1H), 8.13 (m, 2H), 8.41 (d, $^3J_{HH}$ = 5.7 Hz, 1H).

ESI(+)-MS of **7f** in TFE/H_2O doped with dilute HBF_4 [**7f**+H]$^+$: 650.02. Calculated for [**7f**+H]$^+$: 682.06. $C_{23}H_{17}Cl_2N_2O_4PtS$, 681.99.

(C_6H_4-dpms)Pt(3,4-difluorophenyl)(OH), 7g:

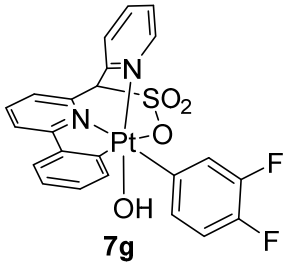

7g

The product was prepared according to General Method B using *o*-difluorobenzene as the arene, Rf: 0.25. Samples of the crude reaction mixture in DMSO-d_6 showed that **7g** is the major LPt^{IV}(Aryl) isomer by no less than 66 %. A third bridging methine singlet was observed, not attributable to **7g** nor **8,** present in half the amount of **7g,** and may be attributable to a second LPt^{IV}(Aryl) isomer derived from C-H activation *ortho* to a C-F bond on *o*-difluorobenzene (Figure S5).

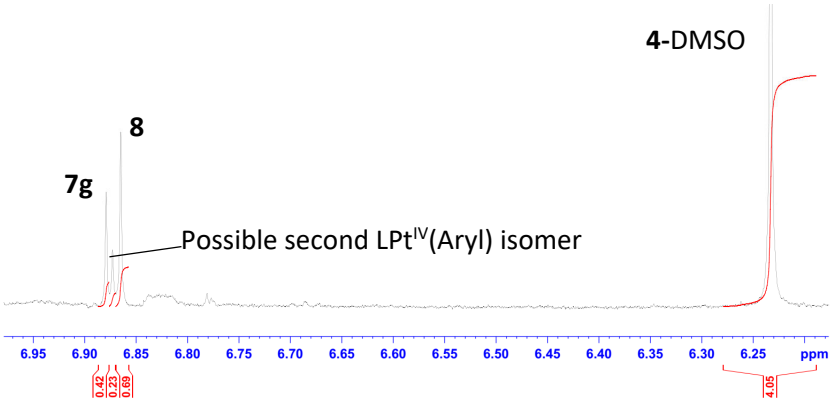

Figure S5. Bridging methine C-H region of ^{1}H-NMR spectrum derived from the crude reaction mixture from the reaction of **4** with O_2 in 1:2 *o*-difluorobenzene:TFE mixture, dissolved in DMSO-d_6 showing **7g**, **4**-DMSO, and the possible second LPt^{IV}(Aryl) isomer.

Isolated yield: 2.3 mg, 14 %.

^{1}H NMR (600 MHz, 22 °C, DMSO-d_6) δ: 1.06 (s, 1H), 6.82 (m, 1H), 6.89 (s, 1H), 7.02 (ddd, $^3J_{HH(F)}$ = 11.3, 8.4 Hz, $^4J_{HH}$ = 1.9 Hz, 1H), 7.20 – 7.30 (m, 4H), 7.57 (ddd, $^3J_{HH}$ = 7.2, 6.7 Hz, $^4J_{HH}$ = 1.5 Hz, 1H), 7.87 (dd, $^3J_{HH}$ =

6.8 Hz, $^{4}J_{HH}$ = 1.8 Hz, 1H), 7.93 (dd, $^{3}J_{HH}$ = 7.88, $^{4}J_{HH}$ = 1.3 Hz, 1H), 8.06 (dd, $^{3}J_{HH}$ = 7.8 Hz, $^{4}J_{HH}$ = 1.4, 1H), 8.27 (ddd, $^{3}J_{HH}$ = 7.8, 7.8 Hz, $^{4}J_{HH}$ = 1.6 Hz, 1H), 8.27 – 8.32 (m, 2H), 8.52 (dd, $^{3}J_{HH}$ = 5.9 Hz, $^{4}J_{HH}$ = 1.5 Hz).

^{1}H NMR (600 MHz, 22 °C, CF_3CH_2OD), δ: 6.20 (s, 1H), 6.85 (m, 1H), 6.98 (ddd, $^{3}J_{HH(F)}$ = 11.3, 8.5 Hz, $^{4}J_{HH}$ = 1.9 Hz, 1H), 7.10 (m, 1H), 7.27 (ddd, $^{3}J_{HH}$ = 8.8, 7.9 Hz, $^{4}J_{HH}$ = 1.3 Hz, 1H), 7.34 (dd, $^{3}J_{HH}$ = 7.8, 7.4 Hz, 1H), 7.42 (m, 2H), 7.74 (dd, $^{3}J_{HH}$ = 7.7 Hz, $^{4}J_{HH}$ = 1.2 Hz, 1H), 7.77 (d, $^{3}J_{HH}$ = 7.6 Hz, 1H), 7.91 (d, $^{3}J_{HH}$ = 7.9 Hz, 1H), 7.99 (d, $^{3}J_{HH}$ = 8.1 Hz, 1H), 8.12 (ddd, $^{3}J_{HH}$ = 8.0, 7.7 Hz, $^{4}J_{HH}$ = 1.3 Hz, 1H), 8.15 (dd, $^{3}J_{HH}$ = 7.9, 7.0 Hz, 1H), 8.42 (d, $^{3}J_{HH}$ = 5.9 Hz, 1H).

^{19}F NMR (376 Mhz, 22 °C, Acetone-d_6), δ: -146.5 (m, 1F), -142.0 (m, 1F).

ESI(+)-MS of **7g** in TFE/H_2O doped with dilute HBF_4 [**7g**+H]$^{+}$: 650.02. Calculated for [**7g**+H]$^{+}$: $C_{23}H_{17}F_2N_2O_4PtS$, 650.05.

IV. Reaction of $(C_6H_4\text{-dpms})Pt^{II}(H_2O)$, 4, with O_2 in TFE

a. Long-term monitoring of the reaction between [4] and O_2 in wet TFE:

$(C_6H_4\text{-dpms})Pt(H_2O)$, **4**, (4.0 mg, 7.4 μmol) was dissolved in 0.55 mL anhydrous TFE and then doped with 50 μL of a 2.0 M solution of H_2O in TFE. The yellow solution was transferred to a sealable NMR J-Young tube along with a sealed capillary containing D_2O for locking and shimming purposes. After initial analysis by ^{1}H-NMR, the tube was pressurized with O_2 and analyzed periodically by ^{1}H-NMR. The solution became dark purple-red over the course of 0.5 h and then gradually changed to light yellow over the next 7 days. A very small amount of white precipitate could be observed after the first week of analysis. The starting material, **4**, along with the Pt(IV) product **8** and the adduct **11** (which is derived from the reversible reaction between **4** and **8**) were tracked via their diagnostic bridging C-H singlets (Fig. S6a).

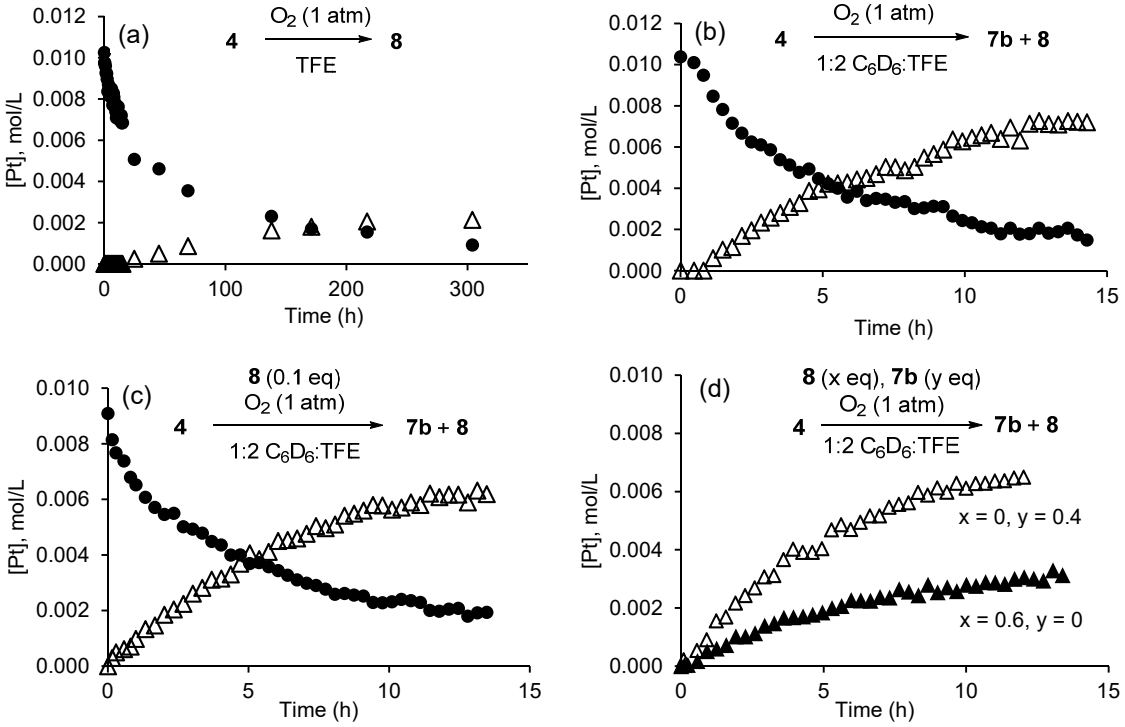

Figure S6. The reaction profile for the oxidation of ~10 mM complex **4** (filled circles) with O_2 to produce Pt^{IV} complexes **7b** and **8** (triangles): a) in wet TFE; b)-d) in wet benzene – TFE mixture (1 : 2, vol.), b) no additives, c) 0.1 eq of **8** added in the beginning, d) 0.6 eq of **8** (filled triangles) vs 0.4 eq of **7b** (open triangles) added in the beginning. The values [**7b**] + [**8**] shown exclude **7b** and/or **8** added in the beginning in the experiments c), b) and d). $[H_2O]$ = 0.150 M and pO_2 = 1 atm in all cases.

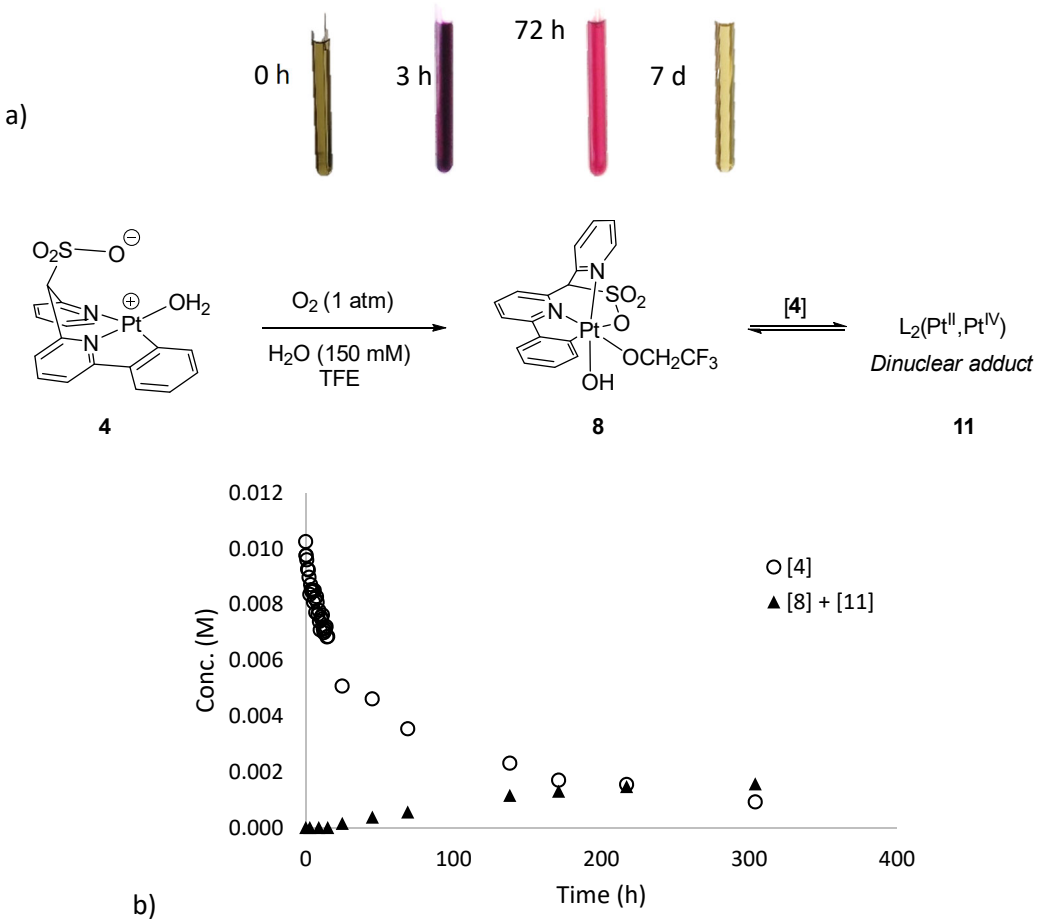

Figure S7. a) Colors of solution of **4** (12.4 µmol) in TFE exposed to O_2 (1 atm) at 0h, 3 h, 72 h, and 1 week. b) Reaction profile showing the consumption of **4** and production of LPt(IV) products (**8** and **11**).

Notable changes to our previous work. First, in our previous work [2] we used DMSO-d_6 as an NMR solvent to follow progress of the 1st reaction in Fig. S7 by ^{1}H NMR after removing TFE solvent form a reaction mixture aliquot. Later we have found that DMSO efficiently and rapidly destroys the paramagnetic intermediates so that their actual contribution to the reaction mass balance was underestimated/unknown to us at that time. Second, the 1st reaction in Fig. S7 was claimed to proceed only under ambient light. Later this conclusion was recognized as one resulting from the presence of some specific impurities in the starting material. The reaction with pure complex **4** does not require light.

b. Reversibility of the initial reaction between [4] and O_2 in TFE:

(C_6H_4-dpms)Pt(H_2O), **4**, (4.0 mg, 7.4 μmol) was dissolved in 0.60 mL anhydrous TFE-d_1 and then transferred to a sealable NMR J-Young tube along with a sealed capillary tube filled with D_2O for locking and shimming purposes. After initial analysis by ^{1}H-NMR, the tube was pressurized with 1 atm pO_2 and monitored for 3 h, during which time the mole % of **4** fell from 37 % to 12 % while the appearance of only one NMR visible intermediate, **S3**, was observed which rose to 10 mole %. The other species, present in the initial mixture is LPt(TFE) which gives rise to broad peaks and made up the other 63 % of total LPt^{II} in solution. Upon addition of O_2, the ^{1}H-NMR peaks corresponding to LPt(TFE) quickly broaden so as to become unintegrable (Figure S6). Assuming that LPt(TFE) and **4** are in fast equilibrium (compared to the initial reaction with O_2), then the total NMR visible content in solution may be assumed to have fallen by 40 %.

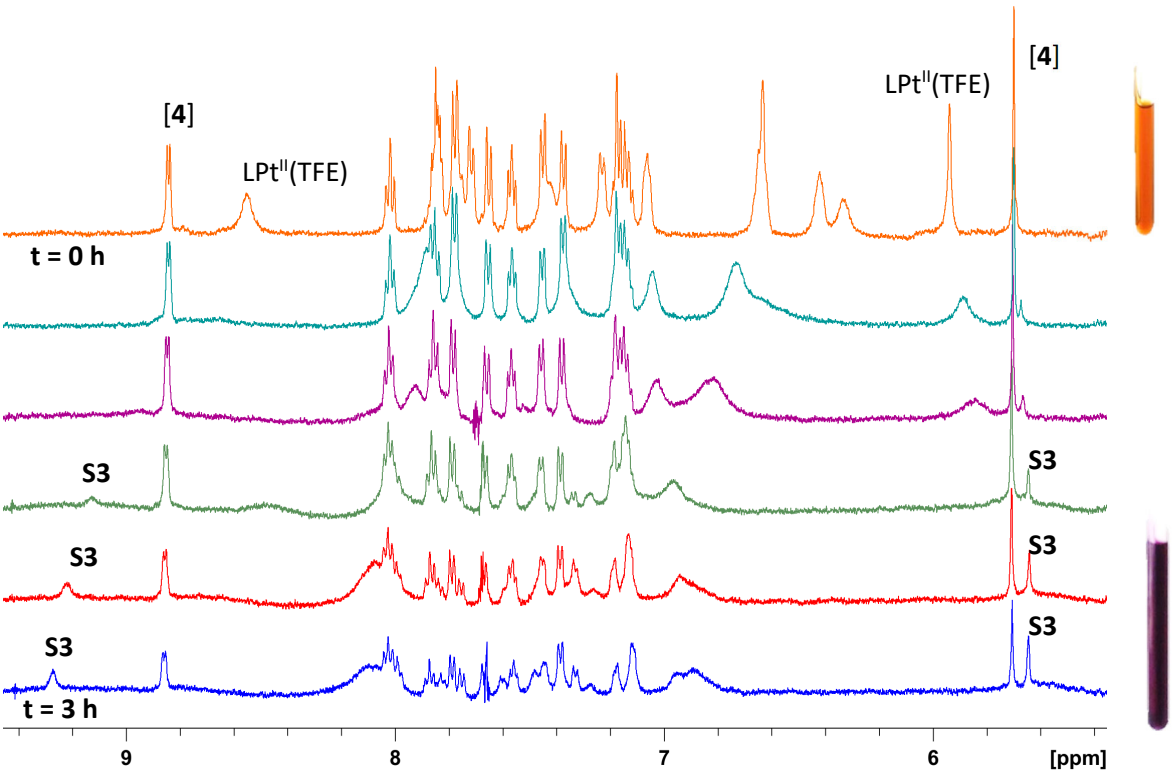

Figure S6. ^{1}H-NMR spectra showing the first 3 h of the reaction between **4** and O_2 in anhydrous TFE-d_1. The top trace is t = 0h while the bottom trace is t = 3 h, taken in 0.6 h increments. On the right, the color of solution is shown.

After 3 h, the now purple solution was doped with H_2O (5 µL), bringing the internal concentration of H_2O to 0.5 M. The color changed almost immediately to light pink and then eventually to yellow. The reaction mixture was then monitored by ^{1}H-NMR which showed [**4**] rise to about 92 mole % while the methine singlet belonging to the intermediate, **S3**, disappeared (Figure S7). The aromatic portion of the ^{1}H-NMR spectrum taken 18 h after addition of H_2O is shown in Figure S8.

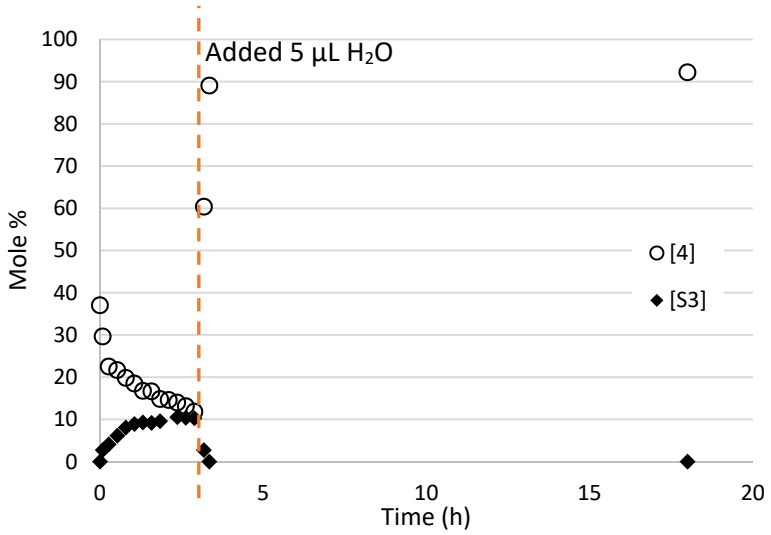

Figure S7. Reaction profiles showing [**4**] and initial unidentified intermediate [**S3**] after exposure of 0.6 mL anhydrous TFE solution of **4** to O_2 for 3 h followed by addition of 5 µL of H_2O.

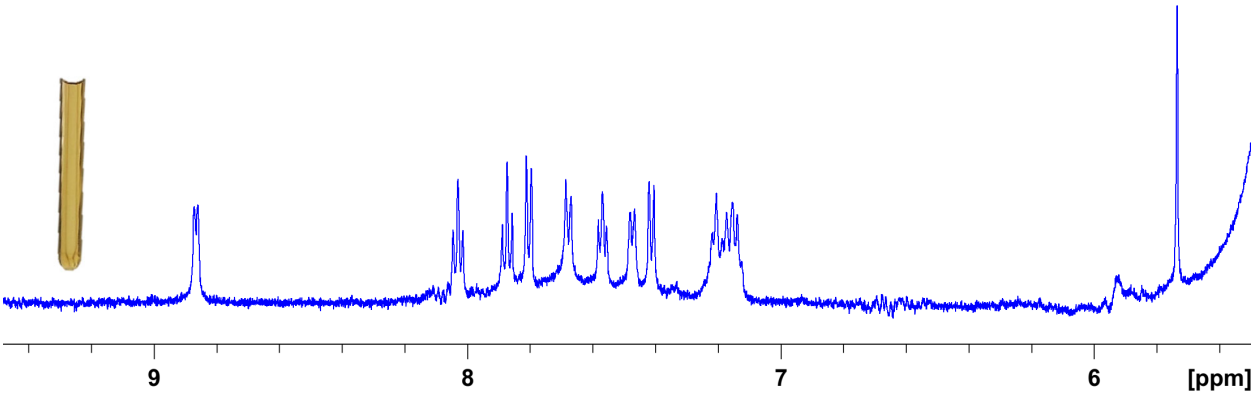

Figure S8. Aromatic region of ^{1}H-NMR spectrum 18 h after adding 5 µL H_2O to reaction between **4** and O_2 in TFE, showing that the only NMR visible species is **4** and the solution color is yellow.

c. Equilibrium formation of 11 from 8 and 4:

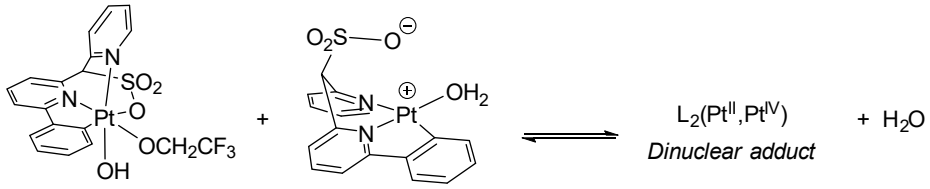

8 **4** **11**

When **8** and **4** are both present in TFE, a third species, **11**, is always observed to form which we propose to be an adduct of **8** and **4**. To find the K_{eq}, (C_6H_4-dpms)Pt(H_2O), **4**, (1.7 mg, 3.1 µmol) was dissolved in 0.5 mL de-gassed TFE-d_1 under argon and then doped with 0.150 M D_2O. A second solution, containing 5.7 mM **8** and 0.150 M D_2O in TFE-d_1 was prepared. The first solution containing **4** was then titrated with

the solution of **8** in 100 µL increments and the concentration of each species measured by ^{1}H-NMR. To test reversibility, 4 uL D_2O was added to the final solution (bringing the internal [D_2O] to 0.40 M). When D_2O was added, [**4**] and [**8**] increased while [**11**] decreased, serving to reverse the equilibrium. This suggests that H_2O is released in the forward reaction. The data was found to agree well with $K_{eq} = \frac{[\mathbf{11}][D_2O]}{[\mathbf{4}][\mathbf{8}]}$ = 95 ± 10.

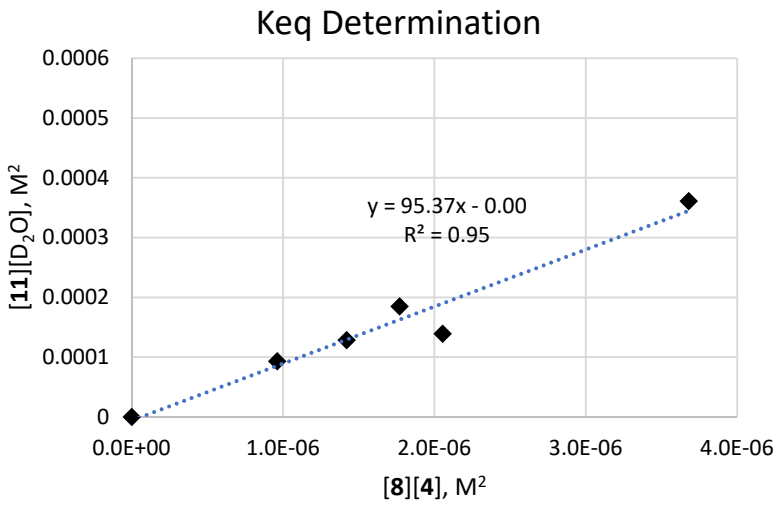

Figure S9. Graph showing [**11**][D_2O] vs [**8**][**4**] used to determine K_{eq} between **8** and **4** and the derived proposed dinuclear adduct **11** which forms with loss of water.

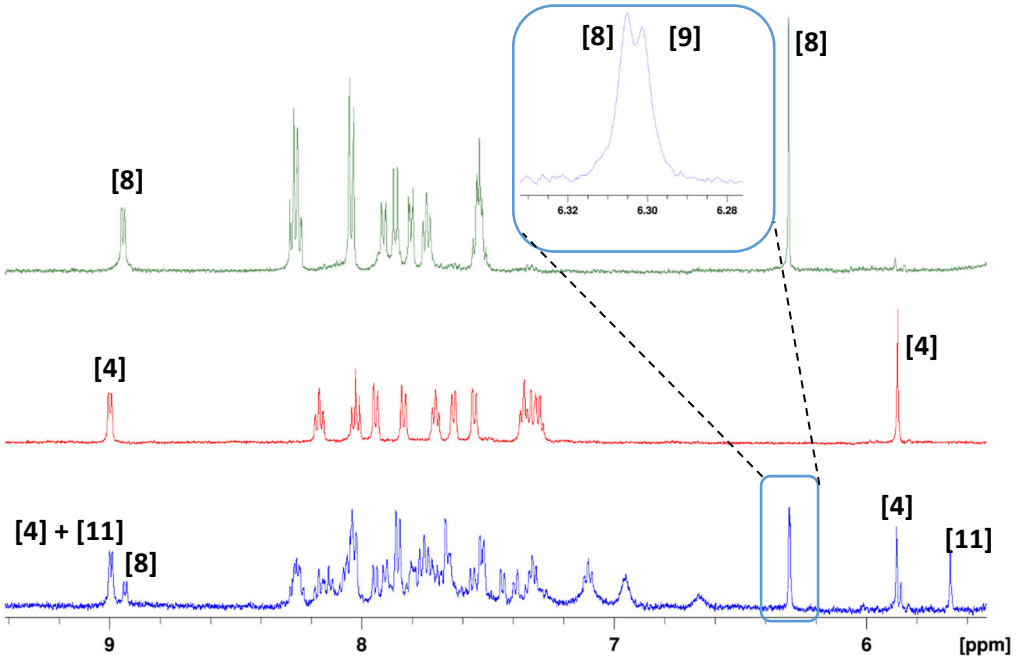

Figure S10. Top green trace – ^{1}H-NMR spectrum of pure **8** in wet TFE. Middle red trace – ^{1}H-NMR spectrum of pure **4** in wet TFE. Bottom blue trace – **8** and **4** combined in wet TFE produces ^{1}H-NMR signals for both species as well as the proposed adduct **11**.

V. Reaction of $LPt^{II}(H_2O)$, 4, with O_2 in TFE/Benzene mixture

Under air, **4** (8.8 mg, 16.4 µmol) was dissolved in 2 mL TFE. After dissolution, the solution was diluted with 1 mL C_6H_6. The solution was then transferred to a 25 mL Schlenk tube and pressurized with 1 atm pO_2. Periodically, a 150 µL aliquot was taken and dried under high vacuum for 1 h before dissolving in DMSO-d_6 to give a yellow solution. The role of DMSO-d_6 is to convert all LPt(solv) species and their derivatives to LPt(DMSO), thereby simplifying ^{1}H-NMR analysis. Each DMSO-d_6 solution was doped with 4 µL of a 0.310 M dioxane solution in D_2O as an internal standard. Thus, the consumption of **4** and appearance of three products, two major and one minor, was followed using the diagnostic singlets in the ^{1}H-NMR spectrum belonging to the ligand bridging methylene C-H (Figure S11).

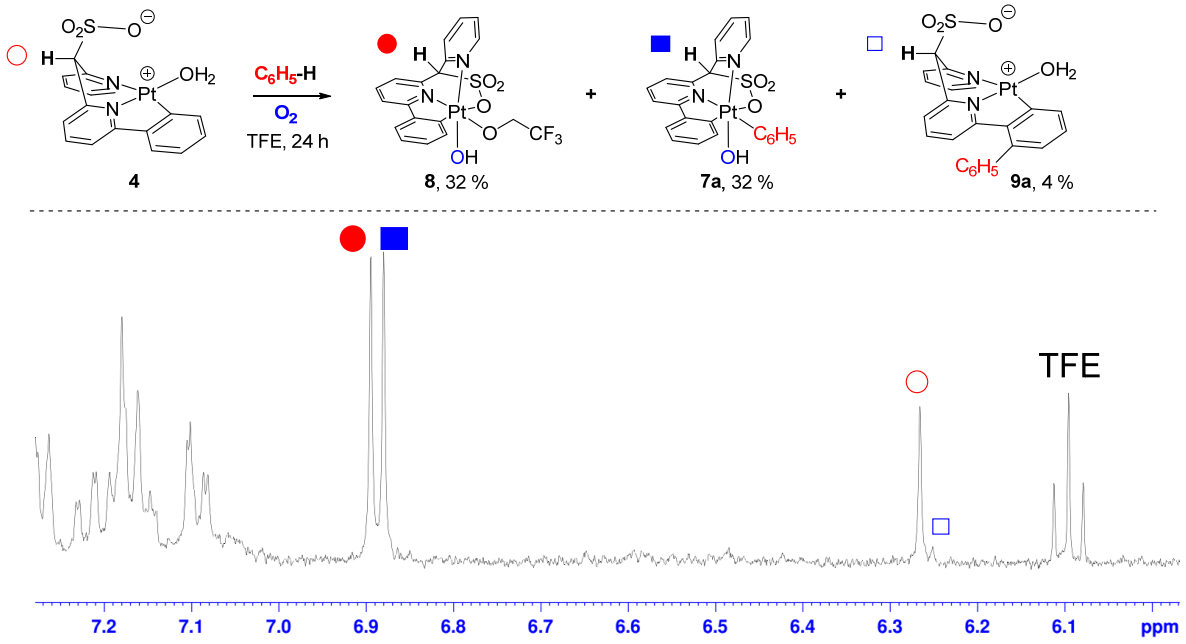

Figure S11. Portion of ^{1}H-NMR spectrum showing diagnostic bridghing C-H singlets, derived from the 24h aliquot of the crude reaction mixture between **4** and O_2 in a 1:2 C_6H_6:TFE mixture, dissolved in DMSO-d_6.

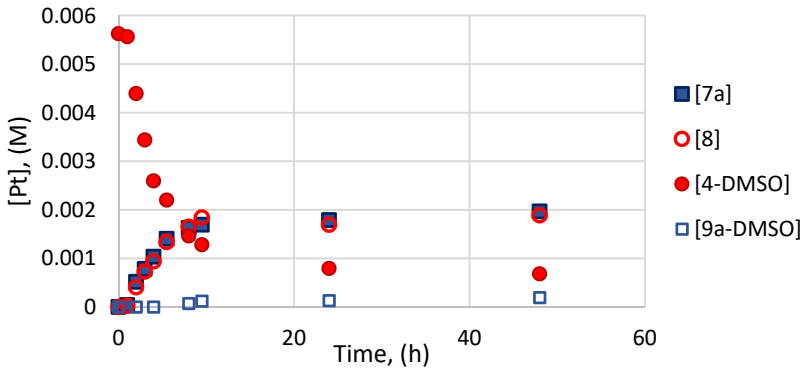

Figure S12. Reaction profile showing product and starting material concentration over the course of the reaction between **4** and O_2 in 1:2 C_6H_6:TFE mixture.

The minor product was identified as **9a** by comparison to the ^{1}H-NMR spectrum of the same complex, independently synthesized via oxidation of Li[(Ph-dpms)PtPh] in TFE. One of the major products, **8**, was also identified by comparison to the independently synthesized complex (prepared by oxidation of **4** by O_2 in TFE). The other major product, **7a**, was isolated from the crude reaction mixture by column chromatography (see "General Method A - For the synthesis of (C_6H_4-dpms)Pt^{IV}(Aryl)(OH) complexes", described above). The ^{1}H-NMR spectrum of pure **7a** in DMSO-d_6 matches that in the samples derived from crude reaction mixture. A single crystal of **7a** suitable for XRD analysis was grown by layering a DCM solution with Et_2O and leaving in the freezer overnight.

a. Attempted reductive elimination from (C_6H_4-dpms)Pt^{IV}(Ph)(OH), 7a

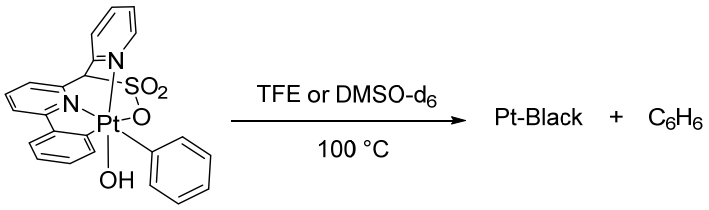

7a

Under air, two solutions containing (C_6H_4-dpms)Pt^{IV}(Ph)(OH), **7a**, (3.0 mg,) were prepared using 0.6 mL of solvent. In one the solvent was DMSO-d_6, in the second the solvent was TFE. Each solution was transferred to a J-Young tube, sealed, and heated at 90 °C. In both solutions, periodic ^{1}H-NMR analysis revealed the slow release of benzene while each gradually became darker in color due to the accumulation of Pt black. Many new small signals, belonging to the ligand, were observed in the ^{1}H-NMR spectrum, however the identification of these decomposition products was not pursued.

b. Procedure for analysis of kinetics data:

First, due to the complex nature of the reaction, which includes multiple reaction pathways with respect to the starting material, **4**, at least one of which is reversible, the analysis of reaction kinetics was undertaken with respect to only the LPt^{IV} products (**7a/b** and **8**) which are formed irreversibly. Since in all cases [**7a/b**] = [**8**], the concentration of **7a/b** (which gives rise to just one set of ^{1}H-NMR signals in solution) was measured and the concentration of **8** was assumed to be equal to that of **7a/b**.

Second, to find the reaction rate law and determine the observed rate constants k_{obs} for the formation of **7a/b**, we used the following methods:

Method A (most suitable for determining reaction rate law). Numerical integration of the pseudo-first order kinetic equation, d[**7a/b**]/dt = k_{obs}[**4**], was utilized using experimental values of [**4**], to obtain best non-linear fit of the experimental values of [**7a/b**] collected, typically, up to 74-85% conversion of **4** (that conversion also accounts for formation of **11**).

Method B (most accurate for determining reaction order and k_{obs}). Fitting the [**7a/b**] in each reaction profile with a third order polynomial and, in some cases, fitting the [**4**] with a fourth order polynomial (the polynomial orders were chosen by best fit) was followed by using resulting analytic polynomial expressions for [**7a/b**] and [**4**] for finding reaction order and k_{obs}. An example is shown in Figure S13.

Method C (may be good for determining reaction order in a specific reactant). Plotting experimental values of [**7a/b**] vs. time corresponding to ≤20% conversion of **4** was used to find the initial rates of formation of **7a/b**. The initial rates were then converted to k_{obs} by dividing them over $[\mathbf{4}]_{init}$ measured at the beginning of the observed reaction period.

In all methods, only the concentrations after the induction period were used in the analyses.

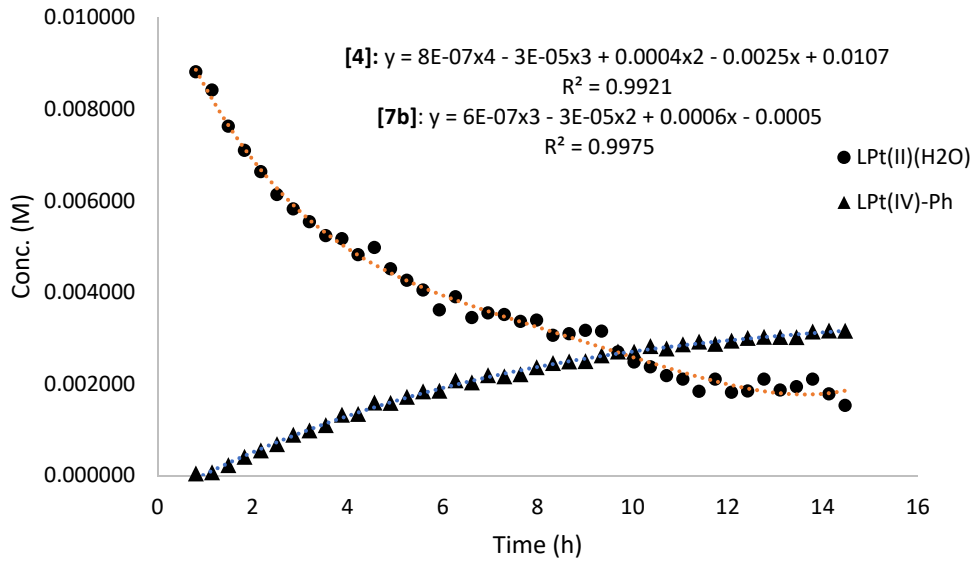

Figure S13. Reaction profile derived from monitoring a 1:2 C_6D_6:TFE solution of **4** (10 mM) doped with H_2O (150 mM) exposed to O_2 (1 atm) by ^{1}H-NMR along with polynomial fittings.

The derivative of the polynomial fitting for [**7a/b**] could then be found and, when plotted against time (Figure S14) gives the instantaneous rate, d[LPt(IV)-Ph]/dt, at each point in time. In this way, the entire data set could be used to make a fair assessment of the initial rate at the time just after the induction period.

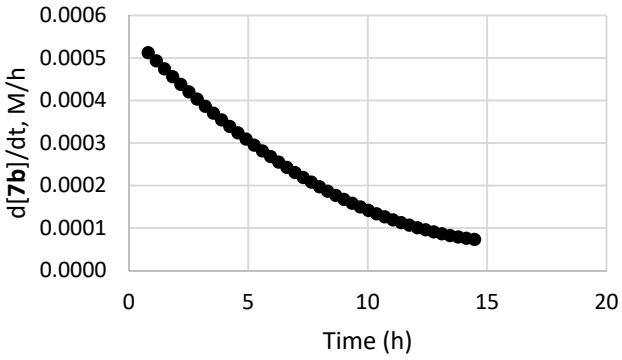

Figure S14. The rate of formation of **7b** (derived from third order polynomial regression) plotted against time (derived from fourth order polynomial regression).

Additionally, considering the first order dependence on [**4**] (Eq. S1), the instantaneous rate, d[**7a/b**]/dt, could be plotted against [**4**] (calculated from the fourth order polynomial regression). A linear fitting then yields the pseudo first order rate constant, k_{obs}, as the slope (Eq. S2). An example of this analysis is provided in Figure S15. In all cases, the dependence was found to deviate from linear after the first few hours of the reaction. Such an effect may be ascribed to inhibition of the reaction by products. Therefore, only the first linear portion of the data was used to find the k_{obs}.

Importantly, both approaches (i) and (ii) lead us to the identical conclusions about the order of the formation reaction of **7a/b**, in [benzene], [**4**] and [O_2].

$$\frac{d[\mathbf{7a/b}]}{dt} = k[Benzene][\mathbf{4}] = k_{obs}[\mathbf{4}] \quad \textbf{(S1)}$$

$$\frac{\frac{d[\mathbf{7a/b}]}{dt}}{[\mathbf{4}]} = k_{obs} \quad \textbf{(S2)}$$

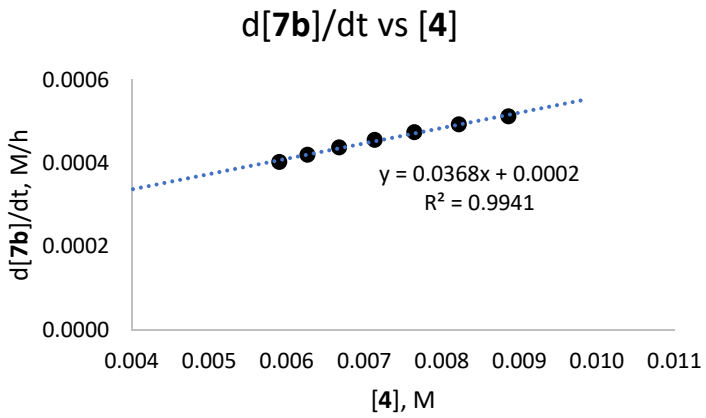

Figure S15. Plot of the instantaneous rate of formation of **7b** vs the corresponding instantaneous concentration of **4** gives an initial slope equal to the pseudo first order rate constant k_{obs}.

c. Kinetics experiments

General procedure: In an argon filled glovebox, an appropriate amount of LPt(H_2O) was loaded into a 5 mL vial. Anhydrous degassed TFE was then added and the vial was shaken until all solids had dissolved, resulting in a red solution. A stock TFE solution containing H_2O was then added to bring the internal [H_2O] to the desired concentration, resulting color change to yellow-orange. Finally, C_6D_6 was added, bringing the total volume to 0.6 mL. The solution was transferred to a J Young tube, sealed, and removed from the glovebox and subjected to ^{1}H-NMR analysis. The tube was then pressurized with O_2 and analyzed by ^{1}H-NMR every 20 minutes for 12 – 20 h at room temperature (Fig. S6, b).

Reaction order in [H_2O]

Following the general procedure, four solutions were produced, each containing 12.4 mM **4** in 1:2 C_6D_6:TFE under 1 atm pO_2 with four different H_2O concentrations: 12.4, 30.3, 74.1, and 150 mM. After monitoring by ^{1}H-NMR for 20 h at RT, the reaction profiles were fit according to the **Method B** outlined above and the initial rate, d[**7b**]/dt, was plotted against the internal H_2O concentration.

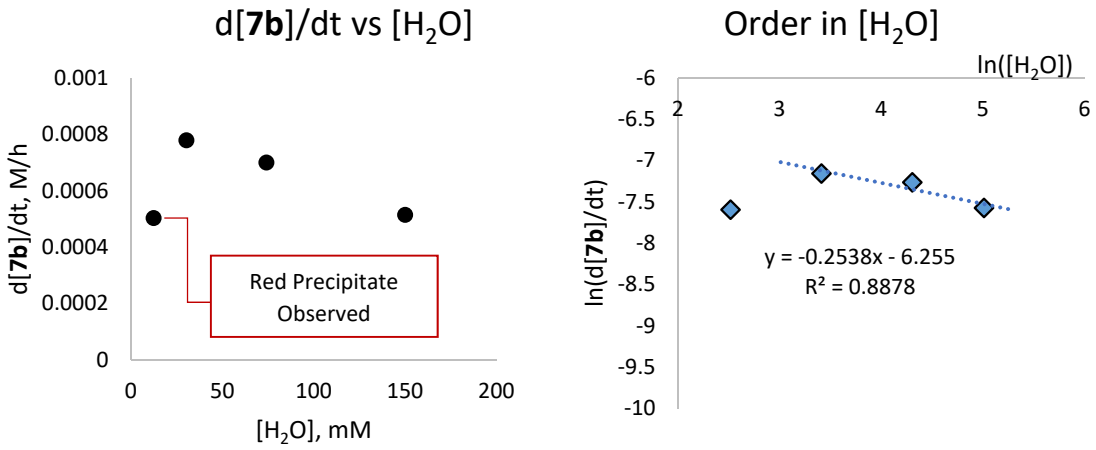

Figure S16. Left – Plot of the initial rate d[**7b**]/dt vs [H_2O]. Right – Plot of the natural log of the initial rate d[**7b**]/dt vs the natural log of [H_2O] with the slope corresponding to the order in [H_2O]. The 4th data point associated with the formation of precipitate is excluded.

A red precipitate, previously postulated to be a dinuclear complex derived from the starting material,[2] was observed to form in the reaction which contained only 12.4 mM H_2O (wherein all the water was derived only from [**4**]) effectively lowering the concentration of [**4**] in solution. This is likely the reason for the anomalously low d[**7b**]/dt at this water concentration. Accordingly, this experiment was excluded when analyzing the order in [H_2O].

The natural log of each initial rate from the other three reactions was then plotted against the natural log of the corresponding H_2O concentration. A linear fitting shows a very small negative order in [H_2O] of -0.26 ± 0.09. Thus, H_2O does serve to inhibit the reaction, but only minimally. An added effect of high, 150 mM, H_2O concentrations is that > 90% of the LPt(II) species in solution exist as LPt(II)(H_2O) which exhibits sharp, easily integrated ^{1}H-NMR signals. Therefore, to simplify analysis, all subsequent experiments were run in the presence of 150 mM [H_2O].

Reaction order in [4]

Following the general procedure, four solutions were produced with varying concentrations of **4**: 6.2, 12.4, 18.6, and 24.8 mM. All were doped with H_2O so that [H_2O] = 150 mM, and the solvent consisted of 1:2 C_6D_6:TFE. After an initial ^{1}H-NMR spectrum taken under argon, each was pressurized to 1 atm pO_2 and monitored for 12 h at RT. The resulting reaction profiles were analyzed as described below.

Method A. The plots demonstrating best fit of experimental [**7b**] using numerical integration of the first-order rate law d[**7b**]/dt = k_{obs}[**4**] are given in Fig. S19. They show good to very good match of experimental vs. calculated concentrations corresponding to the conversion of **4** up to 72-85% and so confirming the reaction 1st order in [**4**].

Method B. The analytical d[**7b**]/dt calculated for up to ~30% conversion of **4** was plotted against the corresponding values of [**4**]$_0$. An acceptable quality linear relationship was observed (Fig. S20).

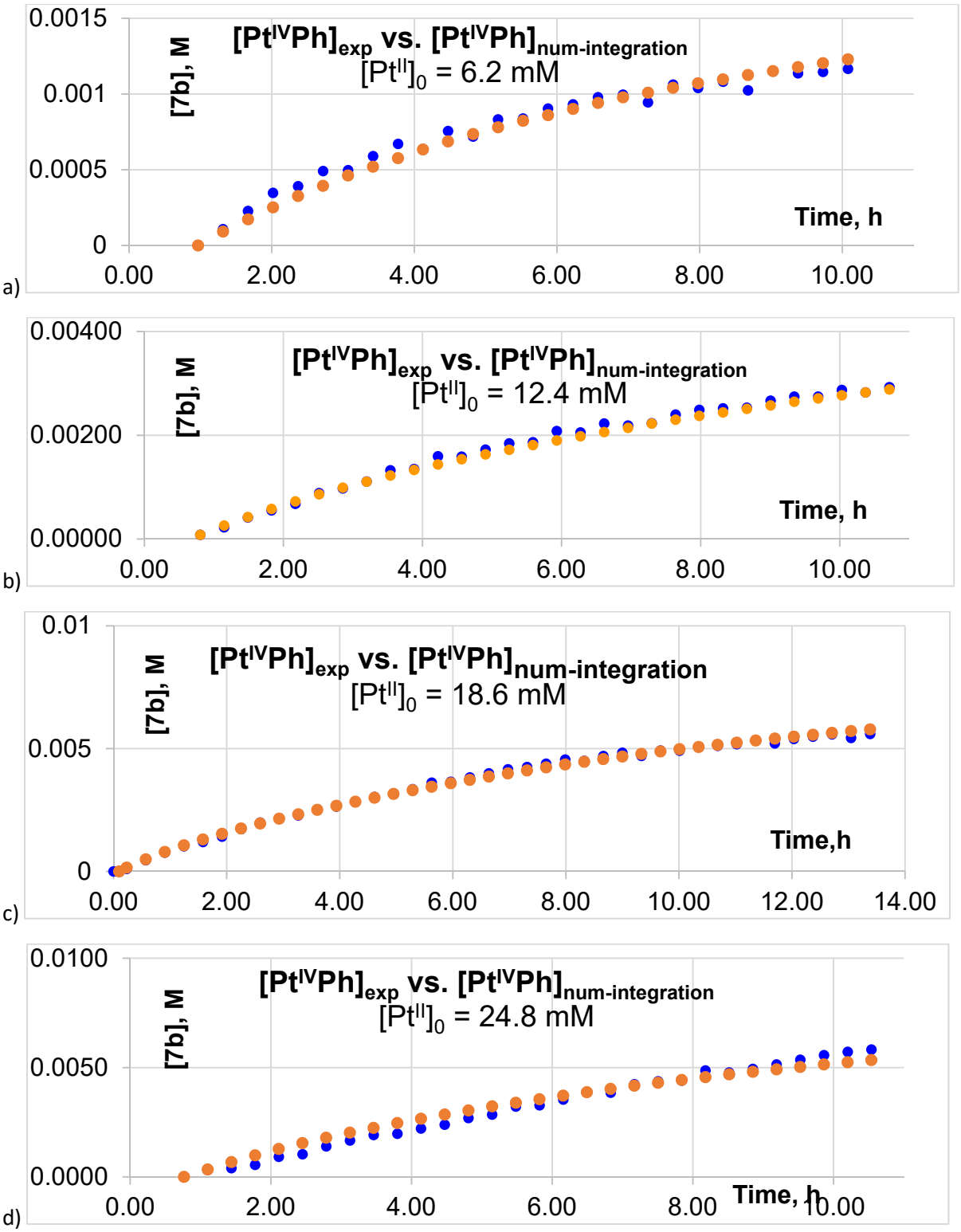

Figure S19. Comparison of [**7b**] found by numerical integration of the equation d[**7b**]/dt = k_{obs}[**4**] (orange circles) and experimental (blue circles) values of [**7b**] as a function of reaction time: a) [**4**]$_0$ = 6.2 mM, 82% conversion of **4**, k_{obs} = 5.7×10^{-2} h^{-1}; b) [**4**]$_0$ = 12.4 mM, 85% conversion of **4**, k_{obs} = 5.2×10^{-2} h^{-1}; c) [**4**]$_0$ = 18.6 mM, 82% conversion of **4**, k_{obs} = 7.9×10^{-2} h^{-1}; d) [**4**]$_0$ = 24.8 mM, 73% conversion of **4**, k_{obs} = 5.4×10^{-2} h^{-1}. In all cases [C_6D_6] = 3.76 M; 21 °C.

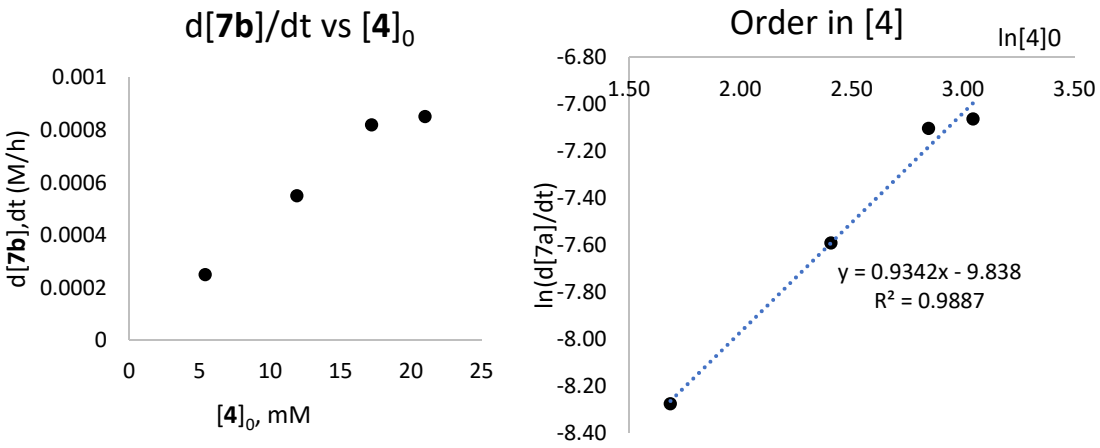

Figure S20. Left – The plot of the initial rate d[**7b**]/dt against the initial concentration [**4**]$_0$. Right – the natural logarithm of the initial rate d[**7b**]/dt plotted against the natural logarithm of the corresponding [**4**]$_0$ with the slope equal to the order in [**4**].

A plot of the natural log of initial d[**7b**]/dt vs. the natural log of [**4**]$_0$ yields a slope of ~0.9, suggesting the rate d[**7b**]/dt is first order dependent on the initial [**4**]$_0$ in this concentration range. Additional evidence for a first order dependence on [**4**]$_0$ is provided by Method A. Subsequent experiments were performed using ~10 mM [**4**]$_0$, ensuring a first order dependence on starting material.

Reaction order in [O_2]

Following the general procedure, four solutions were produced, each containing 10 mM [**4**] in 1:2 C_6D_6:TFE doped with 150 mM H_2O. Each J Young tube was pressurized with a different pO_2: 0.3, 0.5, 1.0, and 2.0 atm. After monitoring by ^{1}H-NMR for ~13 h at RT, the reaction profiles were fit according to the method outlined above and the initial rate, d[**7b**]/dt, was plotted against pO_2. No change in d[**7b**]/dt was observed in this range of O_2 pressure (Method B). Accordingly, when the natural log of each derived k_{obs} is plotted against the natural log of the corresponding pO_2, a slope of 0.02 ± 0.04 is obtained, suggesting 0th order in [O_2] (Figure S17).

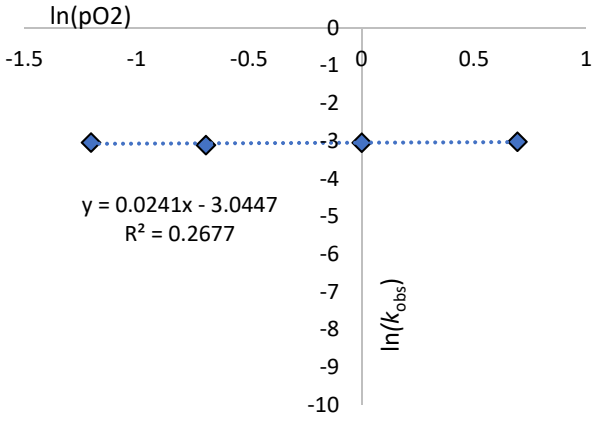

Figure S17. Plot of the natural log of the partial pressure of O_2 against the natural log of each k_{obs} for the reaction between **4** (10 mM) and O_2 in 1:2 C_6D_6:TFE reaction mixture with the slope equal to the order in pO_2.

Reaction order in [Benzene]

Following the general procedure, three solutions were produced, each containing ~10 mM **4**, 150 mM [H_2O], and a varying C_6D_6:TFE solvent ratio: 1:2, 1:5, and 1:9 C_6D_6:TFE. Each J Young tube was pressurized to 1 atm pO_2 and monitored by ^{1}H-NMR for ~13 h at RT. The reaction profiles were analyzed according to the methods outlined below.

Method A. Sample plots showing the best fit of experimental [**7b**] using numerical integration of the first-order rate law d[**7b**]/dt = k_{obs}[**4**] are given in Fig. S22. The plots show very good match of experimental vs. calculated data up to the conversion of **4** of 67-77% observed by 12-13h of reaction, so suggesting that the reaction is 1st order in [C_6D_6].

Method B. The rate of product formation varied linearly with increasing [C_6D_6]. A plot of the natural log of k_{obs} versus the natural log of each corresponding [C_6D_6] yields a slope of ~1 (Figure S18, a), suggesting a first order dependence on [C_6D_6].

Method C. The graphs used for calculation of initial rates of formation of **7b** are given in Fig. S24. The logarithm of the calculated k_{obs} vs. log[C_6D_6] yields a slope of ~1 (Figure S18, b), suggesting a first order dependence on [C_6D_6].

a)

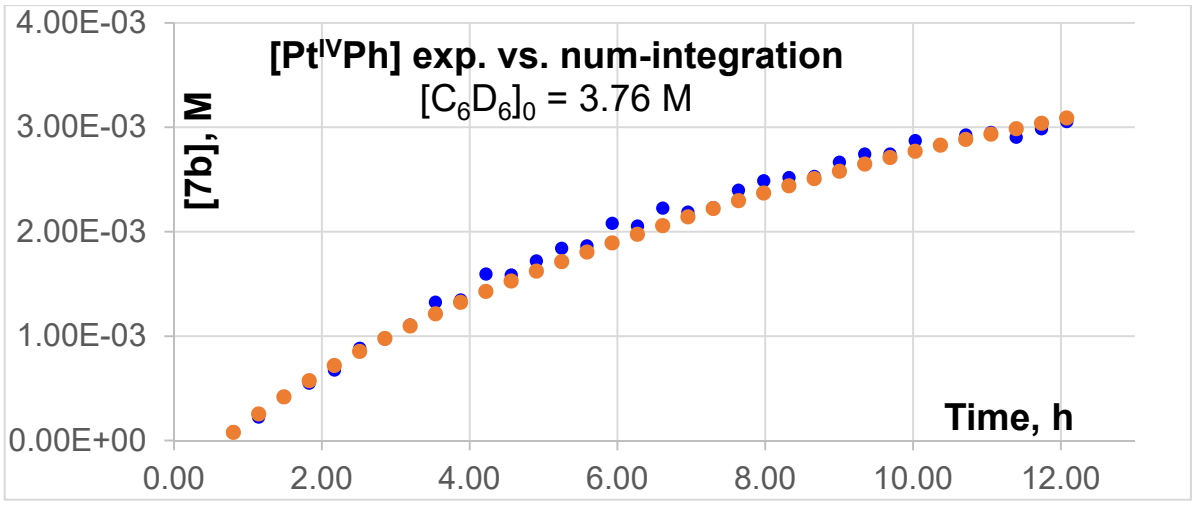

b)

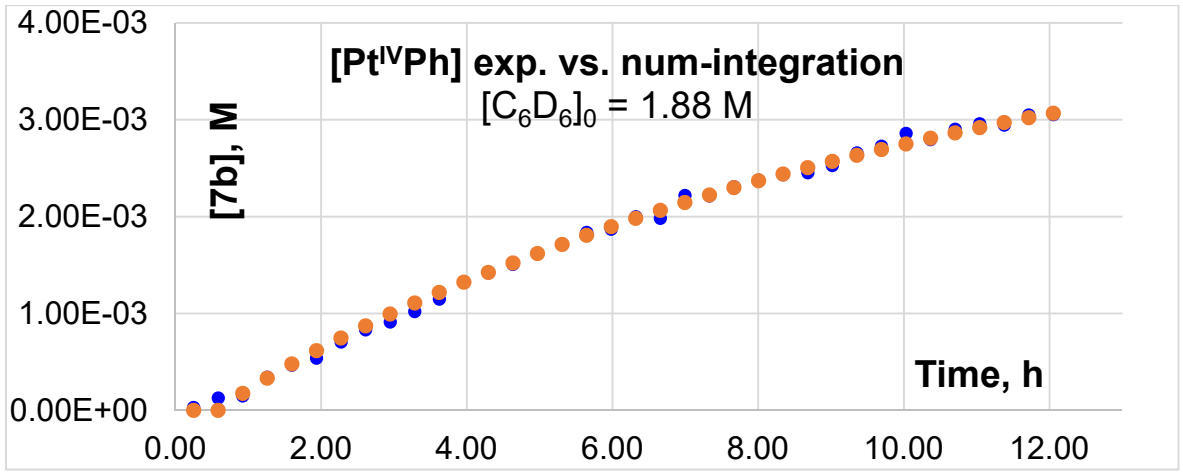

c)

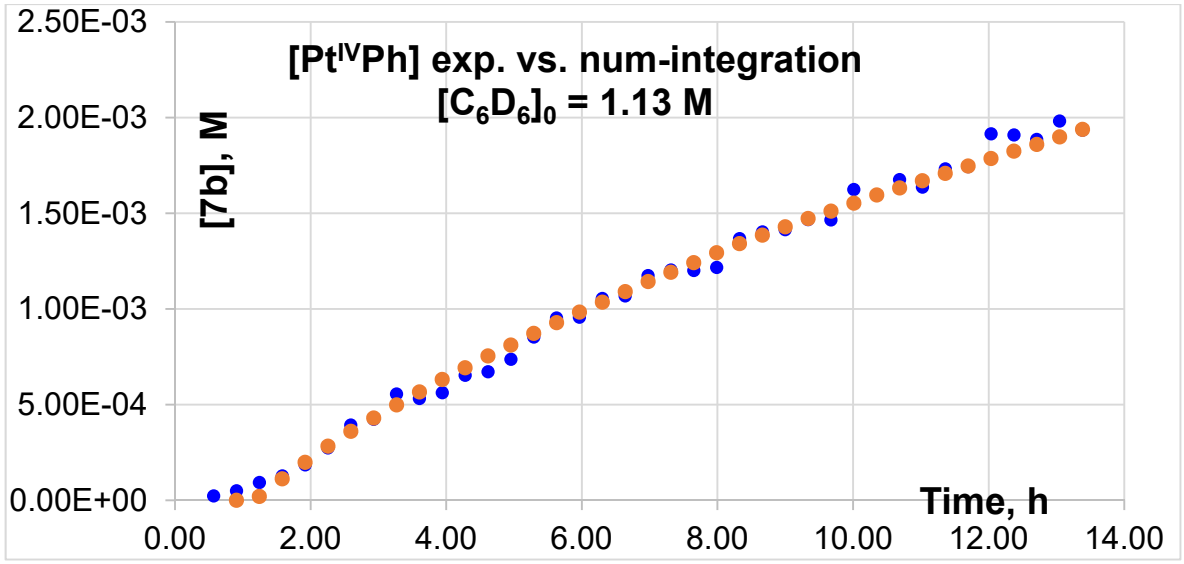

Figure S22. Comparison of experimental [**7b**] (blue circles) and [**7b**] produced using numerical integration of the equation d[**7b**]/dt = k_{obs}[**4**] (orange circles), as a function of reaction time: a) [$\mathbf{C_6D_6}$]$_0$ = 3.76 M, conversion of **4** 75%, k_{obs} = 5.4×10^{-2} h^{-1}; b) [$\mathbf{C_6D_6}$]$_0$ = 1.88 M, conversion of **4** 77%, k_{obs} = 6.2×10^{-2} h^{-1}; c) [$\mathbf{C_6D_6}$]$_0$ = 1.13 M, conversion of **4** 67%, k_{obs} = 3.2×10^{-2} h^{-1}.

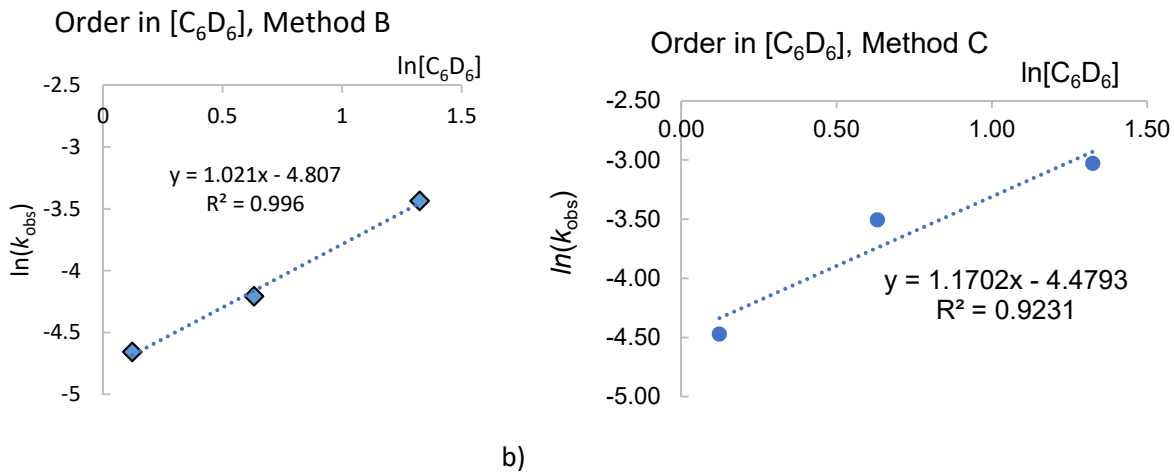

a) b)

Figure S18. Plot of the natural log of the k_{obs} from the reaction between **4** (10 mM) and O_2 in C_6D_6:TFE mixture of different ratios and the natural log of each corresponding [C_6D_6] with the slope equal to the order in [C_6D_6]: a) k_{obs} produced using Method B; b) k_{obs} produced using Method C.

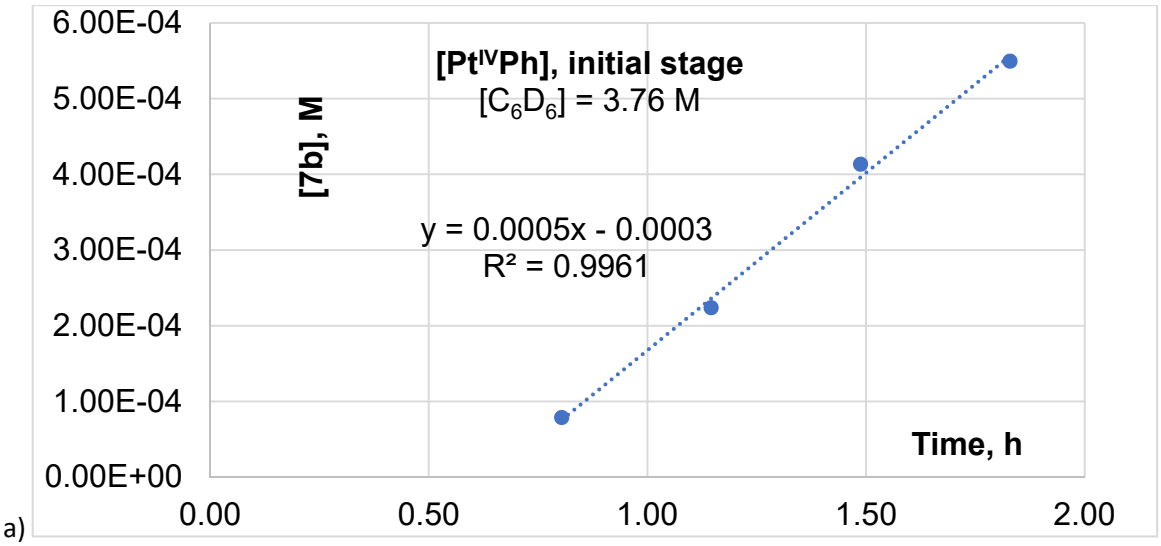

a)

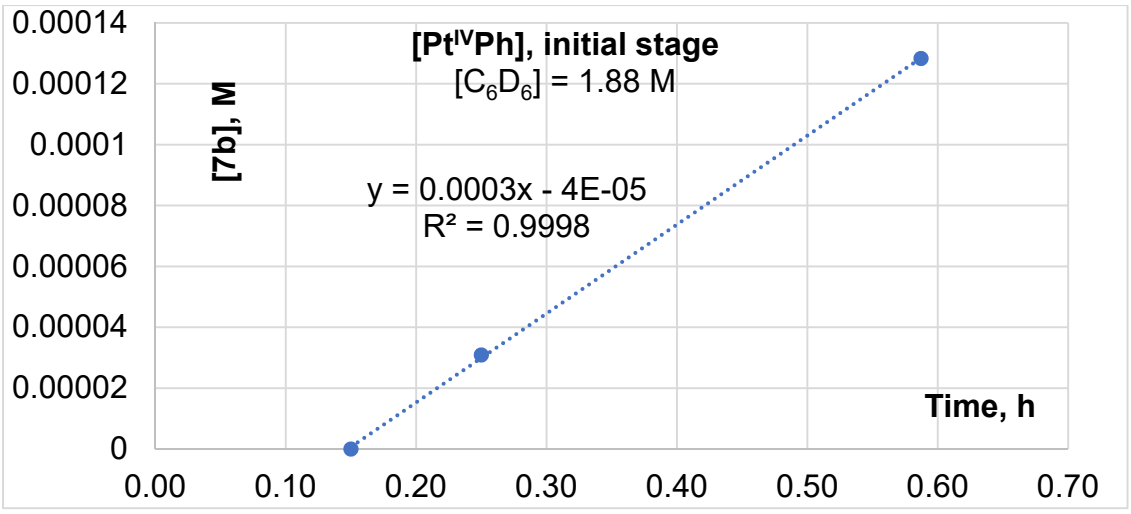

b)

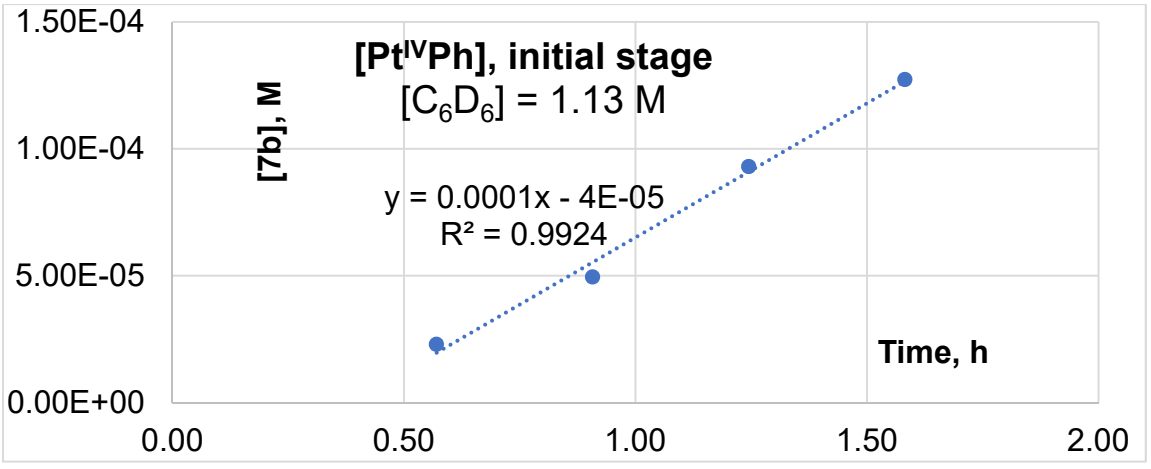

c)

Figure S24. Plots of the experimental values of [**7b**] vs. time corresponding to ≤20% conversion of C_6D_6 and ~10 mM **4** under O_2 atmosphere during the initial post-induction reaction period: a) $[\mathbf{4}]_{init}$ = 9.7 mM, $[C_6D_6]$ = 3.76 M, $k_{obs} = 4.8\times10^{-2}$ h^{-1}, $k_2 = 3.6\times10^{-6}$ M^{-1} s^{-1}; b) $[\mathbf{4}]_{init}$ = 9.7 mM, $[C_6D_6]$ = 1.88 M, $k_{obs} = 3.0\times10^{-2}$ h^{-1}, $k_2 = 4.4\times10^{-6}$ M^{-1} s^{-1}; c) $[\mathbf{4}]_{init}$ = 9.3 mM, $[C_6D_6]$ = 1.13 M, $k_{obs} = 1.14\times10^{-2}$ h^{-1}, $k_2 = 2.8\times10^{-6}$ M^{-1} s^{-1}.

Reaction Hydrogen Deuterium Kinetic Isotope Effect (KIE)

Following the general procedure, two sets of solutions were produced. The first set contained [**4**] (10 mM) in [H_2O] (150 mM) in 1:2 C_6D_6:TFE. The second set consisted of the same concentrations of each reactant except that C_6H_6 was substituted for C_6D_6. The solutions were transferred to NMR J-Young tubes and, after an initial analysis by ^{1}H-NMR, were pressurized to 1 atm pO_2 and monitored by ^{1}H-NMR at RT for 13 h. The data was analyzed as described in the "Procedure for Analysis of Kinetics Data" section and the pseudo first order rate constant k_{obs} for each reaction was found. Finally, each pseudo-first order rate constant k_{obs} was converted to the second order rate constant k (see Eq. S2) by dividing by [Benzene].

To see if there is any H/D KIE due to solvent, a third experiment was run wherein TFE was replaced by TFE-d_1. The k was found to be identical to when protic TFE is used.

Table S2. Pseudo first order rate constants, k_{obs}, and derived second order rate constants, k, derived from the reaction between **4** and O_2 in 1:2 Benzene:TFE solvent mixtures showing a KIE of 1.6 ± 0.1 between protic and per-deuterio benzene.

Solvent Mixture	k_{obs}, (h^{-1})	k, ($M^{-1}\cdot h^{-1}$)	KIE
1:2 C_6D_6:TFE	0.041 ± 0.003	0.0110 ± 0.0008	**1.6 ± 0.1**
1:2 C_6H_6:TFE	0.064 ± 0.001	0.0170 ± 0.0002	
1:2 C_6D_6:TFE-d_1	0.043 ± 0.001	0.0110 ± 0.0003	

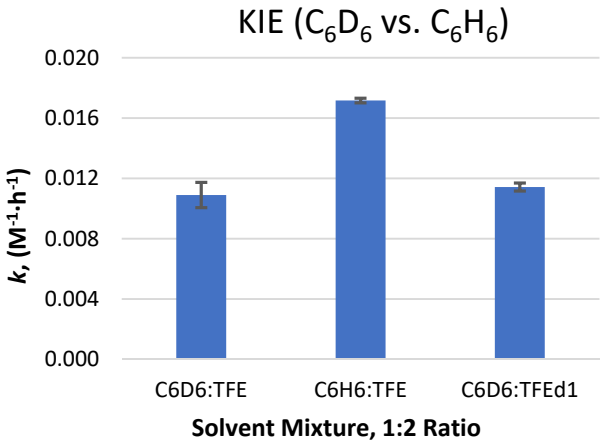

Figure S19. Second order rate constants, k, derived from the reaction between **4** and O_2 in 1:2 Benzene:TFE solvent mixtures.

d. Effect of doping with products and other additives

Doped with both [**7a**] and [**8**]:

Following the general procedure, a solution of [**4**] (10 mM) in 1:2 C_6D_6:TFE doped with [H_2O] (150 mM), [**7b**] (6 mM, 0.6 eq), and [**8**] (6 mM, 0.6 eq) was prepared. Accordingly, much of the [**8**] and [**4**] were in the form of [**11**] at the beginning of the reaction (Figure S20).

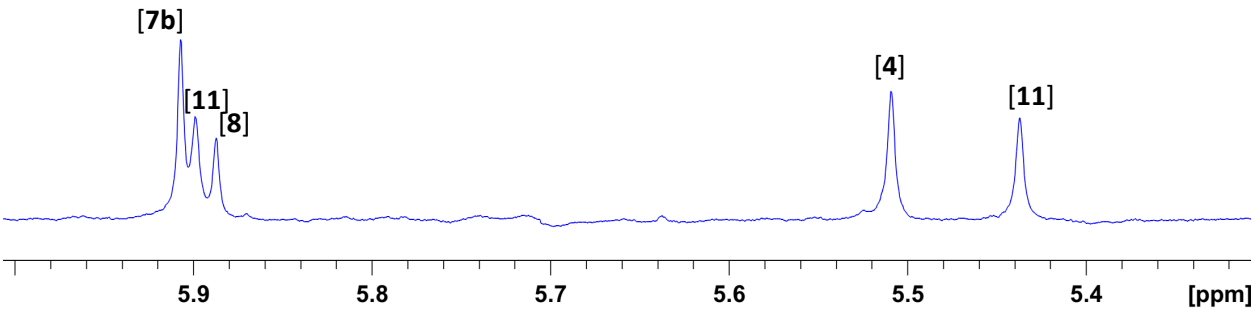

Figure S20. Portion of ^{1}H-NMR spectrum showing diagnostic bridging C-H singlets taken before addition of O_2 to reaction between **4** and O_2 in 1:2 C_6D_6:TFE in the presence of 0.6 eq. each of **8** and **7b** with the dinuclear adduct **11** also visible.

The solution was transferred to an NMR J-Young tube and, after initial ^{1}H-NMR analysis, was pressurized with O_2 (1 atm) and monitored for 13 h at RT by ^{1}H-NMR. Here the total [Pt(IV)] was measured due to the overlap of multiple signals, where $[Pt(IV)]_{total}$ = [**7b**]+[**8**]+[**11**]. The rate of formation of Pt(IV) products was found to be much inhibited in the reaction doped with a large initial concentration of [**8**] and [**7b**] as compared to the normal reaction conditions (Fig. S27).

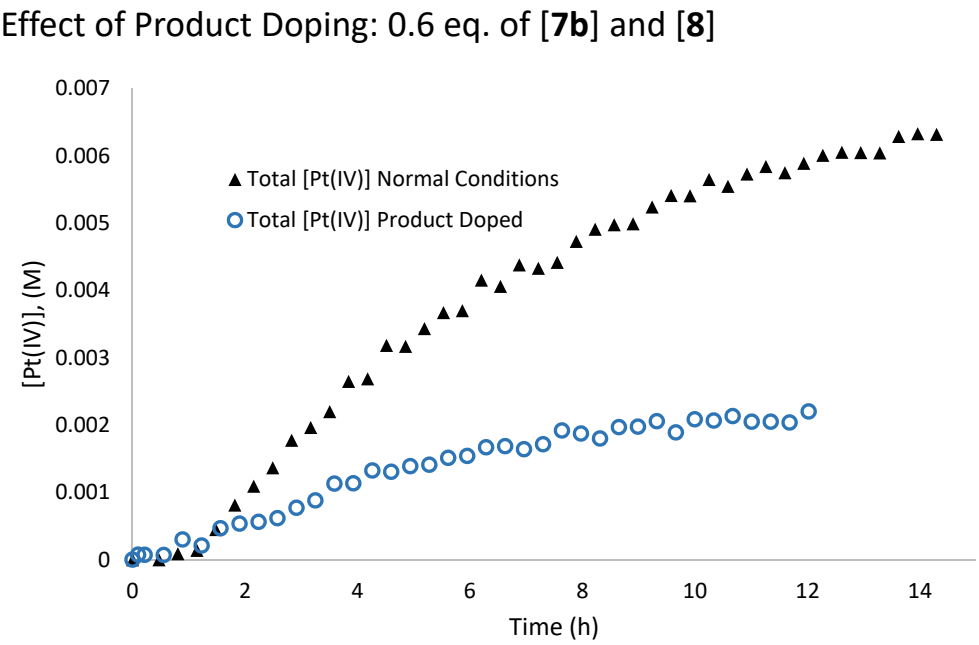

Figure S21. Change in [Pt(IV)] over time (measured as [**8**] + [**7b**] + [**11**]) under normal reaction conditions (black triangles) and doped with 0.6 eq. each of [**8**] and [**7b**] (blue open circles). Normal conditions: **4** (10 mM), H_2O (150 mM), O_2 (1 atm), in 1:2 C_6D_6:TFE.

Doped with just [**7b**]:

To see if the inhibition is due to the presence of [**7b**] or [**8**] (or both), a similar solution was prepared containing [**4**] (10 mM) in 1:2 C_6D_6:TFE doped with [H_2O] (150 mM) and [**7b**] (4 mM, 0.4 eq). No [**8**] was added to the solution. After transferring to a J-Young tube and an initial ^{1}H-NMR spectrum was acquired, the tube was pressurized with 1 atm pO_2 and analyzed periodically by ^{1}H-NMR for 13 h at RT. The rate of accumulation of [Pt(IV)] was unaffected by the initial concentration of **7b** as compared to the normal reaction conditions (Figure S22). More so, the rate of product formation showed no induction period, whereas the normal reaction conditions result in an induction period of ~1 h.

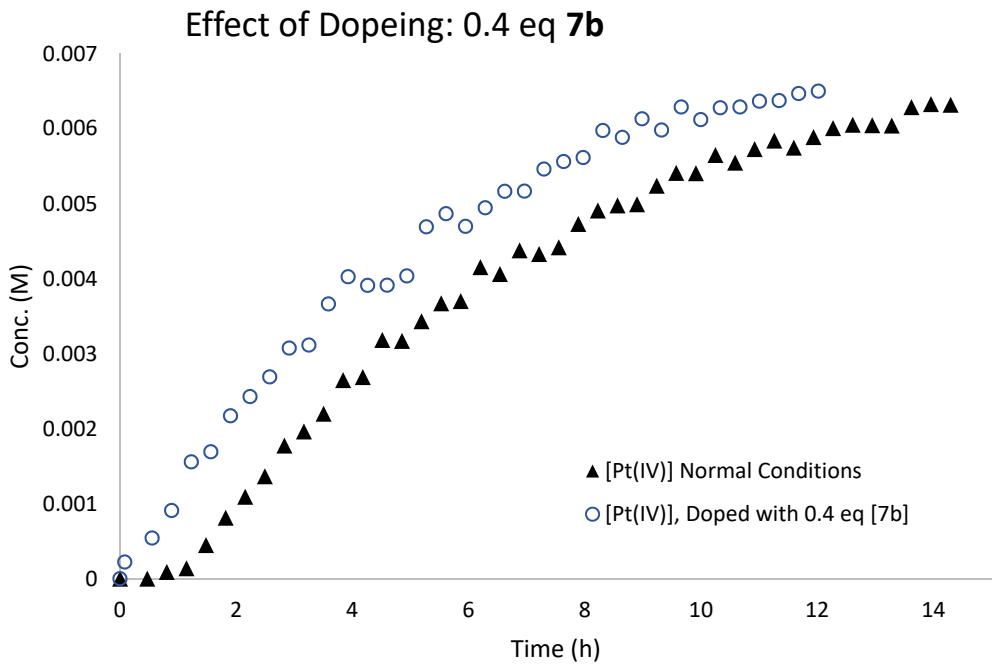

Figure S22. Change in [Pt(IV)] over time (measured as [**8**] + [**7b**] + [**11**]) under normal reaction conditions (black triangles) and doped with 0.4 eq [**7b**] (blue open circles). Normal conditions: **4** (10 mM), H_2O (150 mM), O_2 (1 atm), in 1:2 C_6D_6:TFE.

Doped with just [**8**]:

To see if the initial presence of small amounts of [**8**] may also eliminate the induction period, a similar solution was prepared containing [**4**] (10 mM) in a 1:2 C_6D_6:TFE mixture doped with [H_2O] (150 mM) and [**8**] (1 mM, 0.1 eq.). The solution was transferred to a J-Young tube and, after initial analysis by NMR, the tube was pressurized with O_2 (1 atm) and monitored for 13 h at RT by ^{1}H-NMR. No induction period was observed while a slight inhibition was observed (Figure S23, S6c), as expected by the observed interaction between [**8**] and [**4**]. The inhibition was very much pronounced with 0.6 equ. **8** added in the beginning (Fig. S6, d).

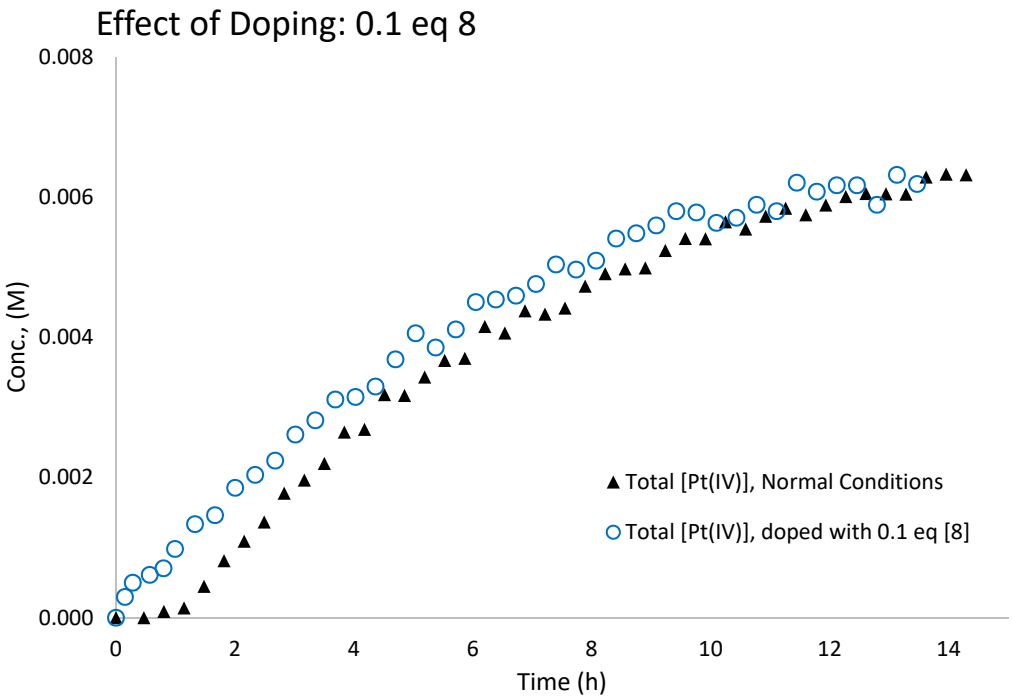

Figure S23. Change in [Pt(IV)] over time (measured as [**8**] + [**7b**] + [**11**]) under normal reaction conditions (black triangles) and doped with 0.1 eq [**8**] (blue open circles). Normal conditions: **4** (10 mM), H_2O (150 mM), O_2 (1 atm), in 1:2 C_6D_6:TFE.

Doped with BHT:

Two solutions were prepared using [**4**] (4.2 mg, 7.8 µmol) along with 0.7 or 10 eq. butylated hydroxy toluene (1.2 mg or 17 mg) dissolved in 0.5 mL TFE. The orange-yellow solution was then diluted with 0.25 mL C_6D_6, transferred to a J-Young tube, and analyzed by ^{1}H-NMR. After the initial spectrum was taken, the tube was pressurized with 1 atm O_2 and then monitored periodically by NMR. In both cases there was no noticeable effect on rate or selectivity and the yield of [**7a**] after 24 h was 32 %.

Doped with Hydroquinone:

In an argon filled glovebox, [**4**] (4.0 mg, 7.4 µmol) was dissolved in anhydrous TFE (0.5 mL) along with hydroquinone (~0.5 mg,~5 µmol, ~0.6 eq). The solution was diluted with 0.25 mL C_6D_6 and transferred to a J-Young NMR tube. An initial ^{1}H-NMR spectrum revealed that hydroquinone was present in 5.3 mM, 0.6 eq. as compared to the total (L)Pt^{II} species present (8.5 mM). The tube was pressurized with O_2 (1 atm) and monitored periodically by ^{1}H-NMR. The color remained a yellow-orange, never chaning to red, while the production of Pt(IV) products was severely hindered with only a 5.5% yield of [**7a**] after 96 h. At the 96 h mark, the temperature was increased to 55 °C for 19 h before the next spectrum was taken, which showed an increase in the yield of [**7a**] to 11 %. Remarkably, the selectivity for [**7a**] was greatly increased in the presence of hydroquinone, maintaining a roughly 4:1 ratio of [**7a**]:[**8**] throughout the reaction. At the end of the experiment, the amount of benzoquinone was measured to be approximately 1 mM. Finally, the solvent was removed under vacuum, and the residue dissolved in DMSO-d_6 which confirmed the 4:1 ratio of [**7a**] to [**8**].

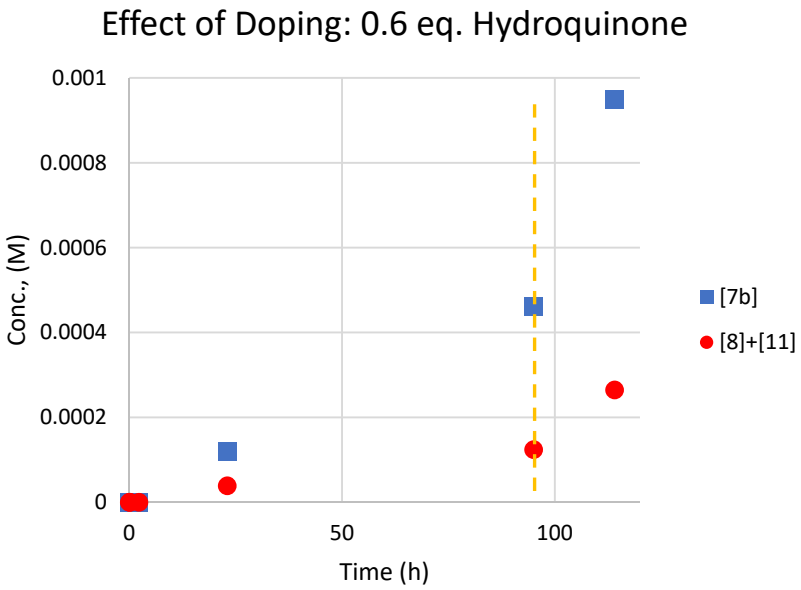

Figure S30. Accumulation of Pt(IV) products in reaction between **4** (8.5 mM) and O_2 (1 atm) in 1:2 C_6D_6:TFE in the presence of 0.6 eq hydroquinone with the orange dotted line representing a change of temperature from RT to 55 °C.

Hydroquinone control experiment

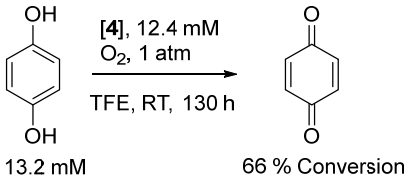

In an argon filled glove box, **4** (4.0 mg, 7.4 µmol) was added to a vial along with anhydrous TFE (0.6 mL). The vial was capped and gently agitated until all had dissolved, giving a red solution. In a separate vial, hydroquinone (0.9 mg, 8 µmol) was weighed out. The red TFE solution of **4** was then transferred to the vial containing hydroquinone. After swirling for 20 min, the hydroquinone had only partially dissolved. The entire mixture was carefully transferred to a J. Young tube and removed from the glovebox. An initial spectrum showed the internal concentration of **4** to be 12.4 mM and hydroquinone to be 12.5 mM. The tube was then pressurized with 1 atm pO_2 and monitored periodically by ^{1}H-NMR. It was observed that after 24 h, all the hydroquinone had dissolved (giving a final concentration of 13.2 mM).

In pure TFE, the singlets belonging to hydroquinone and benzoquinone produce just one signal at 6.76 ppm, preventing their separate integration. To deconvolute the signals, after 133 h reaction time, the reaction mixture was diluted with C_6D_6 such that the final solvent ratio was 1:2 C_6D_6:TFE. In this solvent mixture, benzoquinone appears as a singlet at δ = 6.53 ppm and hydroquinone gives a singlet at δ = 6.91 ppm. The concentration of benzoquinone at t = 133 h was thus measured to be 8.7 mM (**66 % yield**).

A 200 µL aliquot of the reaction mixture was taken and the solvent removed *in vacuo* leaving a reddish residue which was redissolved in DMSO-d_6. Subsequent ^{1}H-NMR analysis showed that **4** was the only Pt complex in solution (none of the oxidized form, **8**, had formed).

Doped with trifluoroacetic acid:

Due to the signal broadening observed in the ^{1}H-NMR spectra of TFE solutions of [**4**] containing trifluoroacetic acid (TFA), the effect of TFA was assessed by removing aliquots from a reaction, removing solvent, and re-dissolving in DMSO-d_6. [**4**] (4.3 mg, 8.0 µmol) was dissolved in 1 mL TFE. The solution was then diluted with 0.5 mL C_6H_6. To the solution was then added 8.0 µL of a 0.34 M stock solution of TFA in TFE (2.7 µmol, ~0.3 eq) which was accompanied by a color change to bright red. The solution was transferred to a 25 mL Schlenk tube and the headspace flushed with O_2. 100 µL aliquots were removed periodically, the solvent removed, and the reddish yellow residue dissolved in DMSO-d_6 and doped with 4.0 µL of a 0.310 M dioxane solution in D_2O as an internal standard.

The reaction was monitored in this way for 24 hours, during which time no changes occurred in the color of the reaction mixture or in the ^{1}H-NMR spectra of the collected aliquots. After 6 days however, the color had changed to yellow. An aliquot was removed which showed nearly all [**4**] had been consumed and the yield of [**7a**] had climbed to 46 %. Surprisingly no [**8**] was detected in solution. Instead ~9 to 10 other unidentified minor products were present, likely resulting from the decomposition of [**8**] in the presence of TFA.

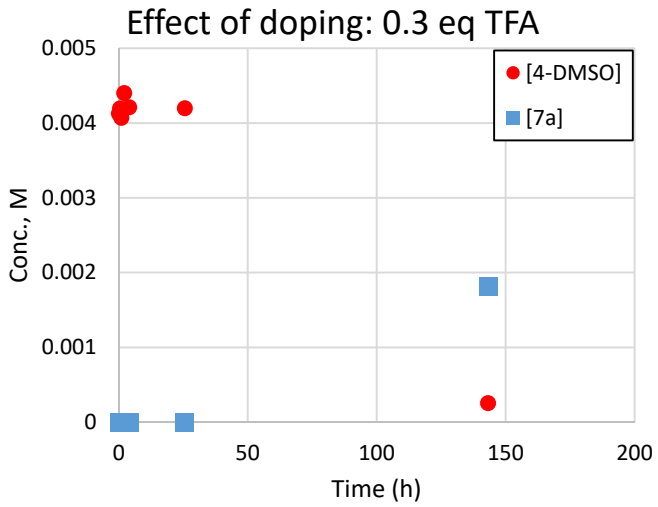

Figure S31. Consumption of **4** (measured as **4**-DMSO in aliquots dissolved in DMSO-d_6 solutions) and the appearance of **7a** upon exposure of a 1:2 C_6H_6:TFE solution of **4** (4.4 mM) to O_2 (1 atm) at RT in the presence of 0.3 eq trifluoroacetic acid.

VI. Kinetics of Li[(C_6H_4-dpms)PtPh], Li(12a), oxidation by O_2

In an argon filled glovebox, Li(**12a**) (3.0 mg) was dissolved in TFE (0.6 mL) to make an 8.3 mM yellow solution. The solution was then doped with 6.2 mM MeCN as an internal standard and transferred to a sealable NMR J-Young tube. After initial analysis by ^{1}H-NMR the, tube was pressurized with 1 atm pO_2 and [Li(**12a**)] was tracked via the diagnostic bridging methine C-H singlet. While Li(**13a**) was the primary product, the reaction was not as clean as when MeCN is not present, possibly due to inhibition of the subsequent reductive elimination and cycloplatination reactions by MeCN. The linear correlation between ln([Li(**12a**)]) and time suggests a first order reaction and gives a $t_{1/2}$ of 2.0 ± 0.3 h.

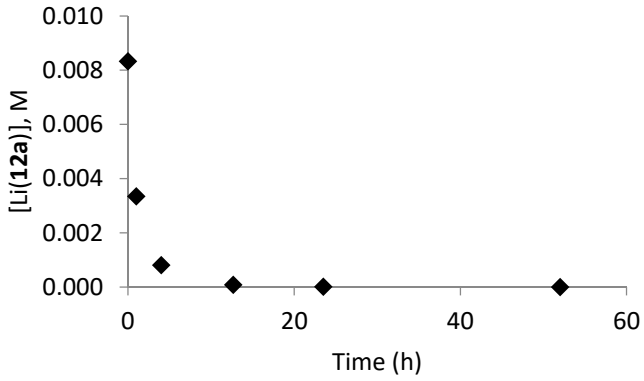

Figure S32. Reaction profile showing the conc. of Li(**12a**) upon exposure to a TFE solution of Li(**12a**) (3.0 mM) to O_2 (1 atm) at RT.

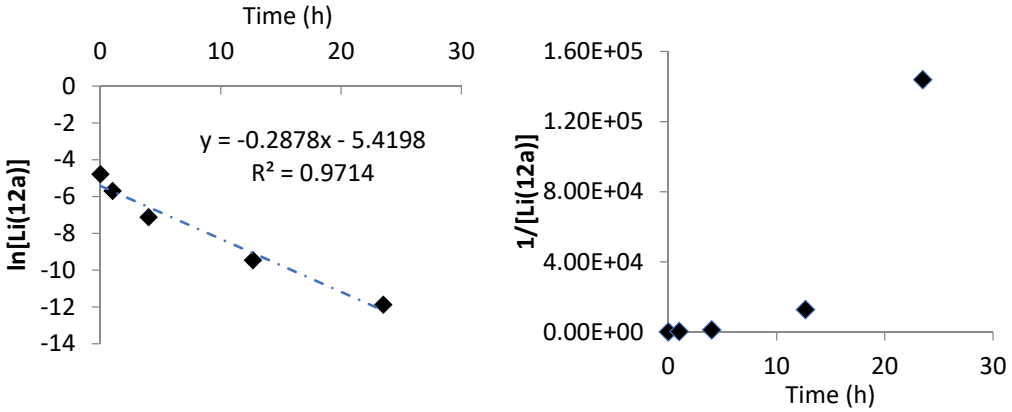

Figure S24. Left – first order fitting of the data in Figure S32. Right – attempted second order fitting of the data in Figure S32.

VII. Crystallographic Details

Crystal Structure Determination for **7a** (Figure S25).

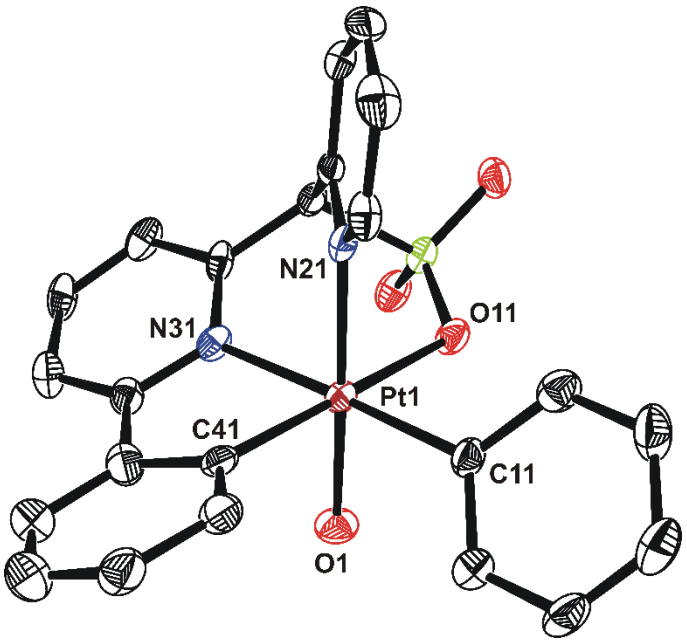

Figure S25. ORTEP plot for **7a**.

A colorless plate-like specimen of $C_{25}H_{22}Cl_4N_2O_4PtS$, approximate dimensions 0.03 mm × 0.13 mm × 0.19 mm, was used for the X-ray crystallographic analysis. The X-ray intensity data were measured on a Bruker APEX-II CCD system equipped with a graphite monochromator and a MoKα sealed tube (λ = 0.71073 Å). Data collection temperature was 150 K.

The total exposure time was 25.25 hours. The frames were integrated with the Bruker SAINT software package using a narrow-frame algorithm. The integration of the data using a triclinic unit cell yielded a total of 34997 reflections to a maximum θ angle of 26.50° (0.80 Å resolution), of which 11312 were independent (average redundancy 3.094, completeness = 99.9%, R_{int} = 4.33%) and 9327 (82.45%) were greater than $2\sigma(F^2)$. The final cell constants of a = 8.3380(8) Å, b = 17.1465(17) Å, c = 19.5150(19) Å, α = 93.214(2)°, β = 101.586(2)°, γ = 92.351(2)°, V = 2725.0(5)Å^3, are based upon the refinement of the XYZ-centroids of 9995 reflections above 20 σ(I) with 4.765° < 2θ < 60.17°. Data were corrected for absorption effects using the multi-scan method (SADABS). The

calculated minimum and maximum transmission coefficients (based on crystal size) are 0.5750 and 0.8680.
The structure was solved and refined using the Bruker SHELXTL Software Package, using the space group P-1, with Z = 4 for the formula unit, $C_{25}H_{22}Cl_4N_2O_4PtS$. The final anisotropic full-matrix least-squares refinement on F^2 with 671 variables converged at R_1 = 4.53%, for the observed data and wR_2 = 9.82% for all data. The goodness-of-fit was 1.134. The largest peak in the final difference electron density synthesis was 1.843 $e^-/Å^3$ and the largest hole was -2.635 $e^-/Å^3$ with an RMS deviation of 0.170 $e^-/Å^3$. On the basis of the final model, the calculated density was 1.910g/cm^3 and F(000), 1520 e^-.

APEX2 Version 2010.11-3 (Bruker AXS Inc.)
SAINT Version 7.68A (Bruker AXS Inc., 2009)
SADABS Version 2008/1 (G. M. Sheldrick, Bruker AXS Inc.)
XPREP Version 2008/2 (G. M. Sheldrick, Bruker AXS Inc.)
XS/XT Version 2014 (G. M. Sheldrick, (2014) University of Gottingen, Germany)
XL Version 2014 (G. M. Sheldrick, (2014) University of Gottingen, Germany)
Platon (A. L. Spek, *Acta Cryst.* (1990). A**46**, C-34)

Table S3. Sample and crystal data for **7a**.

Identification code	2731	
Chemical formula	$C_{25}H_{22}Cl_4N_2O_4PtS$	
Formula weight	783.39	
Temperature	150(2) K	
Wavelength	0.71073 Å	
Crystal size	0.03 × 0.13 × 0.19 mm	
Crystal habit	colorless plate	
Crystal system	triclinic	
Space group	P-1	
Unit cell dimensions	a = 8.3380(8) Å	α = 93.214(2)°
	b = 17.1465(17) Å	β = 101.586(2)°
	c = 19.5150(19) Å	γ = 92.351(2)°
Volume	2725.0(5) $Å^3$	
Z	4	
Density (calculated)	1.910 Mg/cm^3	
Absorption coefficient	5.654 mm^{-1}	
F(000)	1520	

Table S4. Data collection and structure refinement for **7a**.

Diffractometer	Bruker APEX-II CCD
Radiation source	sealed tube, MoKα
Theta range for data collection	2.13 to 26.50°
Index ranges	$-10 \leq h \leq 10$, $-21 \leq k \leq 21$, $-24 \leq l \leq 24$
Reflections collected	34997
Independent reflections	11312 [R(int) = 0.0433]
Coverage of independent reflections	99.9%
Absorption correction	multi-scan
Max. and min. transmission	0.8680 and 0.5750
Structure solution technique	direct methods
Structure solution program	ShelXS-97 (Sheldrick, 2008)
Refinement method	Full-matrix least-squares on F^2
Refinement program	ShelXL-2014 (Sheldrick, 2014)
Function minimized	$\Sigma\, w(F_o^2 - F_c^2)^2$
Data / restraints / parameters	11312 / 0 / 671
Goodness-of-fit on F^2	1.134
Δ/σ_{max}	0.002
Final R indices	9327 data; I>2σ(I) $R_1 = 0.0453$, $wR_2 = 0.0939$
	all data $R_1 = 0.0595$, $wR_2 = 0.0982$
Weighting scheme	$w=1/[\sigma^2(F_o^2)+(0.0283P)^2+19.8722P]$, $P=(F_o^2+2F_c^2)/3$
Largest diff. peak and hole	1.843 and -2.635 eÅ^{-3}
R.M.S. deviation from mean	0.170 eÅ^{-3}

$R_{int} = \Sigma|F_o^2 - F_o^2(\text{mean})| / \Sigma[F_o^2]$
$R_1 = \Sigma||F_o| - |F_c|| / \Sigma|F_o|$
$\text{GOOF} = S = \{\Sigma[w(F_o^2 - F_c^2)^2] / (n - p)\}^{1/2}$
$wR_2 = \{\Sigma[w(F_o^2 - F_c^2)^2] / \Sigma[w(F_o^2)^2]\}^{1/2}$

Crystal Structure Determination for **10a** (Figure S)

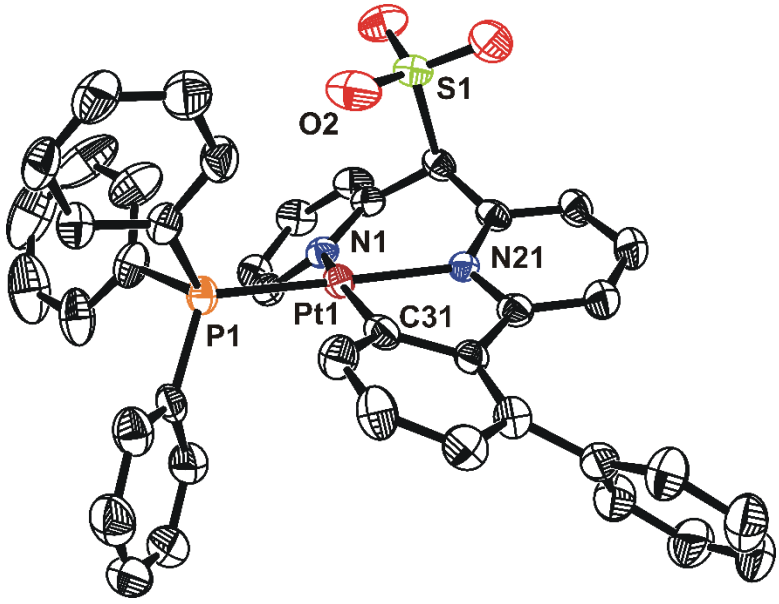

Figure S35. ORTEP plot for **10a**.

A yellow prism-like specimen of $C_{45}H_{41}N_2O_4PPtS$, approximate dimensions 0.08 mm × 0.14 mm × 0.34 mm, was used for the X-ray crystallographic analysis. The X-ray intensity data were measured on a Bruker APEX-II CCD system equipped with a graphite monochromator and a MoKα sealed tube (λ = 0.71073 Å). Data collection temperature was 250 K.

The total exposure time was 8.42 hours. The frames were integrated with the Bruker SAINT software package using a narrow-frame algorithm. The integration of the data using a monoclinic unit cell yielded a total of 49518 reflections to a maximum θ angle of 26.50° (0.80 Å resolution), of which 7940 were independent (average redundancy 6.237, completeness = 100.0%, R_{int} = 6.97%) and 6143 (77.37%) were greater than 2σ(F^2). The final cell constants of *a* = 8.7588(11) Å, *b* = 31.809(4) Å, *c* = 13.8220(17) Å, β = 95.629(2)°, *V* = 3832.4(8) Å^3, are based upon the refinement of the XYZ-centroids of 9973 reflections above 20 σ(I) with 4.845° < 2θ < 49.80°. Data were corrected for absorption effects using the multi-scan method (SADABS). The calculated minimum and maximum transmission coefficients (based on crystal size) are 0.5050 and 0.7380.

The structure was solved and refined using the Bruker SHELXTL Software Package, using the space group P21/n, with Z = 4 for the formula unit, $C_{45}H_{41}N_2O_4PPtS$. The final anisotropic full-matrix least-squares refinement on F^2 with 489 variables converged at R_1 = 3.97%, for the observed data and wR_2 = 8.81% for all data. The goodness-of-fit was 1.064. The largest peak in the final difference electron density synthesis was 1.858 $e^-/Å^3$ and the largest hole was -1.440 $e^-/Å^3$ with an RMS deviation of 0.116 $e^-/Å^3$. On the basis of the final model, the calculated density was 1.615g/cm^3 and F(000), 1864 e^-.

APEX2 Version 2010.11-3 (Bruker AXS Inc.)
SAINT Version 7.68A (Bruker AXS Inc., 2009)
SADABS Version 2008/1 (G. M. Sheldrick, Bruker AXS Inc.)
XPREP Version 2008/2 (G. M. Sheldrick, Bruker AXS Inc.)
XS Version 2008/1 (G. M. Sheldrick, *Acta Cryst.* (2008). A**64**, 112-122)
XL Version 2012/4 (G. M. Sheldrick, (2012) University of Gottingen, Germany)
Platon (A. L. Spek, *Acta Cryst.* (1990). A**46**, C-34)

Table S5. Sample and crystal data for **10a.**

Identification code	2677
Chemical formula	$C_{45}H_{41}N_2O_4PPtS$
Formula weight	931.92
Temperature	250(2) K
Wavelength	0.71073 Å
Crystal size	0.08 × 0.14 × 0.34 mm
Crystal habit	yellow prism
Crystal system	monoclinic
Space group	P21/n
Unit cell dimensions	a = 8.7588(11) Å α = 90°
	b = 31.809(4) Å β = 95.629(2)°

	c = 13.8220(17) Å γ = 90°
Volume	3832.4(8) $Å^3$
Z	4
Density (calculated)	1.615 Mg/cm^3
Absorption coefficient	3.805 mm^{-1}
F(000)	1864

Table S6. Data collection and structure refinement for **10a**.

Diffractometer	Bruker APEX-II CCD
Radiation source	sealed tube, MoKα
Theta range for data collection	1.96 to 26.50°
Index ranges	-10 ≤ h ≤ 10, -39 ≤ k ≤ 39, -17 ≤ l ≤ 17
Reflections collected	49518
Independent reflections	7940 [R(int) = 0.0697]
Coverage of independent reflections	100.0%
Absorption correction	multi-scan
Max. and min. transmission	0.7380 and 0.5050
Structure solution technique	direct methods
Structure solution program	ShelXS-97 (Sheldrick, 2008)
Refinement method	Full-matrix least-squares on F^2
Refinement program	ShelXL-2014 (Sheldrick, 2014)

Function minimized	$\Sigma\, w(F_o^2 - F_c^2)^2$	
Data / restraints / parameters	7940 / 0 / 489	
Goodness-of-fit on F^2	1.064	
Δ/σ_{max}	0.001	
Final R indices	6143 data; I>2σ(I)	$R_1 = 0.0397$, $wR_2 = 0.0800$
	all data	$R_1 = 0.0611$, $wR_2 = 0.0881$
Weighting scheme	$w=1/[\sigma^2(F_o^2)+(0.0318P)^2+9.9600P]$, $P=(F_o^2+2F_c^2)/3$	
Largest diff. peak and hole	1.858 and -1.440 eÅ^{-3}	
R.M.S. deviation from mean	0.116 eÅ^{-3}	

$R_{int} = \Sigma|F_o^2 - F_o^2(\text{mean})| \,/\, \Sigma[F_o^2]$
$R_1 = \Sigma||F_o| - |F_c|| \,/\, \Sigma|F_o|$
$\text{GOOF} = S = \{\Sigma[w(F_o^2 - F_c^2)^2] \,/\, (n - p)\}^{1/2}$
$wR_2 = \{\Sigma[w(F_o^2 - F_c^2)^2] \,/\, \Sigma[w(F_o^2)^2]\}^{1/2}$

VIII. NMR Spectra

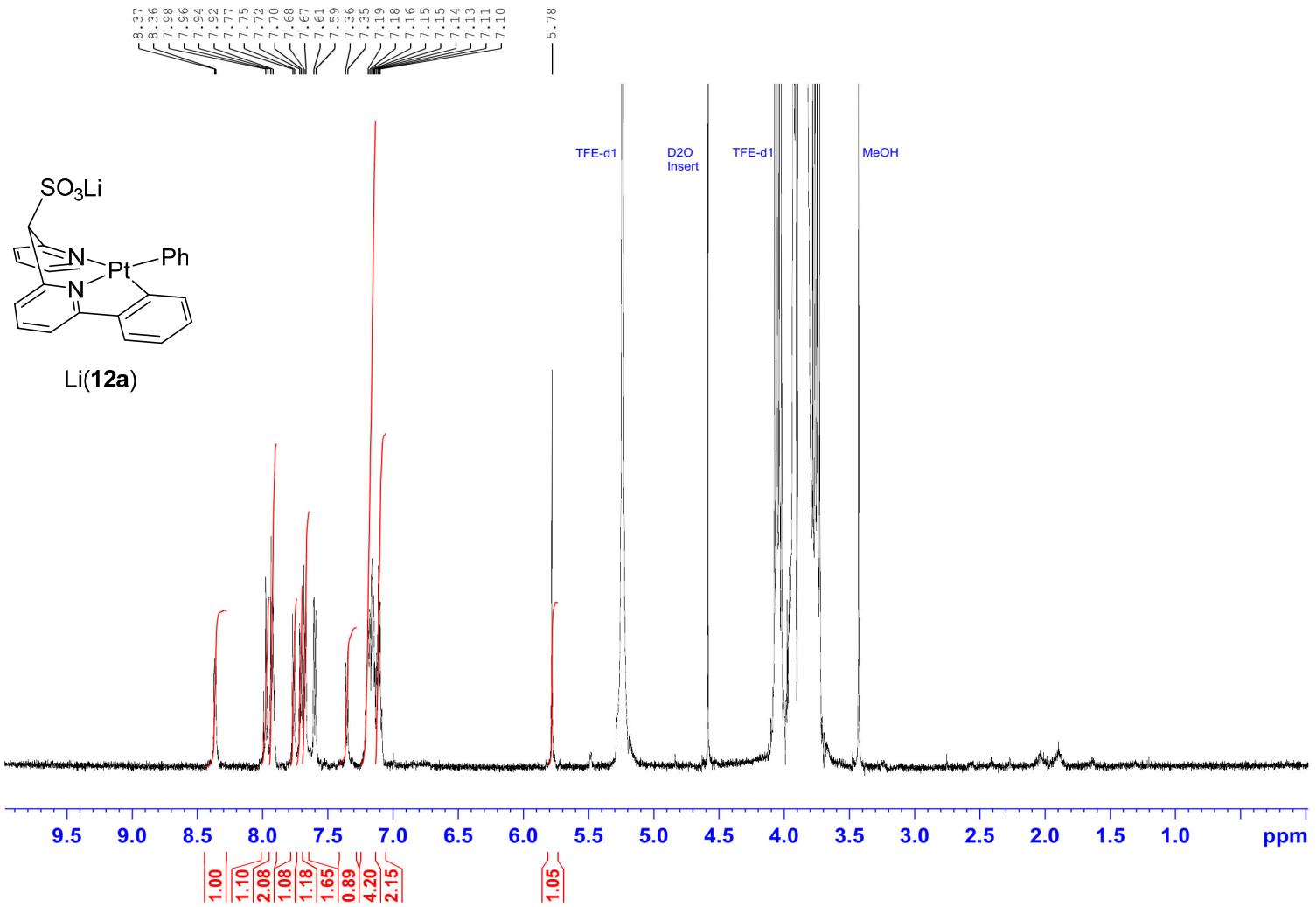

Figure S36. ^{1}H-NMR spectrum of Li(**12a**) in TFE-d_1

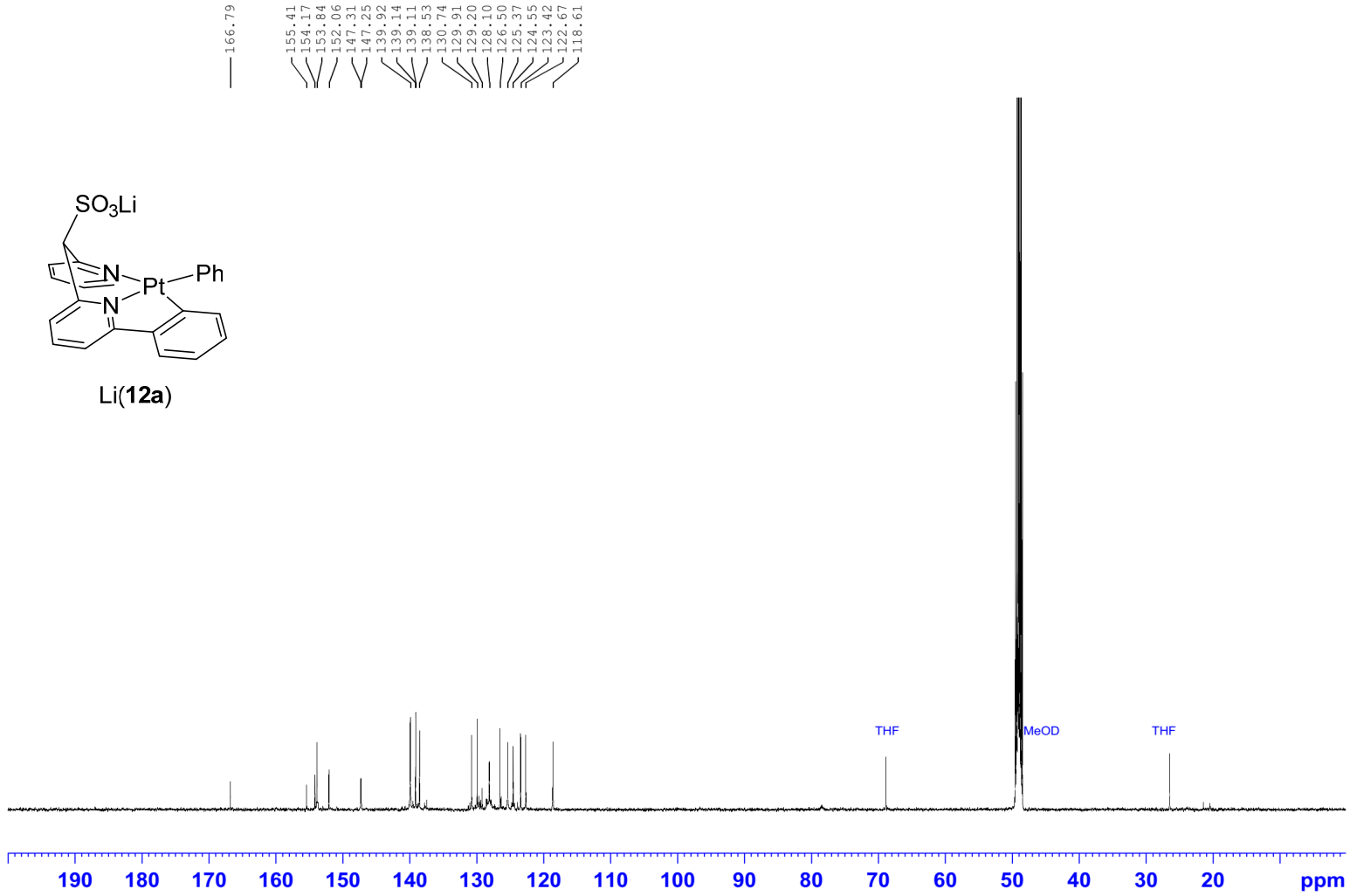

Figure S37. ^{13}C-NMR of Li(**12a**) in MeOD.

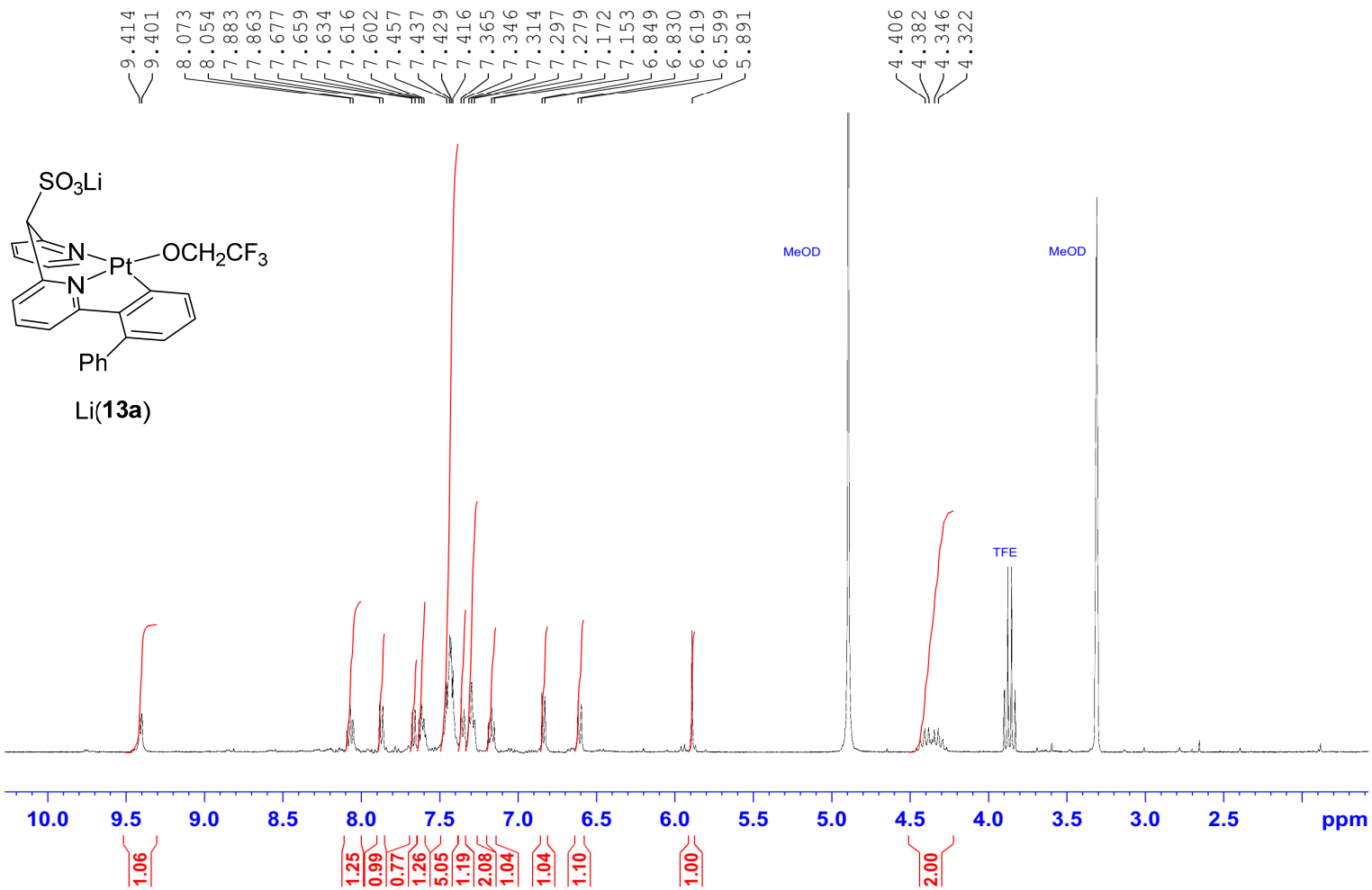

Figure S38. ^{1}H-NMR spectrum of Li(**13a**) in MeOD.

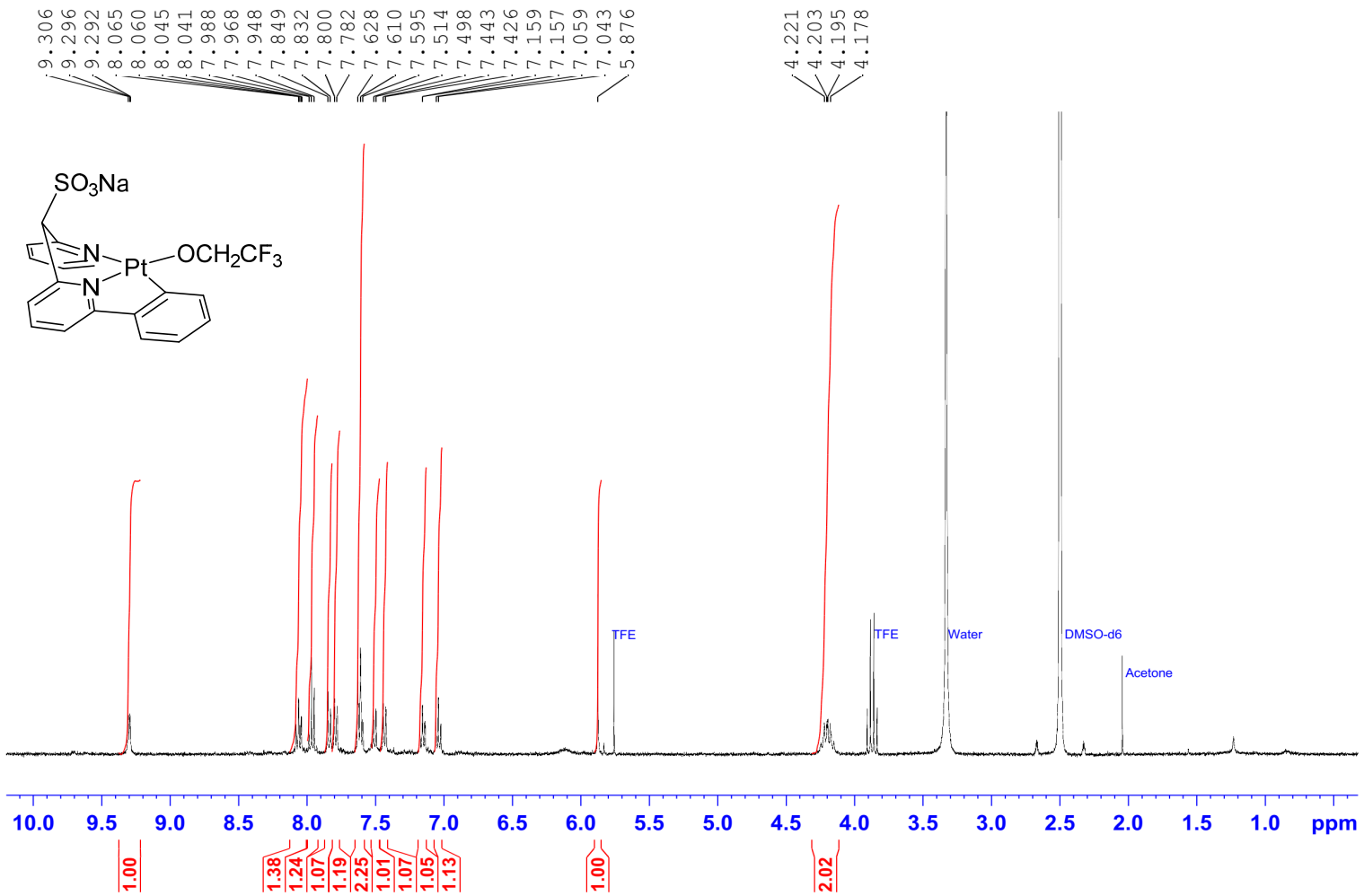

Figure S39. ^{1}H-NMR of Na[(C_6H_4-dpms)Pt(OCH_2CF_3)] in DMSO-d_6.

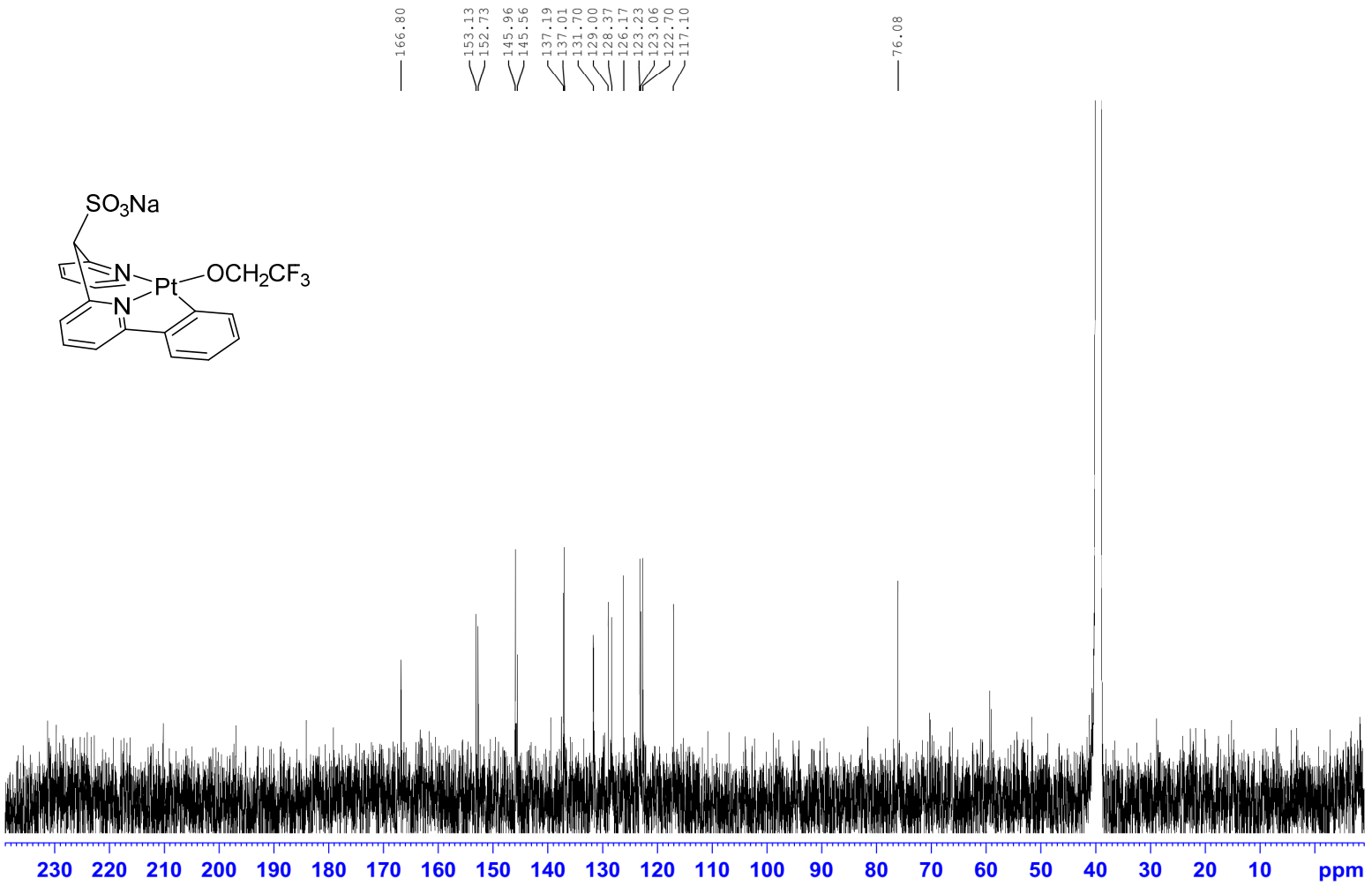

Figure S40. ^{13}C-NMR of Na[(C_6H_4-dpms)Pt(OCH_2CF_3)] in DMSO-d_6.

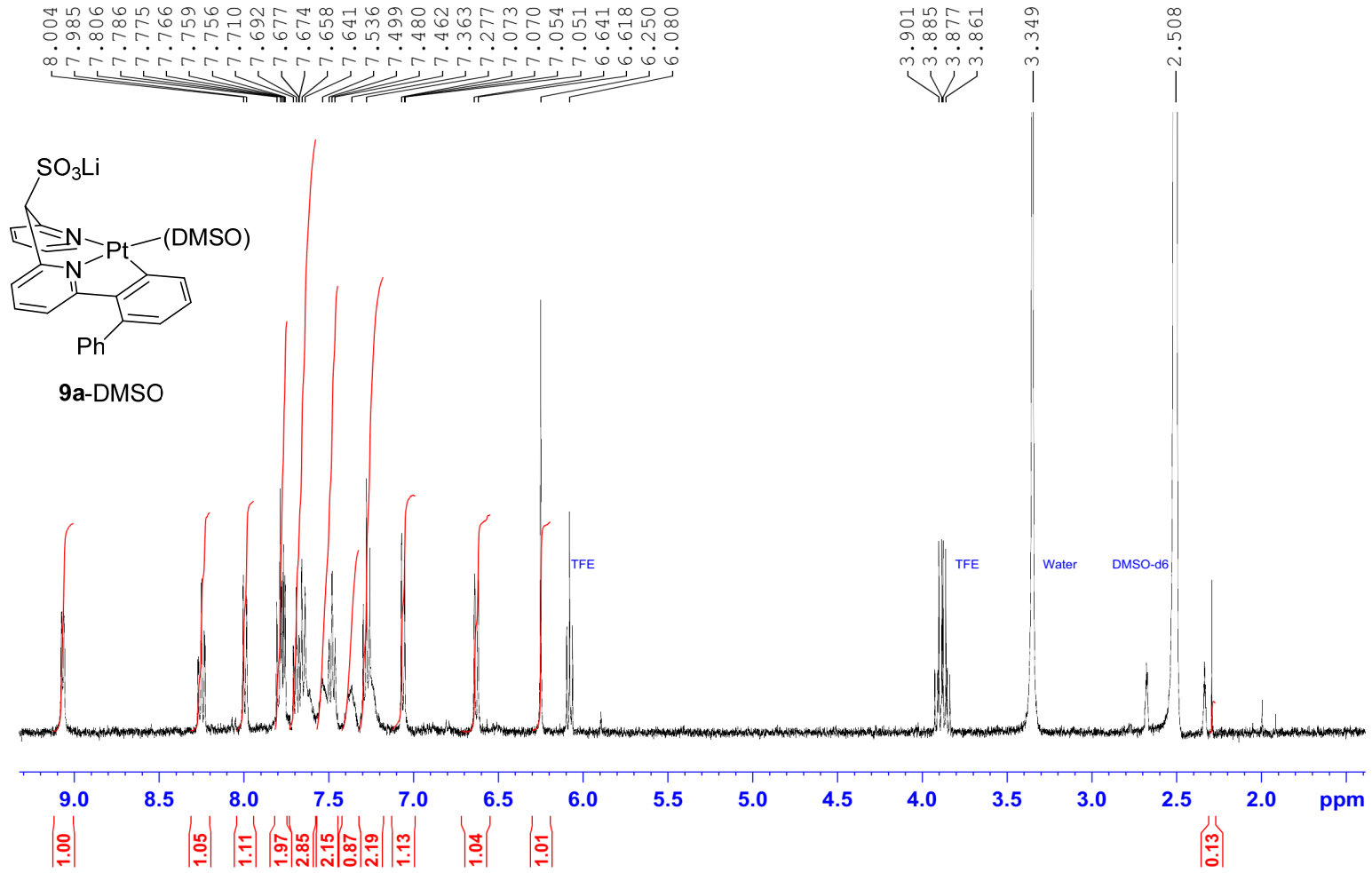

Figure S41. ^{1}H-NMR of **9a**-DMSO in DMSO-d_6.

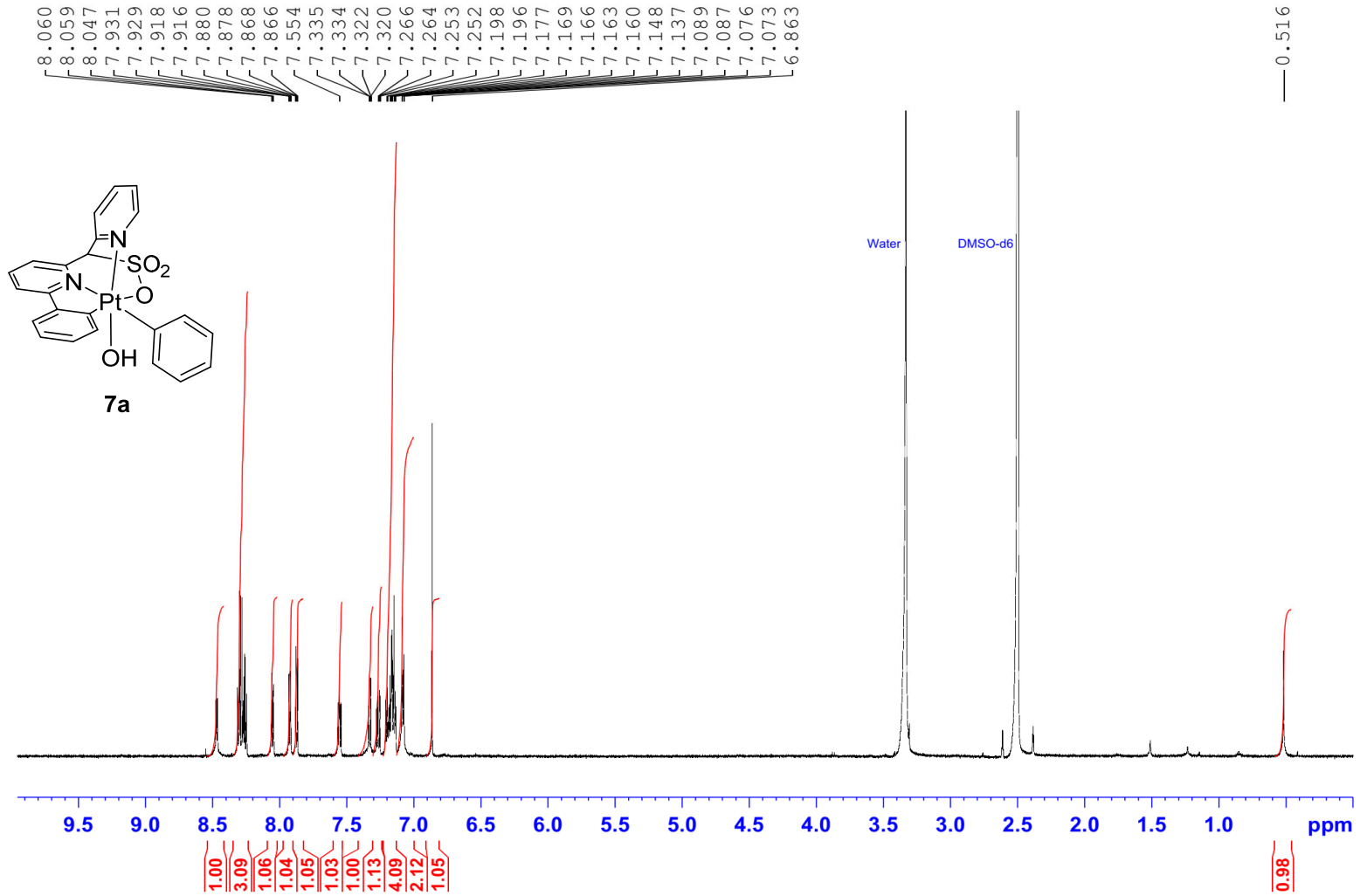

Figure S42. ^{1}H-NMR of **7a** in DMSO-d_6.

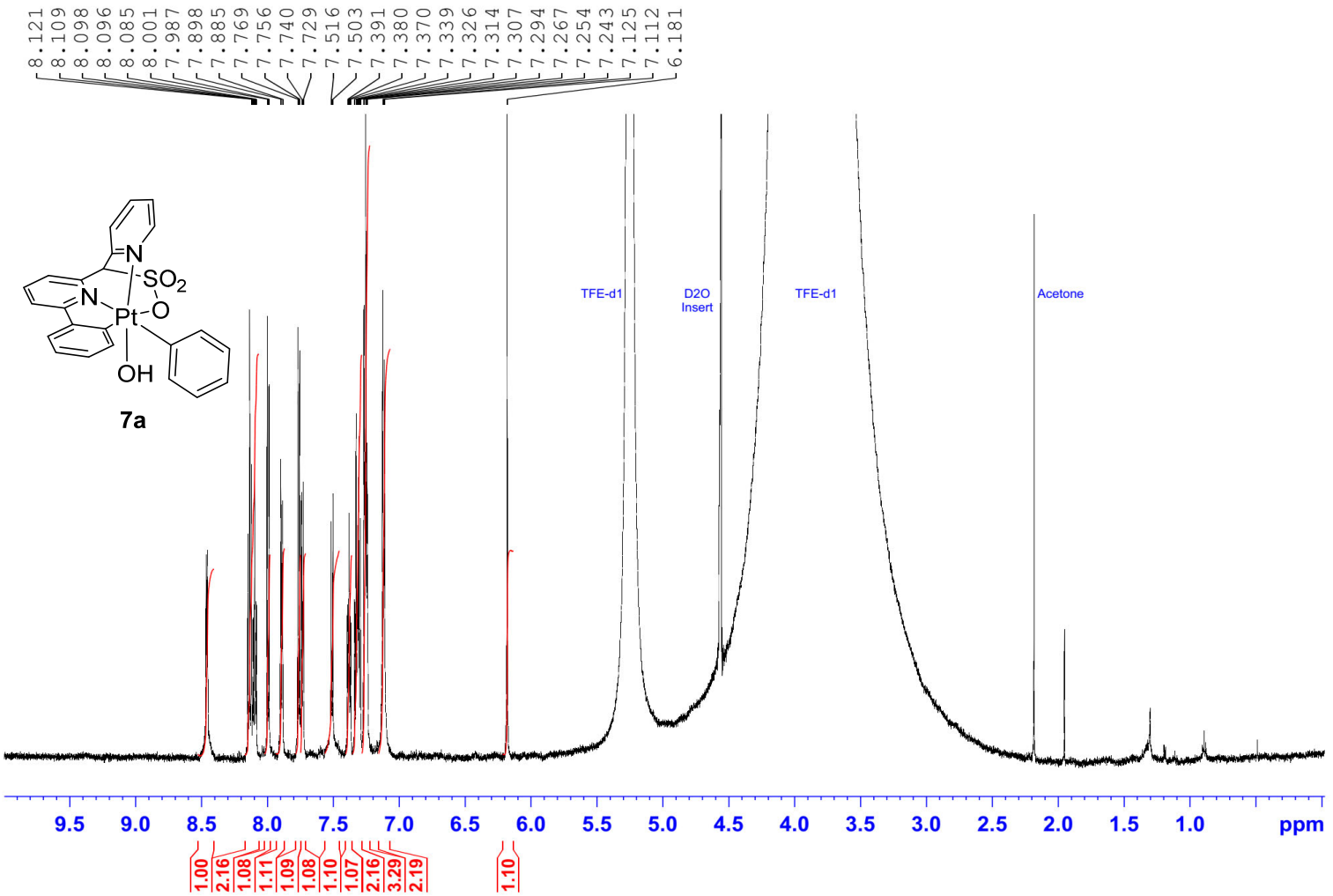

Figure S43. ^{1}H-NMR of **7a** in TFE-d_1.

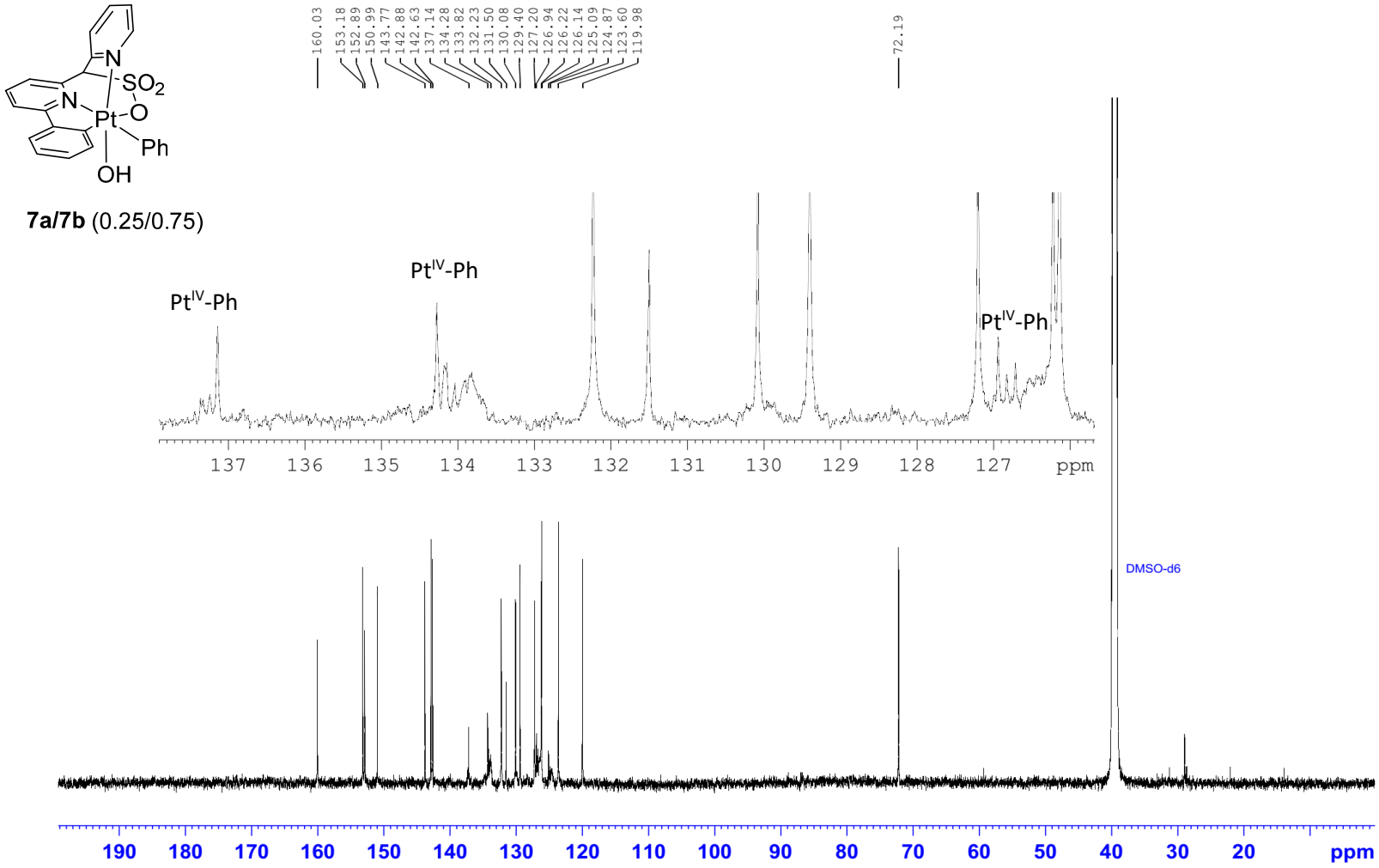

Figure S44. ^{13}C-NMR of a **7a**/**7b** mixture (**7a/7b** ≈ 0.25/0.75) in DMSO-d_6. Inset shows ^{13}C signals, belonging to carbons in the Pt^{IV}-Ph group, split by deuterium.

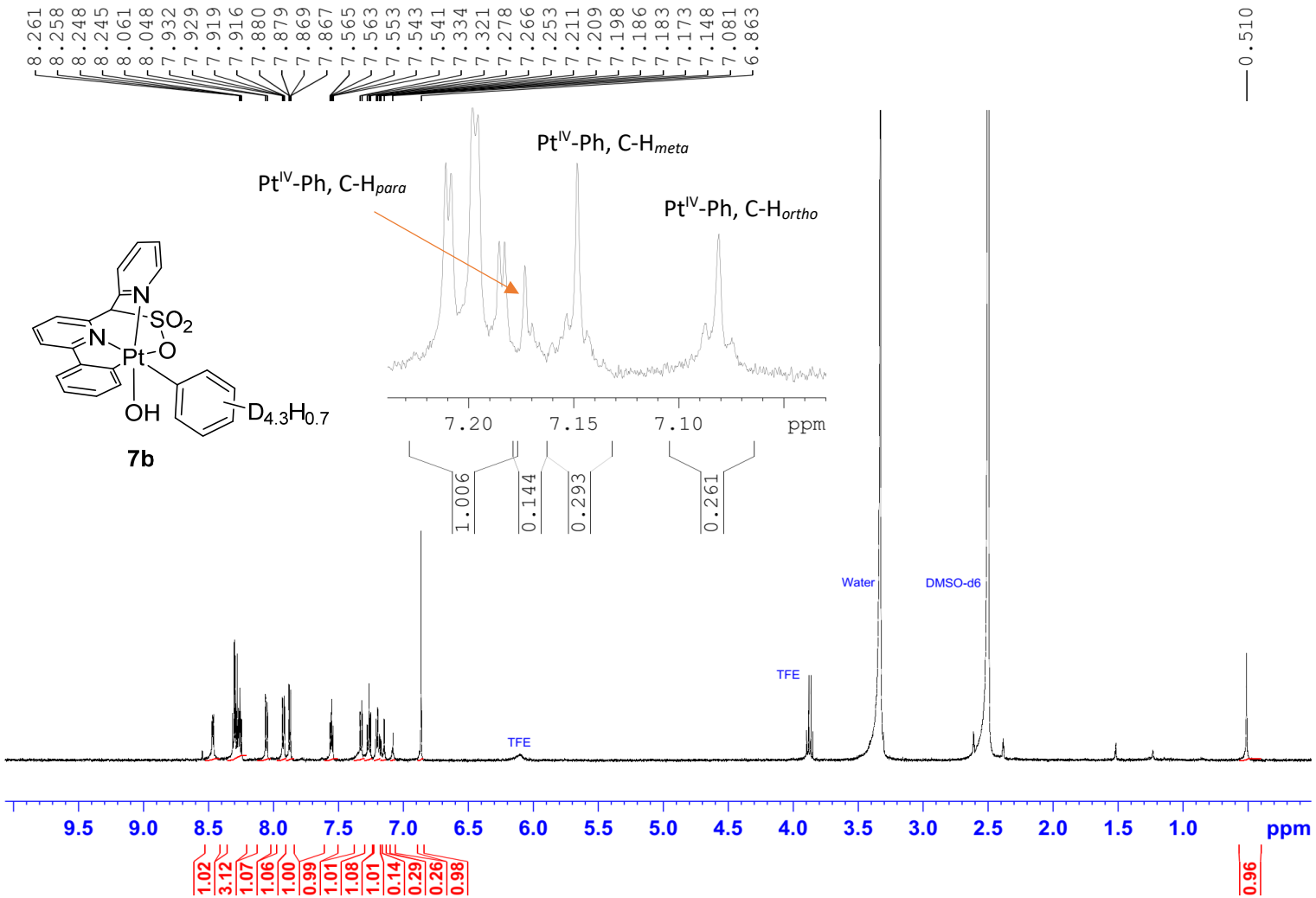

Figure S45. ^{1}H-NMR of **7b** in DMSO-d_6 containing 15 % ^{1}H incorporation into the phenyl group (inset).

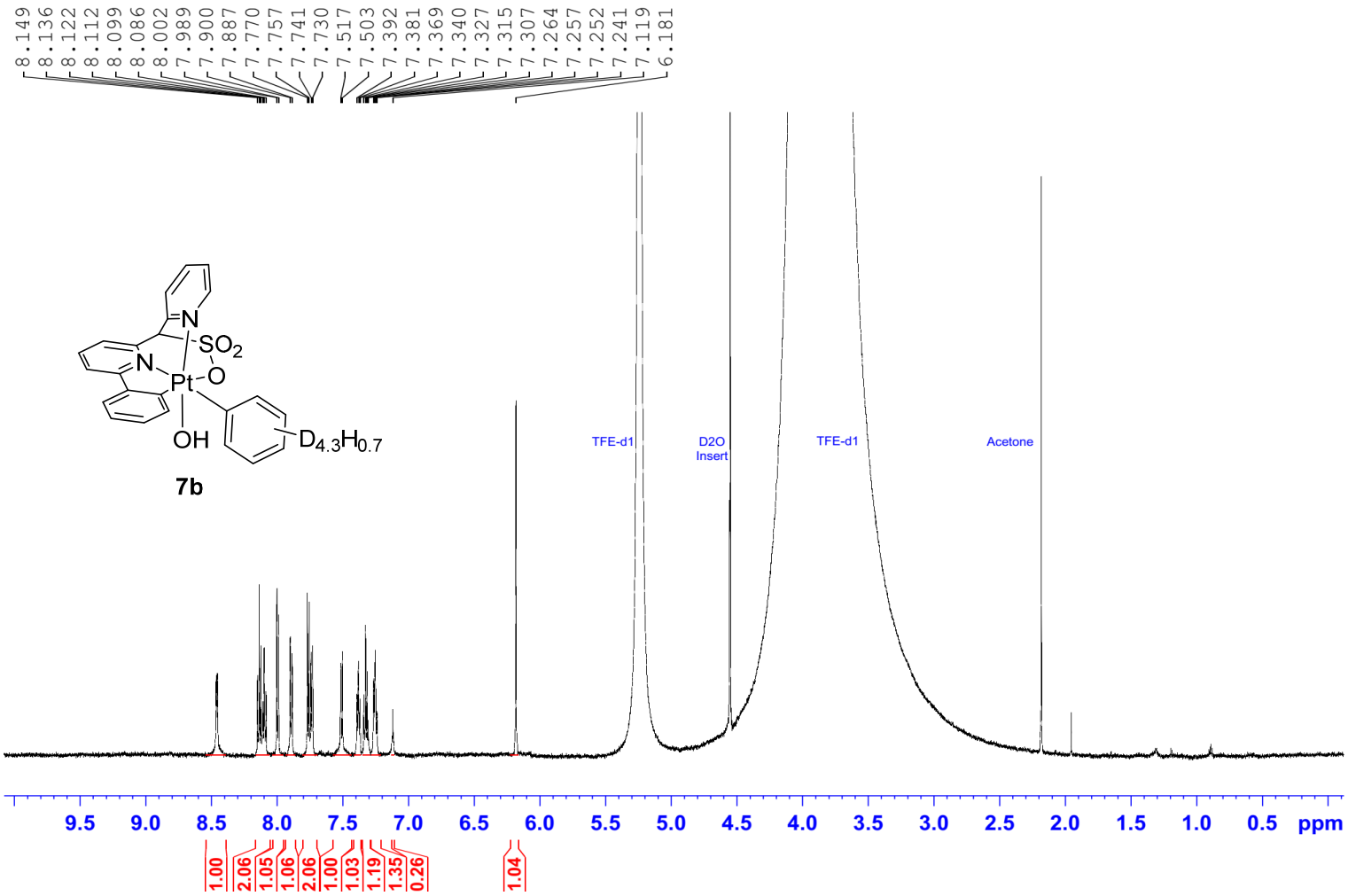

Figure S46. ^{1}H-NMR of **7b** in TFE-d_1.

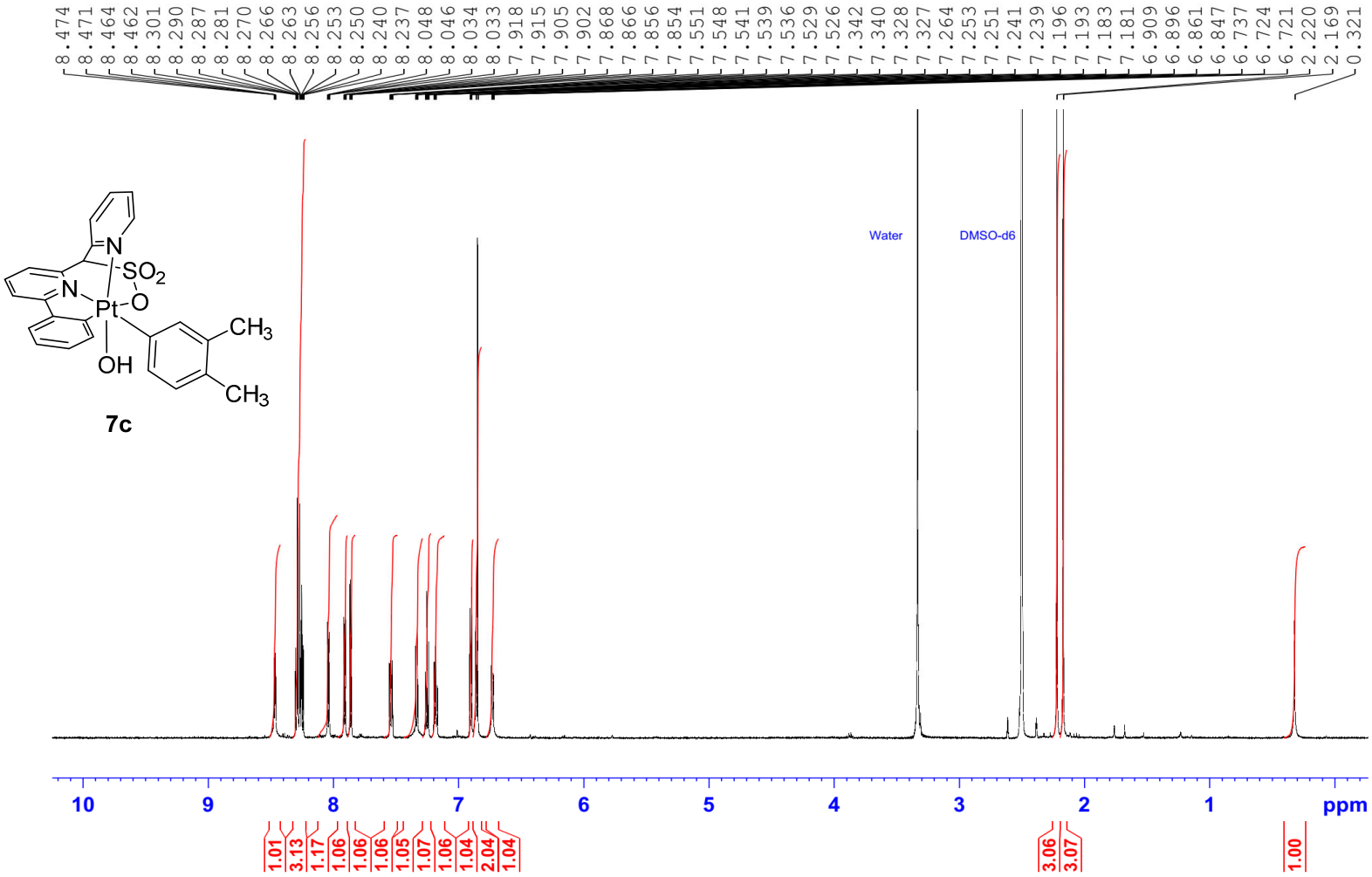

Figure S47. ^{1}H-NMR of **7c** in DMSO-d_6.

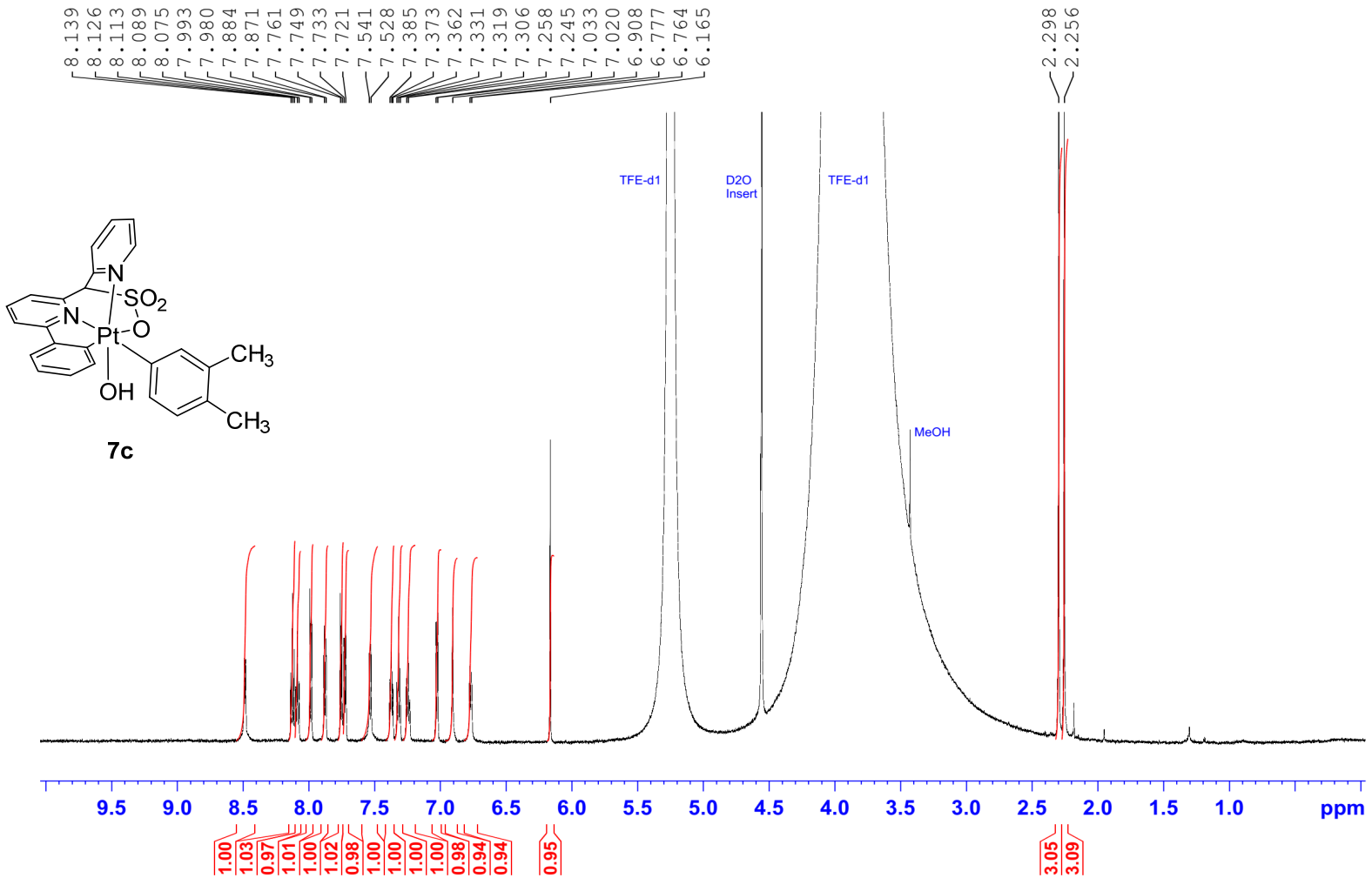

Figure S48. ^{1}H-NMR of **7c** in TFE-d_1.

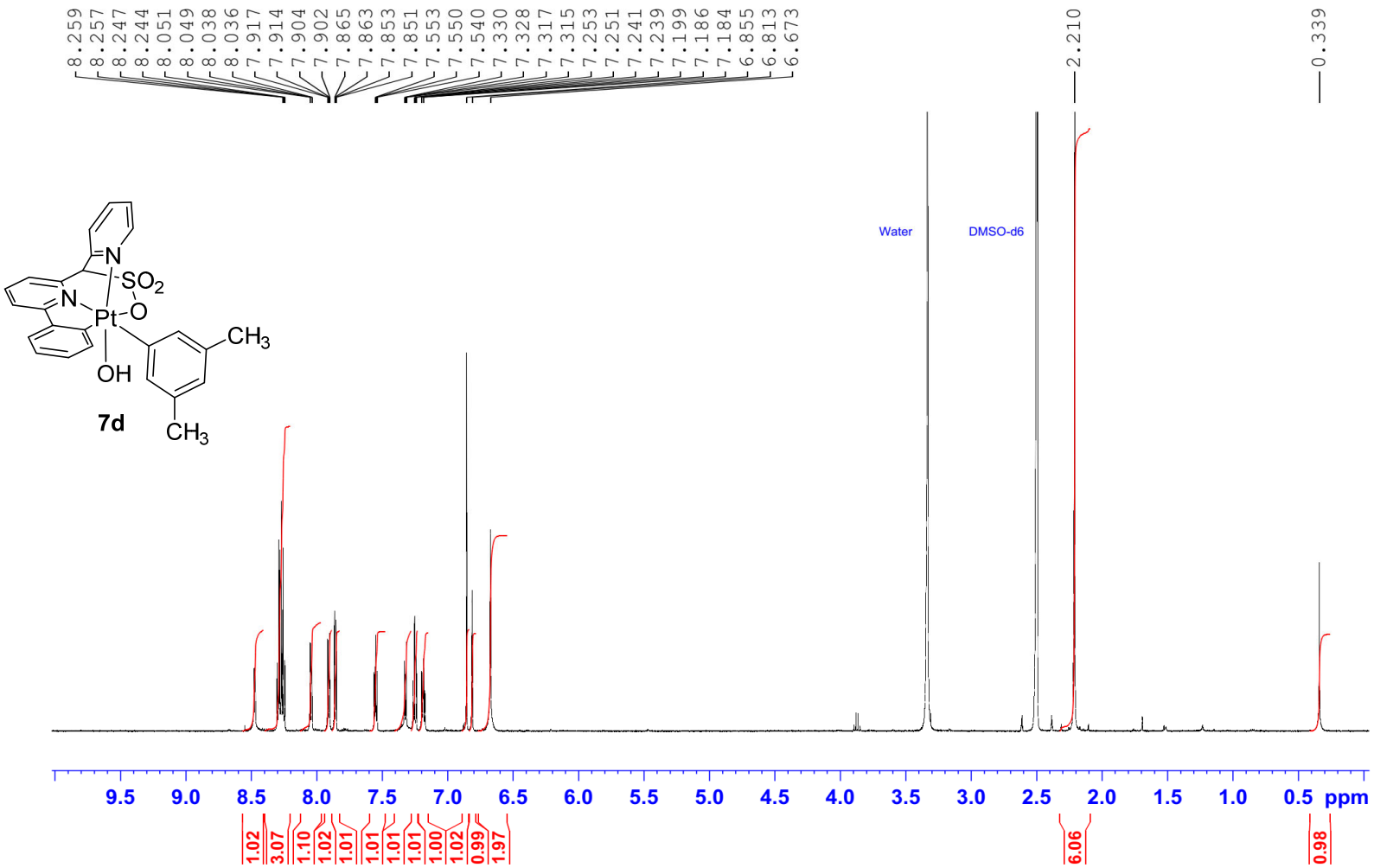

Figure S49. ^{1}H-NMR of **7d** in DMSO-d_6.

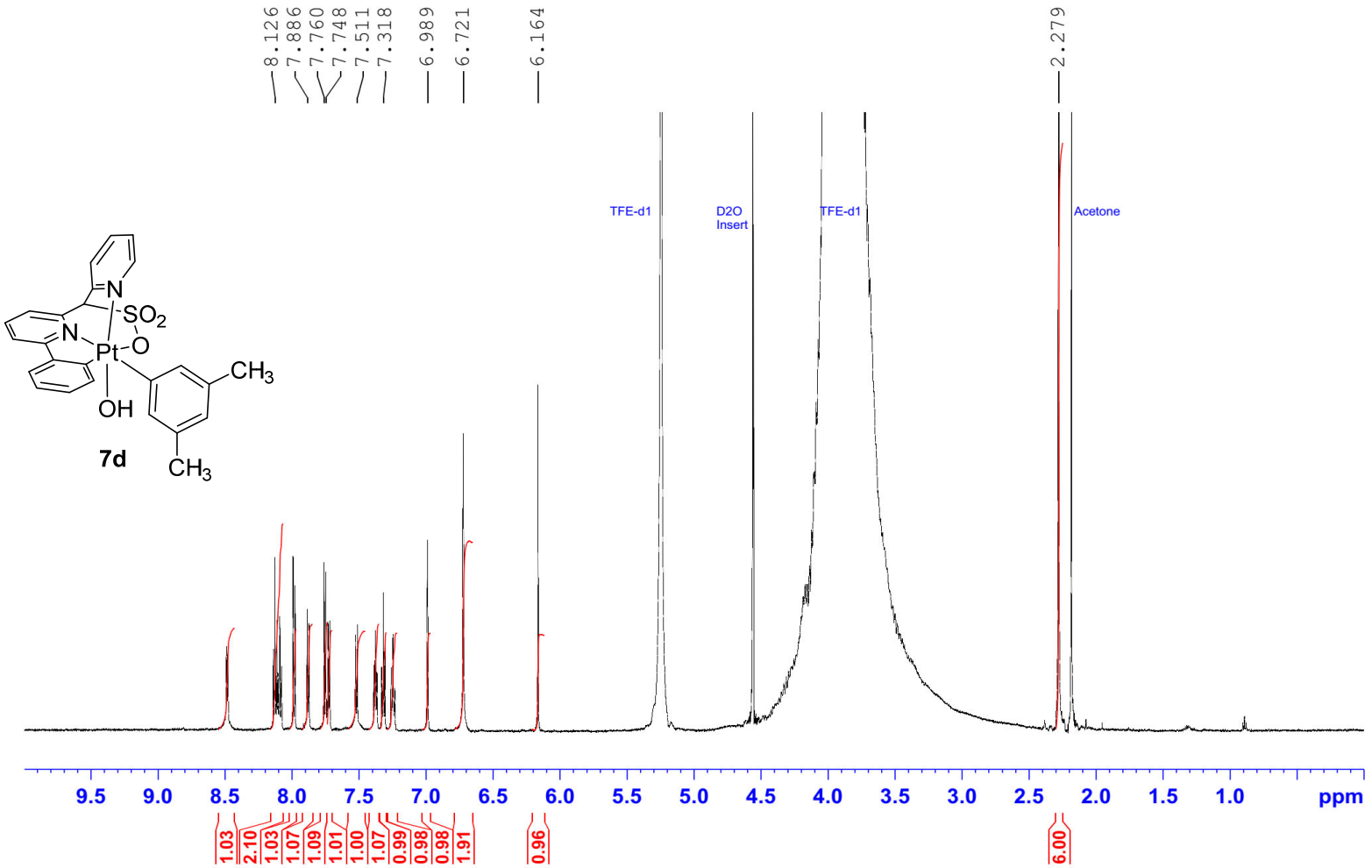

Figure S50. ^{1}H-NMR of **7d** in TFE-d_1.

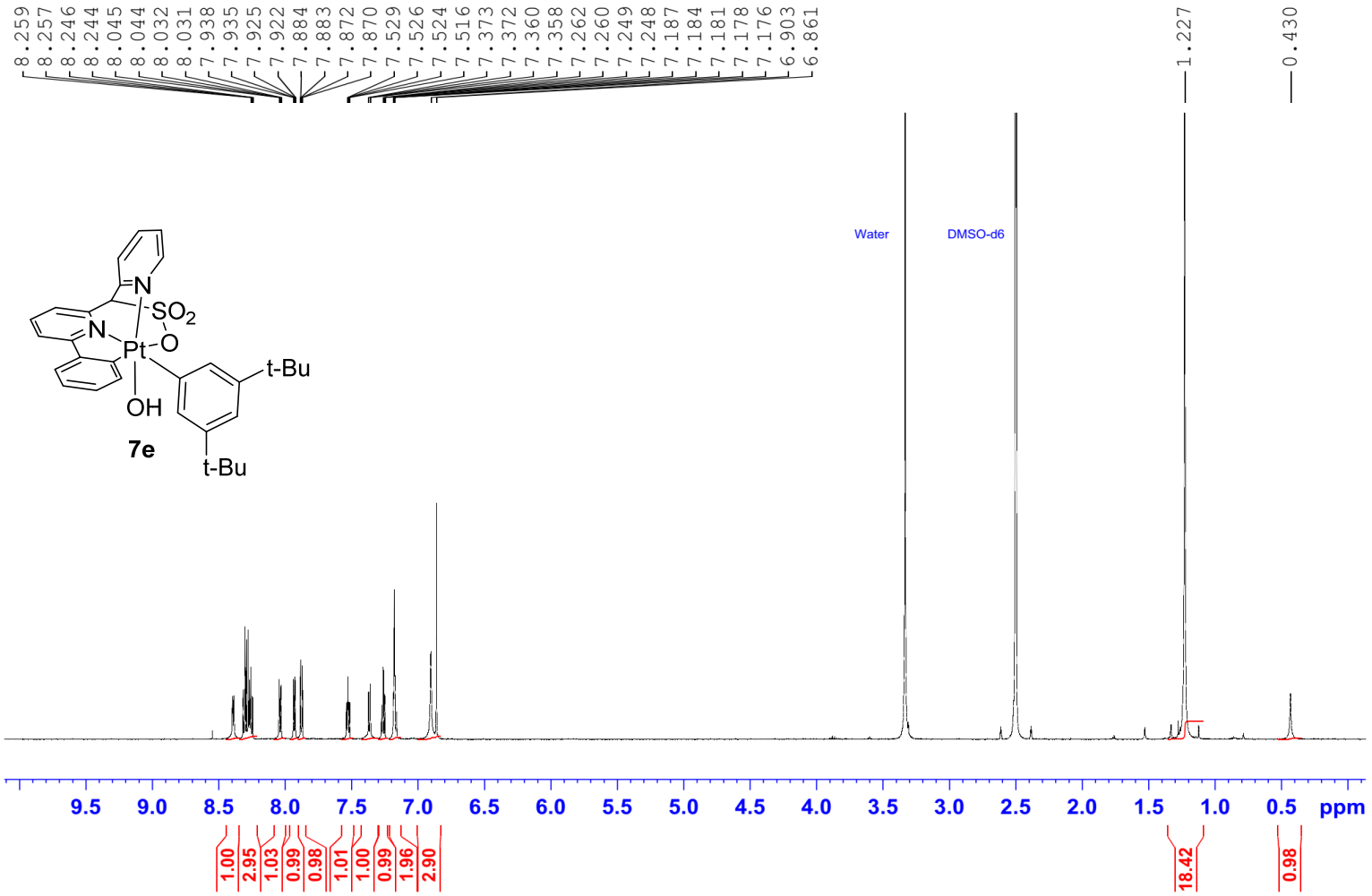

Figure S51. ^{1}H-NMR of **7e** in DMSO-d_6.

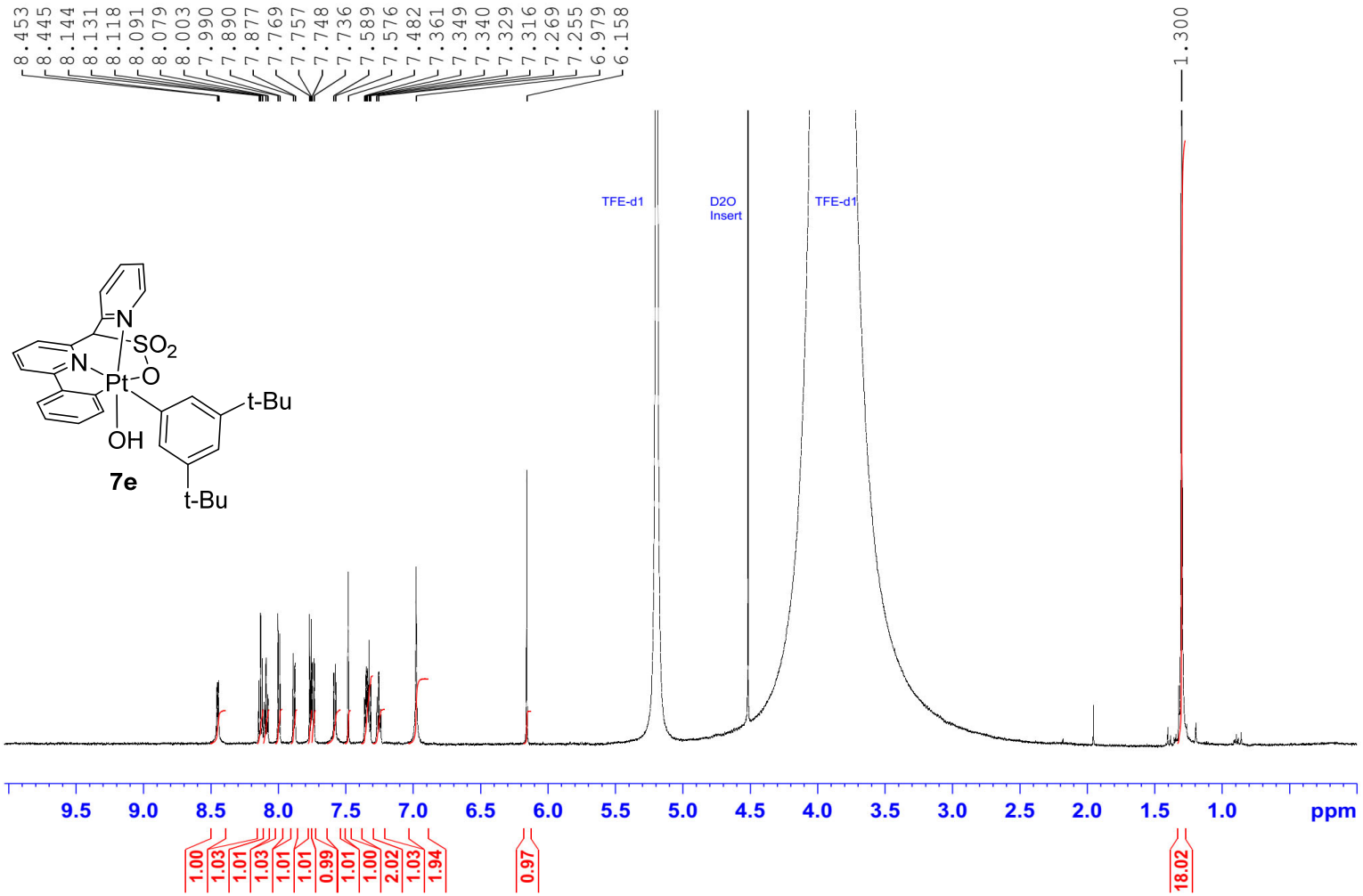

Figure S52. ^{1}H-NMR spectrum of **7e** in TFE-d_1.

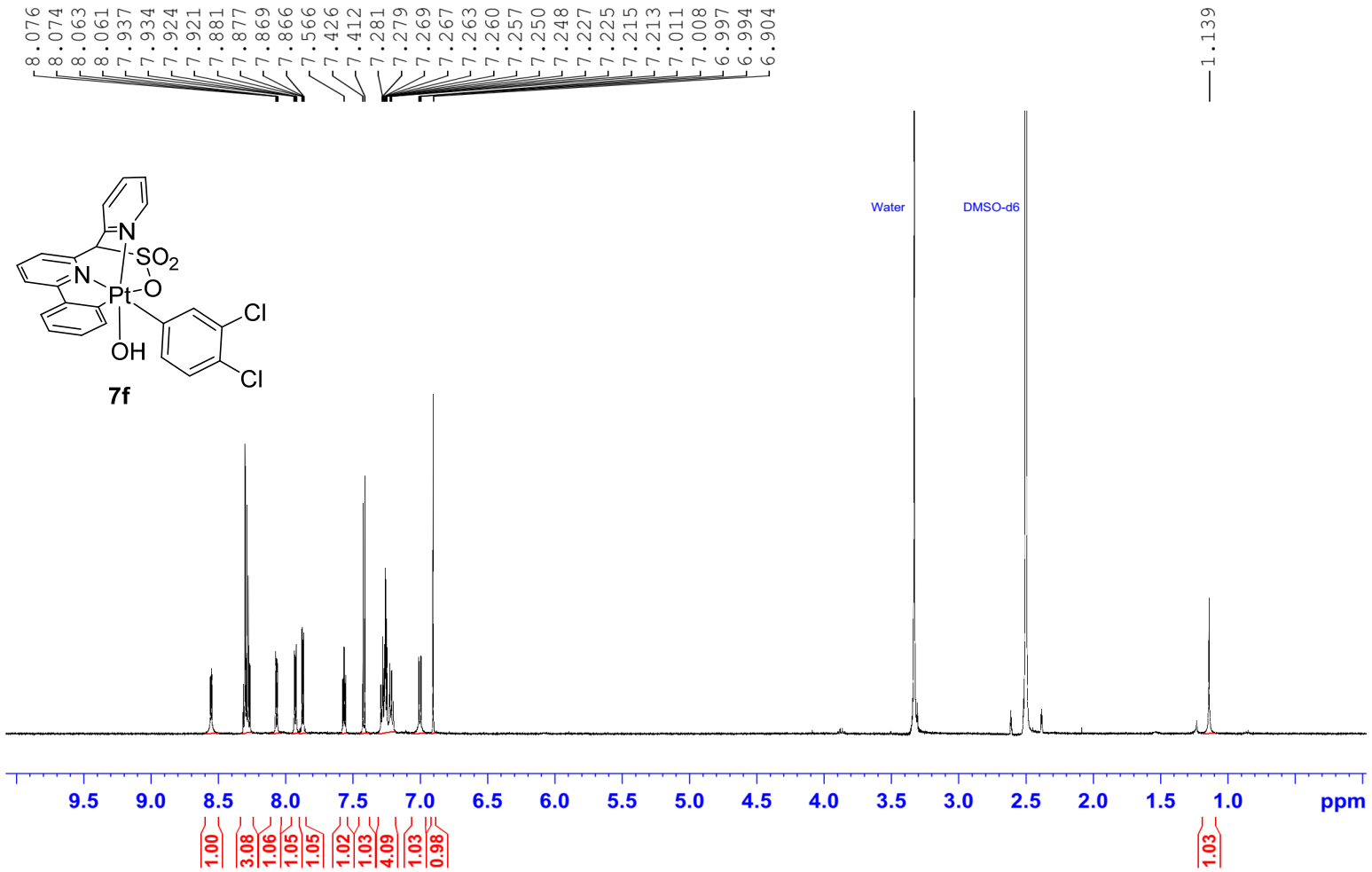

Figure S53. ^{1}H-NMR of **7f** in DMSO-d_6.

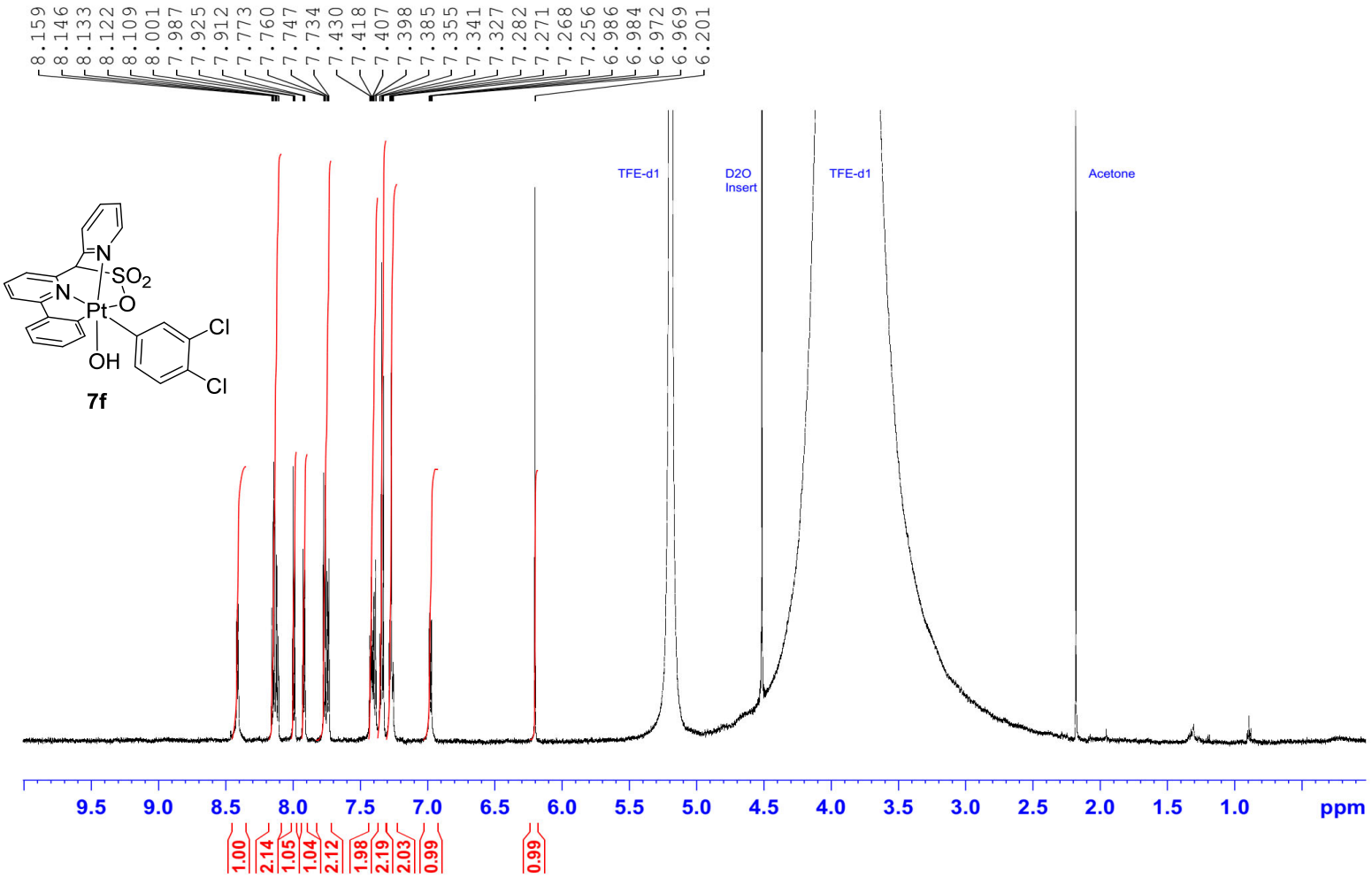

Figure S54. ^{1}H-NMR of **7f** in TFE-d_1.

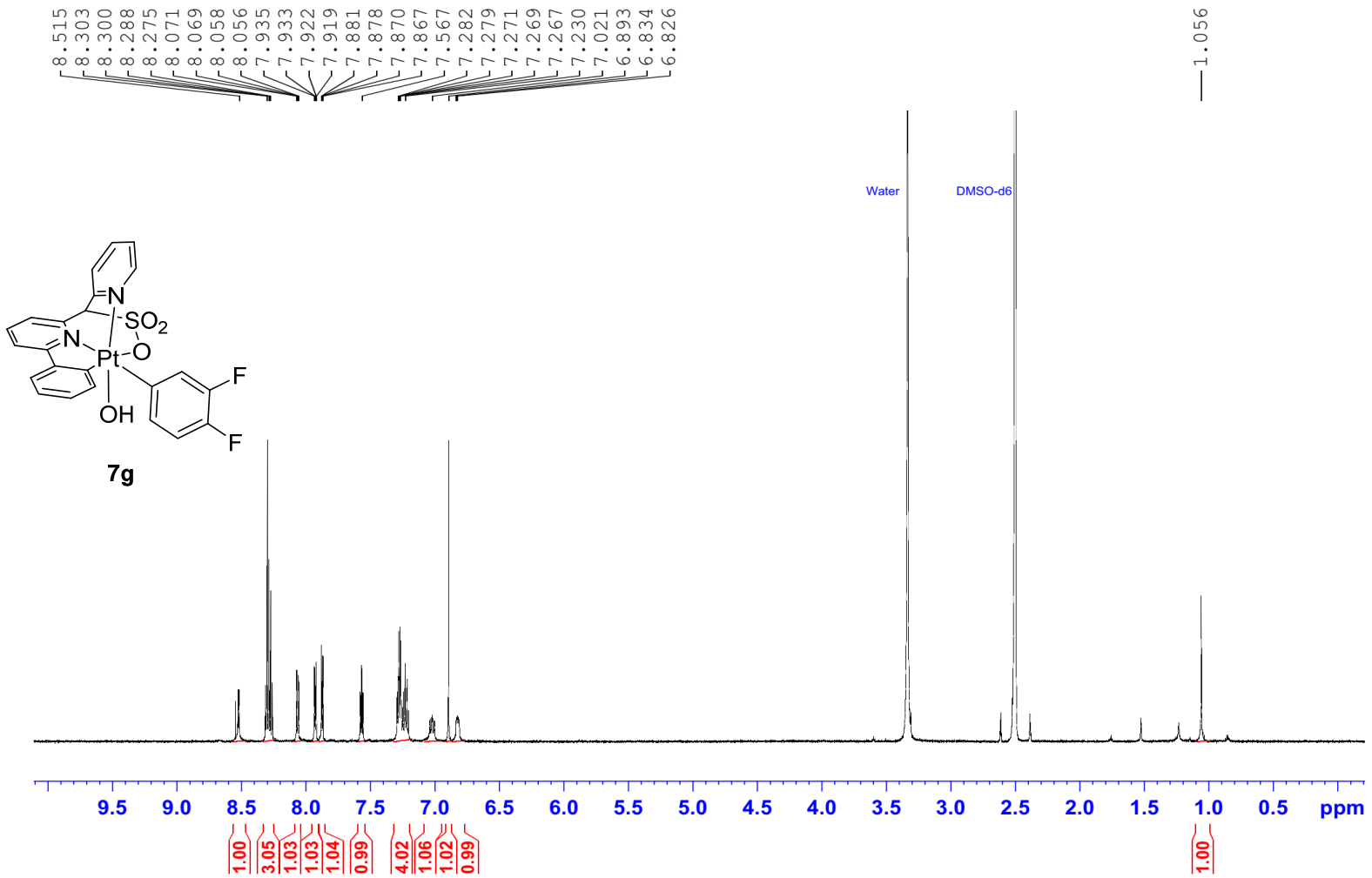

Figure S26. ^{1}H-NMR of **7g** in DMSO-d_6.

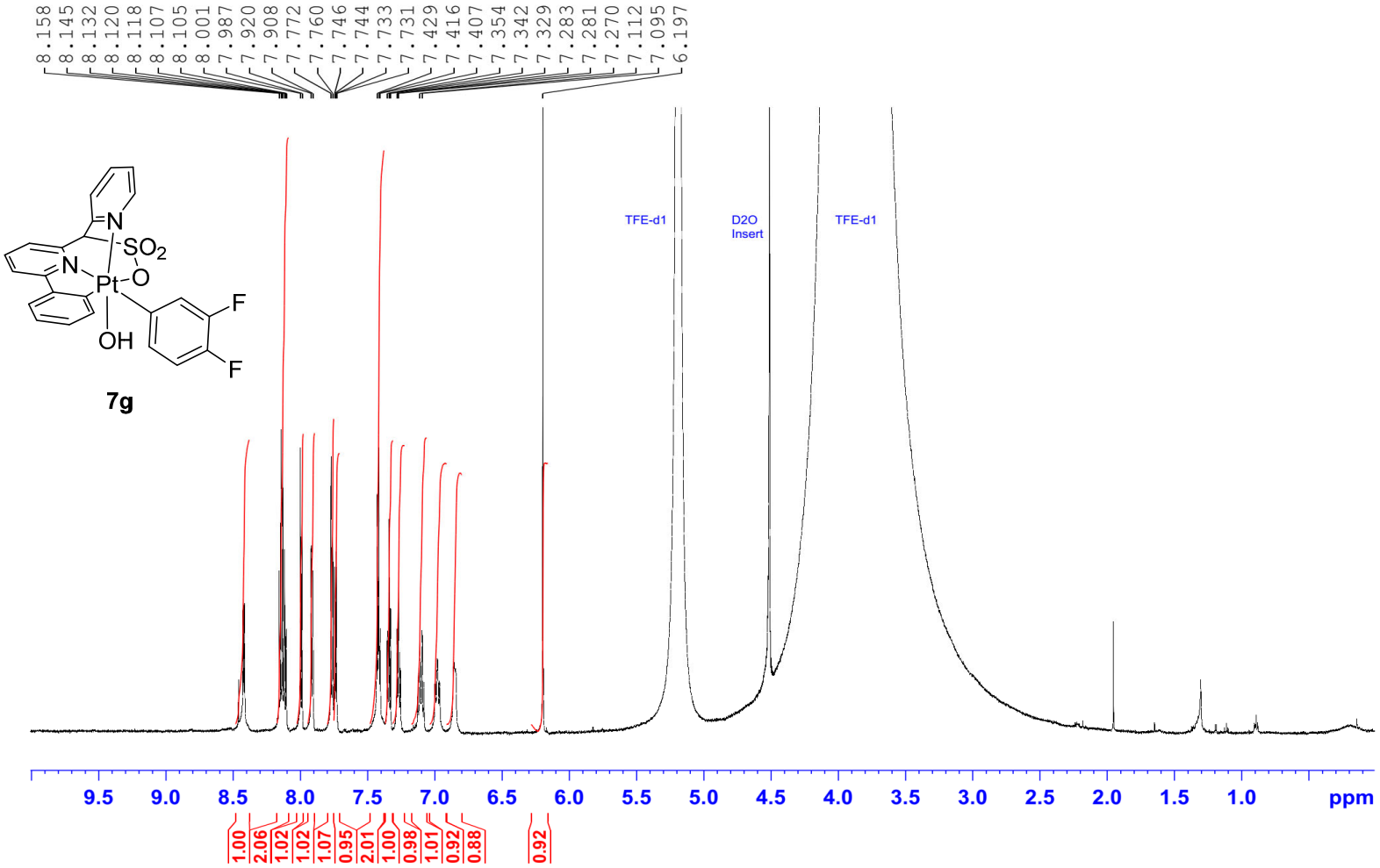

Figure S27. ^{1}H-NMR of **7g** in TFE-d_1.

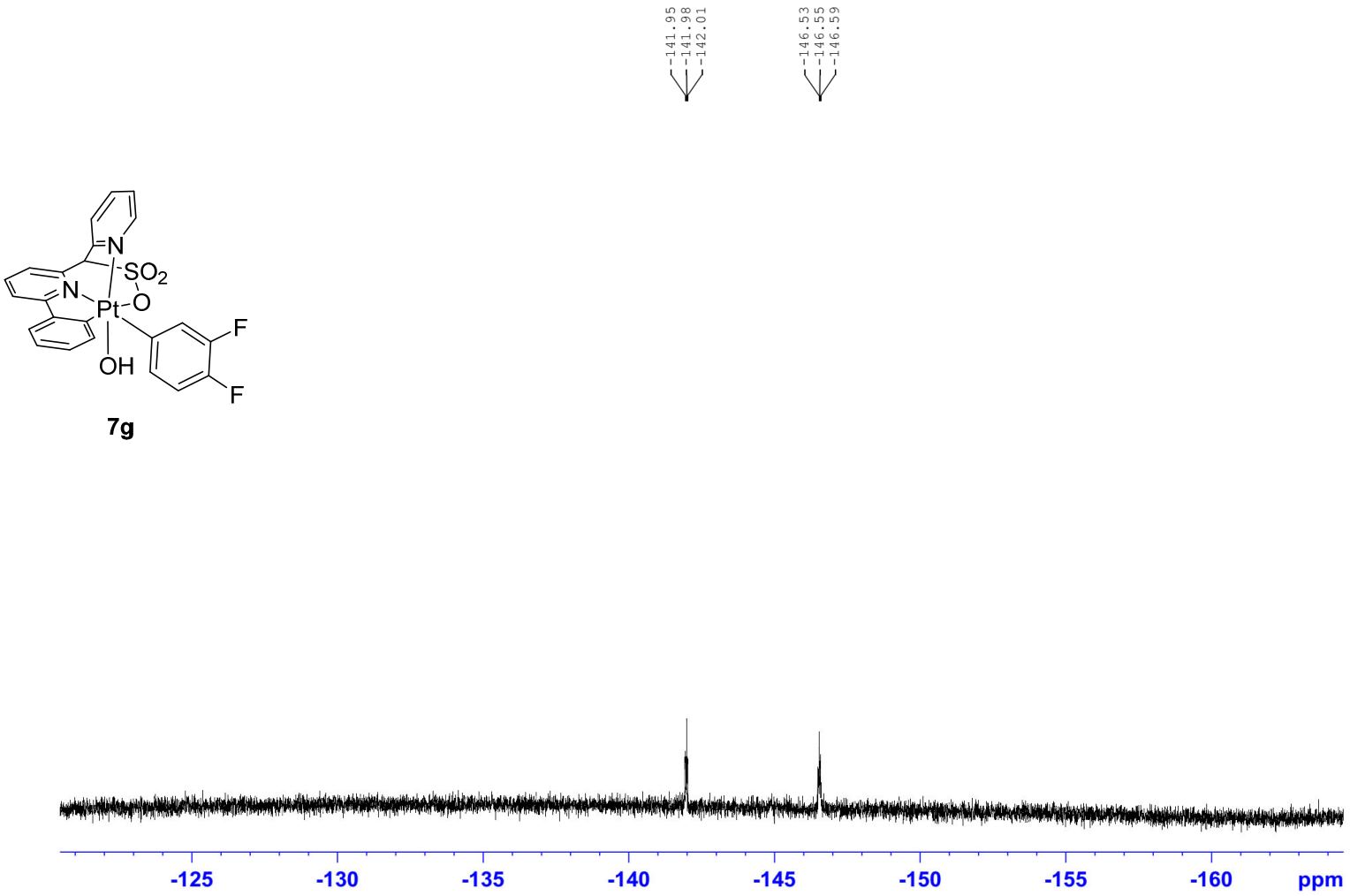

Figure S28. ^{19}F-NMR of **7g** in acetone-d_6.

IX. References

1. Watts, D.; Wang, D.; Zavalij, P. Y.; Vedernikov A. N., *Isr. J. Chem*. **2017**, 1010-1022.
2. Watts, D.; Wang, D.; Adelberg, M.; Zavalij, P. Y.; Vedernikov A. N., *Organometallics* **2017**, 207-219.
3. Hadj-Bagheri, N.; Puddephatt, R., *Polyhederon* **1988**, *7*, 2695-2702.